

การระบุและลักษณะสมบัติของ miRNA ที่เกี่ยวข้องกับการติดเชื้อไวรัสตัวแดงดวงขาวในกุ้งกุลาดำ
Penaeus monodon



บทคัดย่อและแฟ้มข้อมูลฉบับเต็มของวิทยานิพนธ์ตั้งแต่ปีการศึกษา 2554 ที่ให้บริการในคลังปัญญาจุฬาฯ (CUIR)
เป็นแฟ้มข้อมูลของนิสิตเจ้าของวิทยานิพนธ์ ที่ส่งผ่านทางบัณฑิตวิทยาลัย

The abstract and full text of theses from the academic year 2011 in Chulalongkorn University Intellectual Repository (CUIR)
are the thesis authors' files submitted through the University Graduate School.

วิทยานิพนธ์นี้เป็นส่วนหนึ่งของการศึกษาตามหลักสูตรปริญญาวิทยาศาสตรมหาบัณฑิต
สาขาวิชาชีวเคมีและชีววิทยาโมเลกุล ภาควิชาชีวเคมี
คณะวิทยาศาสตร์ จุฬาลงกรณ์มหาวิทยาลัย
ปีการศึกษา 2557
ลิขสิทธิ์ของจุฬาลงกรณ์มหาวิทยาลัย

Identification and characterization of miRNA involved in white spot syndrome virus
infection in black tiger shrimp *Penaeus monodon*

Mr. Napol Kaewkascholkul



A Thesis Submitted in Partial Fulfillment of the Requirements
for the Degree of Master of Science Program in Biochemistry and Molecular Biology
Department of Biochemistry
Faculty of Science
Chulalongkorn University
Academic Year 2014
Copyright of Chulalongkorn University

Thesis Title Identification and characterization of miRNA
involved in white spot syndrome virus infection in
black tiger shrimp *Penaeus monodon*
By Mr. Napol Kaewkascholkul
Field of Study Biochemistry and Molecular Biology
Thesis Advisor Assistant Professor Kunlaya Somboonwiwat, Ph.D.
Thesis Co-Advisor Professor Anchalee Tassanakajon, Ph.D.
Kulwadee Somboonwiwat, Ph.D.

Accepted by the Faculty of Science, Chulalongkorn University in Partial
Fulfillment of the Requirements for the Master's Degree

..... Dean of the Faculty of Science
(Professor Supot Hannongbua, Ph.D.)

THESIS COMMITTEE

..... Chairman
(Assistant Professor Rath Pichyangkura, Ph.D.)

..... Thesis Advisor
(Assistant Professor Kunlaya Somboonwiwat, Ph.D.)

..... Thesis Co-Advisor
(Professor Anchalee Tassanakajon, Ph.D.)

..... Thesis Co-Advisor
(Kulwadee Somboonwiwat, Ph.D.)

..... Examiner
(Associate Professor Teerapong Buaboocha, Ph.D.)

..... External Examiner
(Associate Professor Apinunt Udomkit, Ph.D.)

ฉพล แก้วเกษชกุล : การระบุและลักษณะสมบัติของ miRNA ที่เกี่ยวข้องกับการติดเชื้อไวรัสตัวแดงดวงขาวในกุ้งกุลาดำ *Penaeus monodon* (Identification and characterization of miRNA involved in white spot syndrome virus infection in black tiger shrimp *Penaeus monodon*)
 อ.ที่ปรึกษาวิทยานิพนธ์หลัก: ผศ. ดร. กุลยา สมบูรณ์วิวัฒน์, อ.ที่ปรึกษาวิทยานิพนธ์ร่วม: ศ. ดร. อัญชลี ทศนาขจร, ดร. กุลวดี สมบูรณ์วิวัฒน์, 125 หน้า.

MicroRNAs (miRNAs) เป็น RNA ขนาดเล็กที่ทำหน้าที่ควบคุมกระบวนการต่างๆในสิ่งมีชีวิตรวมถึงระบบภูมิคุ้มกัน โดยยับยั้งการแสดงของยีนผ่านด้วยการย่อยสลาย mRNA หรือยับยั้งกระบวนการแปลรหัสของยีน ในการศึกษาในระดับชนิดของ miRNA ที่แสดงออกในเซลล์เม็ดเลือดของกุ้งกุลาดำที่ติดเชื้อไวรัสตัวแดงดวงขาวโดยเทคนิค next generation sequencing ทำการสร้างห้องสมุดของ RNA ขนาดเล็ก 3 ห้องสมุด จากเซลล์เม็ดเลือดของกุ้งกุลาดำที่ติดเชื้อไวรัสตัวแดงดวงขาวที่เวลา 0 6 และ 48 ชั่วโมง โดยใช้ TruSeq small RNA sample preparation kit และหาลำดับนิวคลีโอไทด์ด้วยเครื่อง MiSeq (Illumina) จากนั้นคัดเลือกข้อมูลลำดับนิวคลีโอไทด์ที่มีคุณภาพสูง มาผ่านกระบวนการกำจัดลำดับนิวคลีโอไทด์ของ 3' และ 5' adapter และ RNA ปนเปื้อน และนำลำดับนิวคลีโอไทด์ที่ผ่านกระบวนการข้างต้นมาเปรียบเทียบกับฐานข้อมูล miRNA ที่เรียกว่า miRBase เพื่อระบุชนิดของ miRNA จากการวิเคราะห์พบ miRNA homolog 60 ชนิด จากเซลล์เม็ดเลือดกุ้งที่ติดเชื้อไวรัสตัวแดงดวงขาว จากนั้นวิเคราะห์ระดับการแสดงออกของ miRNA ที่สนใจ 9 ชนิดต่อการติดเชื้อไวรัสด้วยเทคนิค Northern blot พบว่ามีเพียง miRNA 2 ชนิด คือ let-7-5p และ miR-71-5p ที่สามารถตรวจพบและมีระดับแสดงออกเปลี่ยนแปลงไปในเซลล์เม็ดเลือดกุ้งที่ติดเชื้อไวรัสตัวแดงดวงขาว เนื่องจากข้อจำกัดของความสามารถของตัวติดตามที่ใช้ในการตรวจสอบการแสดงออกของ miRNA ด้วยเทคนิค Northern blot จึงนำเทคนิค stem-loop real-time PCR มาใช้ในการวิเคราะห์ระดับการแสดงออกของ miRNA แทน จากการวิเคราะห์การแสดงออกของ miRNA 16 ชนิดในเซลล์เม็ดเลือดกุ้งที่ติดเชื้อไวรัสตัวแดงดวงขาว พบว่า miRNA 11 ชนิดจาก 16 ชนิดมีการแสดงออกที่เปลี่ยนแปลงไปหลังจากการติดเชื้อไวรัส เพื่อศึกษาหน้าที่ของ miRNA ที่เกี่ยวข้องกับระบบภูมิคุ้มกันในกุ้งกุลาดำต่อเชื้อไวรัสตัวแดงดวงขาว ในงานวิจัยนี้ได้ใช้โปรแกรมซึ่งพัฒนาโดยกลุ่มวิจัย เพื่อระบุชนิดของยีนเป้าหมายของ miRNA แต่ละชนิด โดยอาศัยฐานข้อมูล EST ของกุ้งกุลาดำ ในการศึกษาสนใจ mRNA เป้าหมายที่เป็นยีนในระบบภูมิคุ้มกัน เช่น โปรแกรมการตายของเซลล์ เปปไทด์ต้านจุลชีพ ระบบไพโรพินอลออกซิเดส โปรตีนเนส ตัวยับยั้งโปรตีนเนส การสื่อสารของเซลล์ และ โปรตีนฮีตช็อค จากการทำนายพบ miRNA 46 ชนิด จาก 60 ชนิดในกุ้งกุลาดำ ที่คาดว่าสามารถจับกับบริเวณ 5'UTR ORF และ 3'UTR ของยีนที่เกี่ยวข้องกับระบบภูมิคุ้มกันได้ จากผลการทดลองข้างต้นสรุปได้ว่า miRNA มีหน้าที่ในการควบคุมการแสดงออกยีนในระบบภูมิคุ้มกันที่เกี่ยวข้องกับการตอบสนองต่อการติดเชื้อไวรัสในกุ้ง

ภาควิชา	ชีวเคมี	ลายมือชื่อนิสิต
สาขาวิชา	ชีวเคมีและชีววิทยาโมเลกุล	ลายมือชื่อ อ.ที่ปรึกษาหลัก
ปีการศึกษา	2557	ลายมือชื่อ อ.ที่ปรึกษาร่วม
		ลายมือชื่อ อ.ที่ปรึกษาร่วม

5571963923 : MAJOR BIOCHEMISTRY AND MOLECULAR BIOLOGY

KEYWORDS: MIRNA / PENAUEUS MONODON / WHITE SPOT SYNDROME VIRUS

NAPOL KAEWKASCHOLKUL: Identification and characterization of miRNA involved in white spot syndrome virus infection in black tiger shrimp *Penaeus monodon*. ADVISOR: ASST. PROF. KUNLAYA SOMBOONWIWAT, Ph.D., CO-ADVISOR: PROF. ANCHALEE TASSANAKAJON, Ph.D., KULWADEE SOMBOONVIWAT, Ph.D., 125 pp.

MicroRNA (miRNA) is a small RNA that functions in regulating various biological processes including immune system by suppressing the gene expression via either mRNA degradation or inhibiting gene translation. In this study, miRNAs that are expressed in white spot syndrome virus (WSSV)-infected *Penaeus monodon* hemocyte were identified by next generation sequencing technique. Three small RNA libraries of hemocyte of WSSV-infected *P. monodon* at 0, 6 and 48 hours post infection (hpi) were constructed using TruSeq small RNA sample preparation kits and subjected to MiSeq sequencer (Illumina). Then, the raw data whose quality could pass the quality filter was processed by removing 3'- and 5'-adapter sequences and known contaminated-RNAs. The remaining sequences were searched against miRNA database, miRBase, to identify miRNA homologs. In this study, sixty miRNA homologs from WSSV-infected *P. monodon* hemocyte were identified. In order to analyze the expression of interested miRNAs in response to WSSV challenge, Northern blot analysis of 6 interested miRNAs was performed. Only 2 of them, let-7-5p and miR-71-5p could be detected and they were differentially expressed in hemocyte of WSSV-challenged *P. monodon*. Due to the detection limit of probes used in Northern blot analysis, stem-loop real-time PCR was used instead to further determine the expression of 16 interested miRNAs in hemocyte of WSSV-challenge *P. monodon* at 0, 6 and 48 hpi. The results showed that 11 out of 16 miRNAs were differently expressed upon WSSV infection. Two miRNAs, miR-315 and miR-750, were highly responsive miRNAs upon WSSV infection. To further characterize the involvement of the identified miRNAs in *P. monodon* immunity against WSSV infection, target mRNAs of each miRNA were predicted by in-house software against *P. monodon* EST database. In this study we focused on the target mRNAs that are immune-related genes of apoptosis, antimicrobial peptides, prophenoloxidase system, proteinase and proteinase inhibitor, signaling transduction and heat-shock protein. From the prediction, 46 out of 60 identified *P. monodon* miRNAs were targeted at 5'UTR, ORF and 3'UTR regions of several immune-related genes. These results implied that these miRNAs might play roles as immune gene regulators in shrimp antiviral response.

Department:	Biochemistry	Student's Signature
Field of Study:	Biochemistry and Molecular Biology	Advisor's Signature
		Co-Advisor's Signature
Academic Year:	2014	Co-Advisor's Signature

ACKNOWLEDGEMENTS

On the completion of my thesis, I would like to appreciate for the excellent supports, guidance, encouragement and supervision throughout my three-year study from my advisor, Assistant Professor Dr. Kunlaya Somboonwiwat, and also from my co-advisors, Professor Dr. Anchalee Tassanakajon and Dr. Kulwadee Somboonwiwat. The great suggestion have become important keys for developing my research outcome.

My appreciation is also to Associate Professor Dr. Vichien Rimpanitchayakit, Assistant Professor Dr. Kuakarun Krusong, Dr. Piti Amparyup, Dr. Premruethai Supungul, and Miss Sureerat Tang for instruction, warm support, interesting discussion and helping. Thankfulness are also extended to all members at Center of Excellence for Molecular Biology and Genomics of Shrimp CEMs laboratory for their helps and for friendships that allow me enjoy throughout my study. Thanks to every friends of mine in the department of Biochemistry.

It is a pleasure to thank Assistant Professor Dr. Rath Pichyangkura, Associate Professor Dr. Teerapong Buaboocha, and Associate Professor Dr. Apinunt Udomkit for giving me your precious time on being my thesis's defense committee and for their valuable comments and also useful suggestions.

I would like to express my greatly gratitude to the The Chulalongkorn University Graduate Scholarship to commemorate the 72nd Anniversary of His Majesty King Bhumibol Adulyadej, The 90th Anniversary of Chulalongkorn University Fund grant, 2011 Overseas Research Grants from The Asahi Glass Foundation and Thailand Research Fund (TRF Research Career Development Grant number RSA5580024) for the fellowship.

Finally, indispensable persons and my gratefulness are my parents and all members in my family for their guidance, understanding, encouragement, endless love, and support along my education.

CONTENTS

	Page
THAI ABSTRACT	iv
ENGLISH ABSTRACT	v
ACKNOWLEDGEMENTS	vi
CONTENTS	vii
CONTENT OF TABLES	xii
CONTENT OF FIGURES	xiii
CHAPTER I INTRODUCTION	1
1.1 General introduction of shrimp aquaculture.....	1
1.2 White spot diseases in shrimp.....	2
1.3 Immune response in shrimp.....	5
1.4 miRNA biogenesis and function.....	8
1.5 miRNA identification technique.....	10
1.6 miRNA expression analysis	13
1.6.1 Northern blot	13
1.6.2 Real-time RT-PCR.....	13
1.6.3 Microarray.....	15
1.7 miRNA target identification.....	15
1.8 Current knowledge on miRNA in shrimp	16
1.9 Purpose of the thesis	17
CHAPTER II MATERIALS AND METHODS.....	18
2.1 Materials.....	18
2.1.1 Equipments.....	18

	Page
2.1.2 Chemicals and Reagents	20
2.1.3 Kits	21
2.1.4 Enzymes	22
2.1.5 Antibiotics.....	22
2.1.6 Bacterial, yeast and virus strains	22
2.1.7 Software.....	22
2.2 Shrimp cultivation.....	22
2.3 WSSV-challenged <i>P. monodon</i>	22
2.4 Hemocyte collection.....	23
2.5 Total RNA and total small RNA preparation.....	23
2.6 RNA quantification by spectrophotometry	24
2.7 Denaturing 15% polyacrylamide gel electrophoresis for RNA analysis.....	25
2.8 Identification miRNA involved in WSSV infection in <i>P. monodon</i>	25
2.8.1 Quality analysis of RNA and DNA by Bioanalyzer.....	25
2.8.2 RNA Quantitation using Quant® 2.0 fluorometer.....	28
2.8.3 cDNA library construction	28
2.8.4 Small RNA library validation	31
2.8.4.1 Qualification of small RNA library by Bioanalyzer	31
2.8.4.2 Small RNA library quantification by real-time PCR.....	31
2.9 Small RNA library sequencing on MiSeq instrument (Illumina).....	31
2.9.1 Sample sheet creation.....	31
2.9.2 Small RNA sequencing.....	32
2.10 Small RNA data analysis	32

	Page
2.10.1 FASTQ format generation by MiSeq reporter software.....	33
2.10.2 Small RNA sequence analysis by CLC Genomics workbench.....	33
2.11 miRNA expression analysis	34
2.11.1 Northern blot analysis	34
2.11.1.1 Probe 3' end labeling with DIG-dUTP	34
2.11.1.2 Electrophoresis and blotting.....	35
2.11.1.3 Hybridization.....	36
2.11.1.4 Immunological detection	36
2.11.2 Stem-loop quantitative RT-PCR.....	36
2.11.2.1 Poly (A)-tailed quantitative RT-PCR of U6	37
2.11.2.1.1 Polyadenylation of total RNA.....	37
2.11.2.1.2 First strand cDNA synthesis of poly-A-tailed RNA	37
2.11.2.1.3 Quantitative RT-PCR of U6	38
2.11.2.2 Stem-loop quantitative RT-PCR of interested-miRNA.....	38
2.11.2.2.1 Stem-loop primer design	38
2.11.2.2.2 cDNA synthesis for Stem-loop specific miRNA	39
2.11.2.2.3 Stem-loop quantitative RT-PCR	39
2.11.2.2.4 Data analysis for quantitative RT-PCR.....	41
2.11.2.3 miRNAs and U6 recombinant plasmid construction	42
2.11.2.3.1 miRNAs and U6 amplification.....	42
2.11.2.3.2 PCR product purification	42
2.11.2.3.3 Ligation of U6 and miRNA to TA vector	42
2.11.2.3.4 Recombinant plasmid transformation.....	43

	Page
2.11.2.3.5 Recombinant plasmid extraction	43
2.11.2.4 Determination of PCR efficiency	43
2.12 miRNA Target prediction.....	44
CHAPTER III RESULTS	46
3.1 Determination of WSSV infectivity in shrimp.....	46
3.2 Total RNA and total small RNA preparation.....	46
3.3 Identification of miRNA involved in WSSV infection in <i>P. monodon</i> by next generation sequencing.....	47
3.3.1 First preparation	48
3.3.1.1 Qualitative analysis of total RNA.....	48
3.3.1.2 Small RNA library preparation and validation	48
3.3.2 Second preparation.....	50
3.3.2.1 Quantitative and qualitative analyses of total small RNA.....	50
3.3.2.2 Small RNA sequencing.....	53
3.3.3 Third preparation	55
3.3.3.1 Small RNA fragment analysis.....	55
3.3.3.2 Small RNA library preparation and validation	56
3.3.3.3 Small RNA sequencing.....	57
3.5 miRNA expression analysis	60
3.5.1 Northern blot analysis	60
3.5.1.1 Determination of labeling probe efficiency	60
3.5.1.2 miRNA expression determined by Northern blot analysis	61
3.5.2 miRNA expression analysis by stem-loop real-time PCR.....	62

	Page
3.6 miRNA target prediction.....	71
CHAPTER IV DISCUSSIONS.....	93
REFERENCES.....	103
APPENDIX.....	123
VITA.....	125



CONTENT OF TABLES

		Page
Table 2. 1	Amount of total RNA and total small RNA for cDNA preparation in NGS.....	29
Table 2. 2	Sequences of specific-miRNA oligonucleotide probe for Northern blot analysis.....	35
Table 2. 3	Primers used for quantitative stem-loop RT-PCR.....	40
Table 3. 1	The number of raw reads and the passed filter (PF) reads of small RNA libraries (2 nd preparation).....	53
Table 3. 2	Nucleotide sequences and length of miRNA homologs (2 nd preparation).....	55
Table 3. 3	The number of raw reads and the passed filter (PF) reads of small RNA libraries (3 rd preparation).....	58
Table 3. 4	Summary of sequences identified from small RNA libraries (3 rd preparation).....	59
Table 3. 5	Nucleotide sequences and length of known miRNAs (3 rd preparation).....	59
Table 3. 6	The PCR efficiency for each amplified miRNA, melting temperature and fold-change of expression upon WSSV infection.....	71
Table 3. 7	miRNA targets of the identified <i>Penaeus monodon</i> miRNAs predicted against <i>P. monodon</i> EST and transcriptome databases.....	73
Table 3. 8	Prediction of miRNA-target mRNA duplex structure using RNAhybrid software.....	76

CONTENT OF FIGURES

	Page
Figure 1. 1 Shrimp production by region	2
Figure 1. 2 Shrimp aquaculture production in major farming nation in Asia.....	2
Figure 1. 3 General structure of the white spot syndrome virus genome and morphology	4
Figure 1. 4 A proposed model of the morphogenesis of WSSV.....	5
Figure 1. 5 A schematic model of the shrimp immune system.....	6
Figure 1. 6 The current model for the biogenesis and post-transcriptional suppression of microRNAs and small interfering RNAs	10
Figure 1. 7 Next generation sequencing on Illumina platform with terminator-based method	12
Figure 2. 1 RNA 6000 nano chip and high sensitivity DNA chip on Agilent 2100 Bioanalyzer	26
Figure 2. 2 Chip priming station for RNA 6000 nano chip and high sensitivity DNA chip	26
Figure 2. 3 Small RNA libraries preparation workflow using TruSeq® small RNA sample preparation kit	29
Figure 2. 4 Small RNA data analysis workflow.....	33
Figure 2. 5 Northern blot transfer cassette on the Trans-Blot® SD (Bio-Rad)	35
Figure 2. 6 miRNA target identification software	45
Figure 3. 1 Analysis of VP28 gene expression in gills of WSSV-infected shrimp at 0, 6 and 48 hours post-injection.....	46
Figure 3. 2 Verification the quality of total RNA and total small RNA extracts by denaturing 15% acrylamide gel.....	47
Figure 3. 3 Analysis of total RNA quality by Bioanalyzer (1 st preparation)	48

Figure 3. 4	Quantitative and quantitative analysis of small RNA libraries by bioanalyzer using Agilent high sensitivity DNA kit (1 st preparation)	49
Figure 3. 5	Quantitative real-time PCR of miHcW0_1 small RNA library (sets 1 and 2).....	50
Figure 3. 6	Analysis of small RNA libraries constructed from total small RNA of WSSV-infected <i>Penaeus monodon</i> hemocyte at 0 and 6 hpi by 6% acrylamide gel electrophoresis.....	51
Figure 3. 7	Quantitative analysis of small RNA libraries using bioanalyzer (2 nd preparation).....	52
Figure 3. 8	Quantitative real time PCR analysis of small RNA libraries (2 nd preparation) prepared from WSSV-infected shrimp hemocyte	52
Figure 3. 9	Size distribution of small RNA libraries after 3' and 5' adapter trimming of small RNA sequencing in the second preparation	54
Figure 3. 10	Total small RNA extracted from WSSV-infected shrimp hemocyte at 0, 6, and 48 hpi by bioanalyzer using Agilent RNA 6000 Nano kit.....	56
Figure 3. 11	Qualitative and quantitative analysis of small RNA libraries after amplification electrophoresed by Agilent high sensitivity DNA kit.....	57
Figure 3. 12	Size distribution of small RNA libraries after 3' and 5' adapter trimming in the third preparation.....	58
Figure 3. 13	Determination of oligonucleotide probe efficiency.....	60
Figure 3. 14	Northern blot analysis of miRNAs in WSSV-infected <i>P. monodon</i>	61
Figure 3. 15	Amplification efficiency curves of reference U6 recombinant plasmid.....	62
Figure 3. 16	Standard curves of miRNAs determined by stem-loop real-time RT-PCR.....	64
Figure 3. 17	The dissociation curves of interested miRNAs	67
Figure 3. 18	Relative expression analysis of miRNAs in response to WSSV infection	68
Figure 4. 1	Predicted interactions between miRNAs and mRNAs involved in shrimp immune responses.....	102

CHAPTER I

INTRODUCTION

1.1 General introduction of shrimp aquaculture

Since 1992, shrimp farming in Thailand had become a multi-billion dollar industry. Thailand was the world's leading exporter and the largest producer of Black (or Giant) Tiger shrimp, *Penaeus monodon*, supplying 20 percent of the world trade in shrimp and prawn (Wyban, 2007). Unfortunately, the production of the black tiger shrimp had rapidly been decreased because the outbreaks of bacterial and viral diseases (Mohan et al., 1998). Due to the serious problems of the black tiger shrimp production loss, Thailand had switched to culture the white shrimp, *Litopenaeus vannamei*.

The *L. vannamei* has several advantages over the *P. monodon* including its rapid growth rate, tolerance of high stocking density, tolerance of low salinities and temperature and high survival during larval rearing. The importation of *L. vannamei* also has disadvantages including its act as a carrier of various viral pathogens such as *Baculovirus penaei*, infectious hypodermal and hematopietic necrosis virus and Taura syndrome virus. These viruses can be transmitted to the penaeid shrimp, *P. monodon*, and increases the spreading of diseases (Overstreet et al., 1997).

The 2014 Global Aquaculture Alliance survey production trends in shrimp farming from Asia/Oceania, Latin America and Africa showed that the world production was fell 13.3 percent in 2013 when compared with that in 2012 (Figure 1.1). Because of the outbreak of the early mortality syndrome (EMS) or Acute hepatopancreatic necrosis disease (AHPND) in shrimp farming, the shrimp production dramatically decreased. Recently, the shrimp production in Thailand has been substantially dropped from 2012 to 2013 about 50 % because the crisis disease, EMS (Figure 1.2).

Due to the disease outbreaks in shrimp farming, the pathogen-resistance *P. monodon* should be developed. Therefore, researches in *P. monodon* must be continued in various fields concerning the shrimp immunity, pathology and physiology.

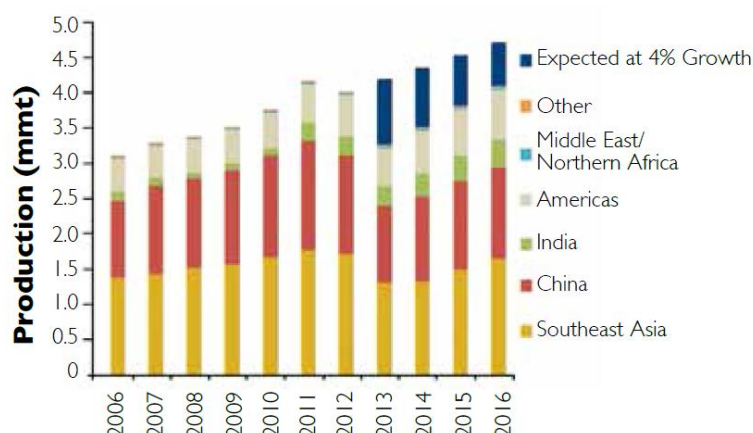


Figure 1. 1 Shrimp production by region (Sources: FAO for 2009-2012 and GOAL survey for 2013-2016)

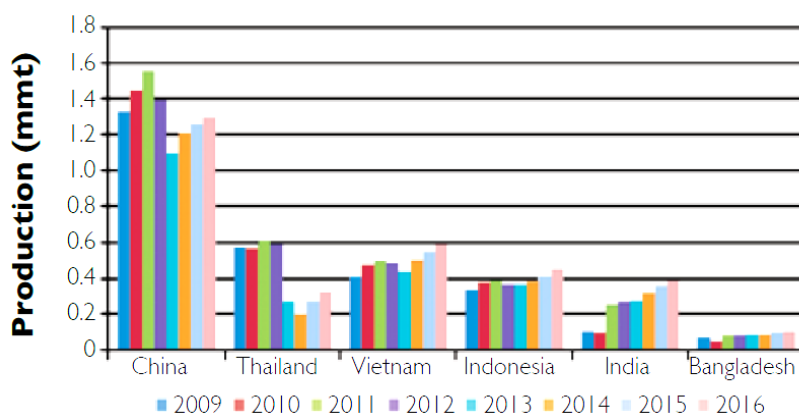


Figure 1. 2 Shrimp aquaculture production in major farming nation in Asia (Sources: FAO for 2009-2012 and GOAL survey for 2013-2016)

1.2 White spot diseases in shrimp

The diseases, especially viral diseases, become serious problems in shrimp industry worldwide. For over decade years, Thailand shrimp farming industry encountered a severe problem from uncontrollable viral diseases. The major viral pathogens, in order with the greatest to the least economic impact, are white spot syndrome virus (WSSV), yellow head virus (YHV), infectious hypodermal and hematopoietic necrosis virus (IHHNV), hepatopancreatic parvo-like virus (HPV) and monodon baculovirus (MBV) (Flegel, 2007). In *P. monodon*, WSSV and YHV caused high mortality (Kiatpathomchai et al., 2004; Mohan et al., 1998; Sithigorngul et al., 2000; Soowannayan et al., 2003; Wongteerasupaya et al., 2003). In this research, we focused only on WSSV.

White spot syndrome (WSS) disease is one of the most important viral diseases, causing severe mortality of the shrimp aquaculture and shrimp farming industry (Chou et al., 1995b; Flegel, 1997; Flegel and Alday-Sanz, 1998; Lightner, 1996). WSSV was first discovered in Taiwan in 1992 (Chou et al., 1995b), the virus has spread rapidly to all shrimp farming countries of the world (Escobedo-Bonilla et al., 2008; Rodriguez et al., 2003). In 1994, WSSV was reported in Thailand (Lo et al., 1996). The clinical signs of WSSV include white spots on the carapace, cuticle over abdomen, display signs of lethargy and reddish coloration of the hepatopancreas (Chou et al., 1995b).

WSSV is the type species of the genus *Whispovirus* in the viral family *Nimaviridae* with double-stranded circular DNA molecule of about 305 kb (Figure 1.3, A) (Chen et al., 2002; van Hulsten et al., 2001a; Yang et al., 2001). Sequence analysis shows that WSSV genome contains between 531 and 684 open reading frames (ORFs). However, 92% of the genetic information of WSSV genome encode functional proteins (van Hulsten et al., 2001a; Yang et al., 2001). About 21-29% of encoded-WSSV proteins were shared identity with other known proteins. These protein involved in nucleic acid metabolism such as DNA polymerase, non-specific nuclease, small and a large subunit of ribonucleotide reductase, thymidine kinase, thymidylate kinase, chimeric thymidine-thymidylate kinase, thymidylate synthase and dUTPase (Chen et al., 2002; Li et al., 2005; Li et al., 2004; Liu and Yang, 2005; Tsai et al., 2000; Witteveldt et al., 2001). Other proteins with other functions include a collagen-like protein, chitinase, kunitz-like proteinase inhibitor and anti-apoptotic protein (Marks, 2005; van Hulsten et al., 2001b; Yang et al., 2001).

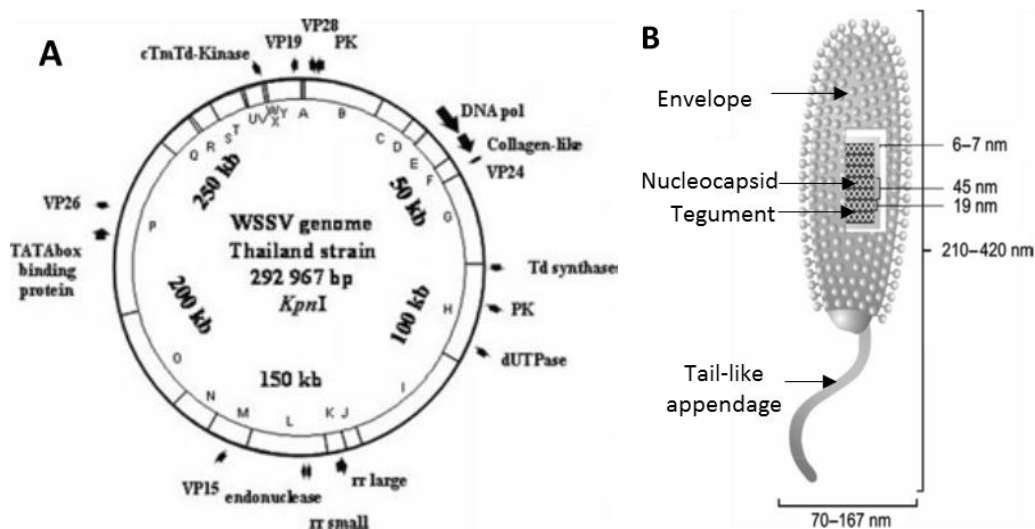


Figure 1. 3 General structure of the white spot syndrome virus genome (A) and morphology (B) (Escobedo-Bonilla et al., 2008)

The morphology of WSSV is a bacilliform with non-occluded enveloped virus (Chou et al., 1995a; Chou et al., 1995b). Intact enveloped virions are between 210 nm and 380 nm in length and 70 -167 nm in maximum width (Flegel and Alday-Sanz, 1998; Park et al., 1998; Rajendran et al., 1999). The structure of intact virion consist of envelope, tegument, nucleocapsid and tail-like appendage (Figure 1.3, B). The viral envelope is 6-7 nm thick and has the structure of an apparently lipidic bilayer membrane. The nucleocapsids, which contain a DNA-protein core bounded by a distinctive capsid layer giving it a cross-hatched appearance, are wrapped singly into an envelope to shape in the virion (Figure 1.3, B) (Durand et al., 1997).

There are six stages of WSSV morphogenesis to development of cellular lesions (Figure 1.4) (Escobedo-Bonilla et al., 2008). At the early stage of cell infection the WSSV particles entry into host cells and show gently hypertrophied nuclei. A viral nucleosome appears before the formation of viral particles. It composes of viral proteins organized in fibrillar fragments. In the nucleus, the fibrillar material induces the formation of circular membranes that are soon filled with viral core material starting viral assembly. The nucleocapsid is completed with 12–14 rings of globular protein units arranged in a stacked series. Each nucleocapsid has one round and one square end. The nucleocapsid becomes completely enclosed by the envelope. The viral particles become ovoid in shape and a long tail-like projection derived from the

envelope is observed. The final phase, the mature virions are elliptical with complete smooth envelopes enclosing an electron-dense nucleocapsid and with a tail-like projection at the last enclosed end.

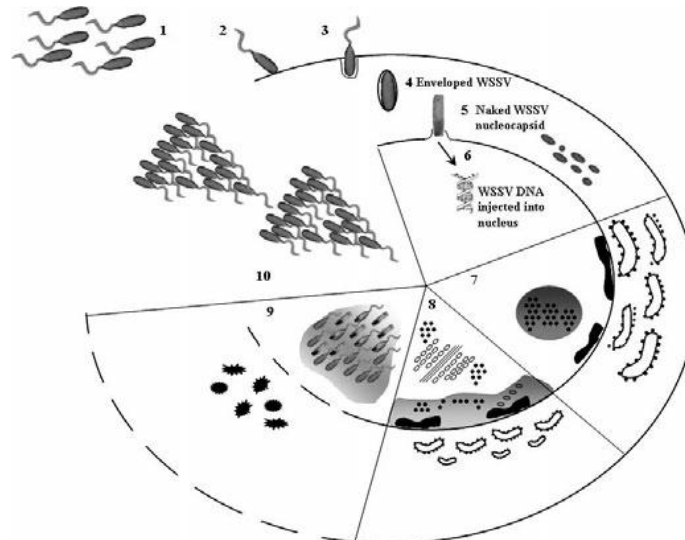


Figure 1. 4 A proposed model of the morphogenesis of WSSV (Escobedo-Bonilla et al., 2008)

1.3 Immune response in shrimp

Shrimp defense system, relies on humoral and cellular innate immune response (Figure 1.5) (Bachère et al., 2004). The humoral responses involve the synthesis and release of several immune proteins including antimicrobial peptides (AMPs), proteinase inhibitors, cytokine-like factor, etc., whereas the cellular immune reactions are phagocytosis, nodulation and encapsulation. The major immune reactions take place in shrimp hemolymph, which contains three different types of hemocytes including hyaline, granular and semigranular hemocytes. The bacteria or fungal cell wall components, such as peptidoglycan (PG), lipopolysaccharides (LPS) and β -glucans (BGs), activate immune molecules which are stored in hemocytes and releases into hemolymph to eliminate the pathogens (Johansson and Soderhall, 1989). Moreover, the hard cuticle covering all external surfaces of crustaceans is the first line of defense between them and the environment.

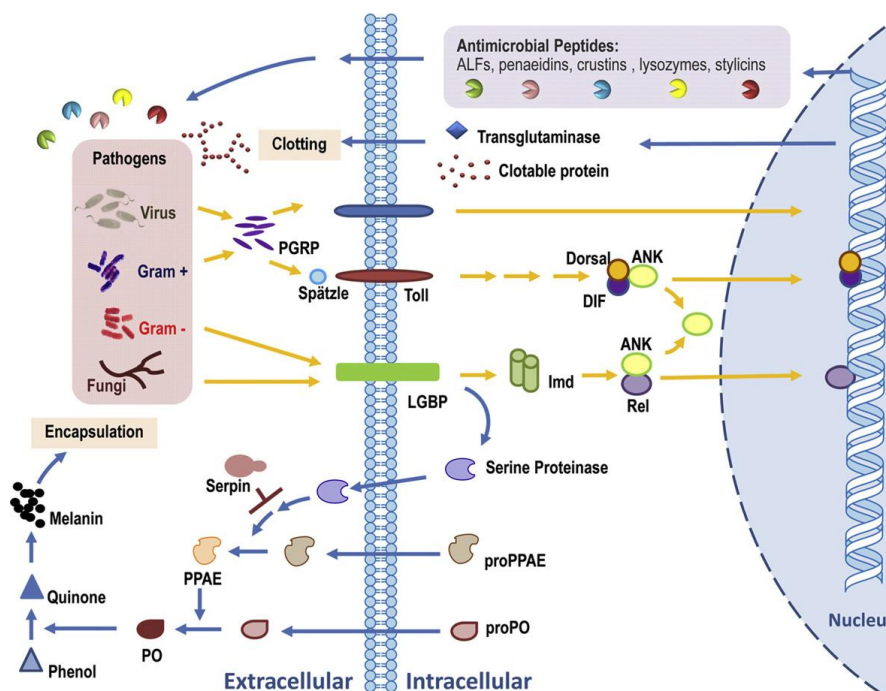


Figure 1. 5 A schematic model of the shrimp immune system. (Tassanakajon et al., 2013)

The exoskeleton of the crustaceans, chitin, is an important barrier against pathogens. However, shrimp was damaged and then breached the protective barrier properties. To prevent the loss of hemolymph upon such injury and the invasion of infected microorganisms, the rapid blood coagulation system at the site of injury is a prominent immune mechanism. The shrimp coagulation relies on the formation of clottable protein polymer by transglutaminase. In shrimp, transglutaminase and clottable proteins have been found in *Penaeus monodon* (Chen et al., 2005b; Cheng et al., 2008; Yeh et al., 1999; Yeh et al., 2006), *Fenneropenaeus chinensis* (Liu et al., 2007), *Marsupenaeus japonicus* (Cheng et al., 2008; Liu et al., 2007) and *Litopenaeus vannamei* (Cheng et al., 2008; Yeh et al., 2009).

Pattern recognition receptors (PRRs), or pattern recognition proteins (PRPs), recognized pathogen associated molecular patterns (PAMPS), such as peptidoglycan, lipopolysaccharides and β -glucans, which was the surface of microorganisms (Medzhitov and Janeway, 2000). The signaling pathways of the immune responses including phagocytosis, nodule formation, encapsulation and synthesis of AMPs, were triggered by different PRRs recognized specific PAMPS (Gillespie et al., 1997; Yu and

Kanost, 2002). Several penaeid shrimps PRRs, including LGBP, BG-binding protein (GBP) and lectin were identified and characterized.

Antimicrobial peptides (AMPs) function as a first line of defense to fight against invading pathogens (Hancock and Diamond, 2000). AMPs are small size biomolecules approximately less than 150-200 amino acid residues and have an amphipathic structure with cationic or anionic properties. AMPs are active against a wide range of microorganisms, such as bacteria, virus, yeast, parasite and fungi (Hancock and Diamond, 2000; Krepstakies et al., 2012). Several families of shrimp AMPs, such as penaeidins, lysozymes, crustins, ALFs and stylicins, have been identified and characterized (Rolland et al., 2010; Tassanakajon et al., 2011).

Proteinases and proteinase inhibitors are ubiquitous in all living organisms and play crucial roles in various biological and physiological processes. Proteinases are key components of the innate immune response of shrimps which function in several proteolytic cascades. Proteinases, such as clip domain serine proteinases (clip-SPs) and their homologs (clip-SPHs), are important in many pathways including apoptosis and melanization (Charoensapsri et al., 2009; Jiang and Kanost, 2000). On the other hand, protease inhibitors regulate the protease cascade in order to prevent excessive activation and consequent damage to host tissue. In penaeid shrimp, three families of serine protease inhibitors; Kazal-type serine proteinase inhibitors (KPIs), serine proteinase inhibitors (SERPINs) and alpha-2-macroglobulins (A2Ms), have been identified and characterized (Cassar and Hunter, 2013; Lin et al., 2007; Rimphanitchayakit and Tassanakajon, 2010).

Melanization is one of important immune defense components of crustaceans. Prophenoloxidase (proPO)-activating system, which is an enzymatic cascade involving several enzymes including the key enzyme, phenoloxidase (PO) (Gorman et al., 2008). The proPO-activating system is initiated whenever PRPs can recognize microbial cell wall components, such as peptidoglycan, lipopolysaccharides and β -glucans. To date several genes associated with *P. monodon* proPO-activating system have been identified and characterized such as clip-SPs, *PmproPO1*, *PmproPO2*, proPO-activating enzymes 1 (*PmPPAE1*) and 2 (*PmPPAE2*) (Amparyup et al., 2009; Charoensapsri et al.,

2009). Also, they have been identified from many shrimp species (Amparyup et al., 2010; Jang et al., 2011; Ren et al., 2009; Vaseeharan et al., 2011).

Apoptosis is a genetically regulated cell death program that eliminate leftover, damaged, or harmful cell (Liu et al., 2009a; Portt et al., 2011). In penaeid shrimps, it has been reported that the shrimp viral pathogens, WSSV and YHV, can induce apoptosis upon infection (Molthathong et al., 2008; Wang et al., 2008). Caspases are the important effector molecules that mediate the apoptotic process (Wang et al., 2008). Inhibitors of apoptotic proteins have also been identified in shrimps, including the defender against apoptotic death 1 (DAD1), controlled tumor protein (TCTP/fortilin) and the inhibitor of apoptosis protein (IAP) (Bangrak et al., 2004; Deveraux and Reed, 1999; Molthathong et al., 2008).

Several conserved signaling pathways are involved in the antiviral immune responses. The essential roles of Toll, Immunodeficiency (IMD) and the Janus kinase-signal transducer and activator of transcription (JAK/STAT) pathways in shrimp immunity have been reported, and the shrimp IMD pathway component was discovered and characterized (Li and Xiang, 2013).

1.4 miRNA biogenesis and function

MicroRNAs (miRNAs) are endogenous approximately 22 nucleotides RNA that can play important regulatory roles in animals and plants by targeting mRNA for cleavage or translational repression. The first miRNAs, lin-4 and let-7, were discovered through genetic screens in *Caenorhabditis elegans* as gene important for developmental timing (Lee et al., 1993; Reinhart et al., 2000). Since their discovery in *C. elegans*, miRNAs have been found across animal and plant species. In many cases the expression patterns and recognition of target mRNAs by specific miRNAs are conserved as well (Bartel, 2009).

The biogenesis of miRNAs is a multiple step process (Figure 1.6). miRNAs are initially transcribed in the cell nucleus from intragenic or intergenic regions by RNA polymerase II to form primary miRNAs (pri-miRNAs) with length of 1-3 kb (Lee et al., 2004). These pri-miRNAs are cleaved in the nucleus by the RNase III enzyme Drosha and a double-stranded RNA-binding protein Pasha into approximately 70-100

nucleotide-long stem-loop structures called precursor miRNAs (pre-miRNAs) (Gregory et al., 2004; Lee et al., 2003). The pre-miRNAs are then transported from the nucleus to the cytoplasm by Exportin-5 (Bohnsack et al., 2004), where the pre-miRNAs are further cleaved into the 18-24 double-stranded oligonucleotides by the RNase-III enzyme Dicer into mature double-stranded miRNA:miRNA* (Hammond et al., 2000).

After strand separation, one of the double strands becomes a mature miRNA molecule, called guide strand, incorporated into RNA-induced silencing complex (RISC), while another passenger strand is often degraded or plays a functional role in the regulation of miRNA homeostasis as well as downstream regulation effect (Bartel, 2009; Suzuki and Miyazono, 2011). The RISC complex functions by perfectly or imperfectly matching with its complementary target mRNA at 3'-untranslated region (3'UTR), and induces target mRNA degradation or translational inhibition or sequestration of mRNA from translational machinery (Liu et al., 2005; Olsen and Ambros, 1999). On the other hand, it has also been reported that the target sequence for miRNA binding were located at 5'UTR (Jopling et al., 2005) or even within coding DNA sequence of mRNAs (Lewis et al., 2003; Ryan et al., 2010; Tay et al., 2008).

Importantly, a single gene can be regulated by multiple miRNAs, and likewise, a single miRNA might have more than one target due to the imperfectly matching between the miRNA and its target. The increasing evidence has indicated that miRNAs play critical regulatory roles in a vast range of biological processes including early development (Brennecke et al., 2003), cellular differentiation (Dostie et al., 2003), proliferation (Wang et al., 2009), apoptosis (Xu et al., 2003), developmental timing (Ambros, 2003), and hematopoiesis (Chen et al., 2004), etc. The percentage of complementarity between miRNA and the target is a major determinant factor distinguishing the miRNA-mRNA interaction mechanism. In case of near-perfect complementarity to the miRNA, target mRNA can be cleaved and degraded. Otherwise, in case of partial complementarity to miRNA, the translation of target mRNA is repressed (Bushati and Cohen, 2007; Hutvagner and Zamore, 2002; Martinez and Tuschl, 2004).

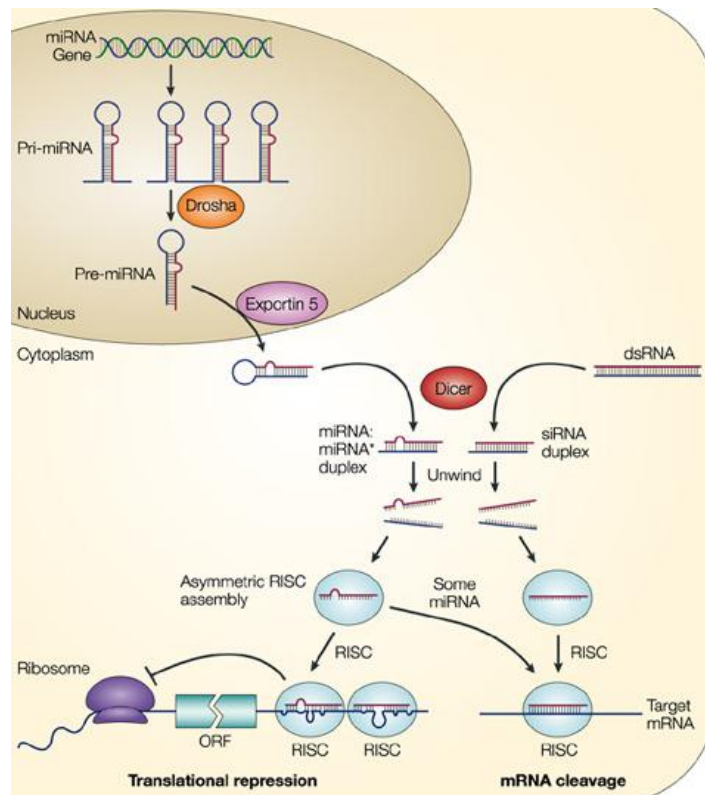


Figure 1. 6 The current model for the biogenesis and post-transcriptional suppression of microRNAs and small interfering RNAs (He and Hannon, 2004)

1.5 miRNA identification technique

The first known miRNAs, *lin-4* and *let-7*, were discovered using forward genetic experiments by isolating mutant genes from an organism showing abnormal phenotypic characteristics (Lee et al., 1993). However, this method is also time consuming and costly for miRNA discovery. Subsequently, miRNA identification was made when directional cloning was used to construct a cDNA library for endogenous small RNAs (Ambros and Lee, 2004). This approach has advantage that it can be applied to any organism but the limitation of low level miRNA expression would be difficult to find.

The next generation sequencing (NGS) technologies (also called deep sequencing), from Illumina/Solexa, ABI/SOLiD, 454/Roche, can detect many small RNAs with high-throughput detection (Friedlander et al., 2008). These technologies produce a number of sequence fragments in the 20–300 bp range by detecting and profiling

known and novel miRNAs (Git et al., 2010). Nowadays. There are three main NGS platforms technologies for miRNAs discovery including Illumina/Solexa (Bentley et al., 2008), ABI/SOLiD (Valouev et al., 2008) and 454/Roche (Petrosino et al., 2009). Because the Illumina/Solexa technology is the most successful and widely-adopted next-generation sequencing platform worldwide, in this study we use this technology to identified miRNA.

The Illumina/Solexa technology support parallel sequencing using reversible terminator-based method that detected a single base as it is incorporated into growing DNA strands (Figure 1.7). A fluorescent-labeled terminator is imaged as each dNTP is added and then cleaved to allow incorporation of the next base. The Illumina/Solexa utilizes a unique “bridged” amplification reaction that occurs on the surface of the flow cell (Olson et al., 2008). In this process, one end of single DNA molecule is attached to a solid surface using an adapter; the molecules subsequently bend over and hybridize to complementary adapters (creating the “bridge”), thereby forming the template for the synthesis of their complementary strands. After the amplification step, flow cell clusters are produced, where the cluster station amplifies DNA on the flow cell surface to create clusters of each molecule. Single-stranded, adapter-ligated fragments are bound to the surface of the flow cell exposed to reagents for polymerase-based extension. The first cycle of sequencing consists first of the incorporation of a single fluorescent nucleotide, followed by high resolution imaging of the entire flow cell. These images represent the data collected for the first base. Any signal above background identifies the physical location of a cluster, and the fluorescent emission identifies which of the four bases was incorporated at that position (Metzker, 2010). So, the major advantage by NGS is the ability to produce an enormous volume of data and in some cases in excess of one billion short reads per instrument run.

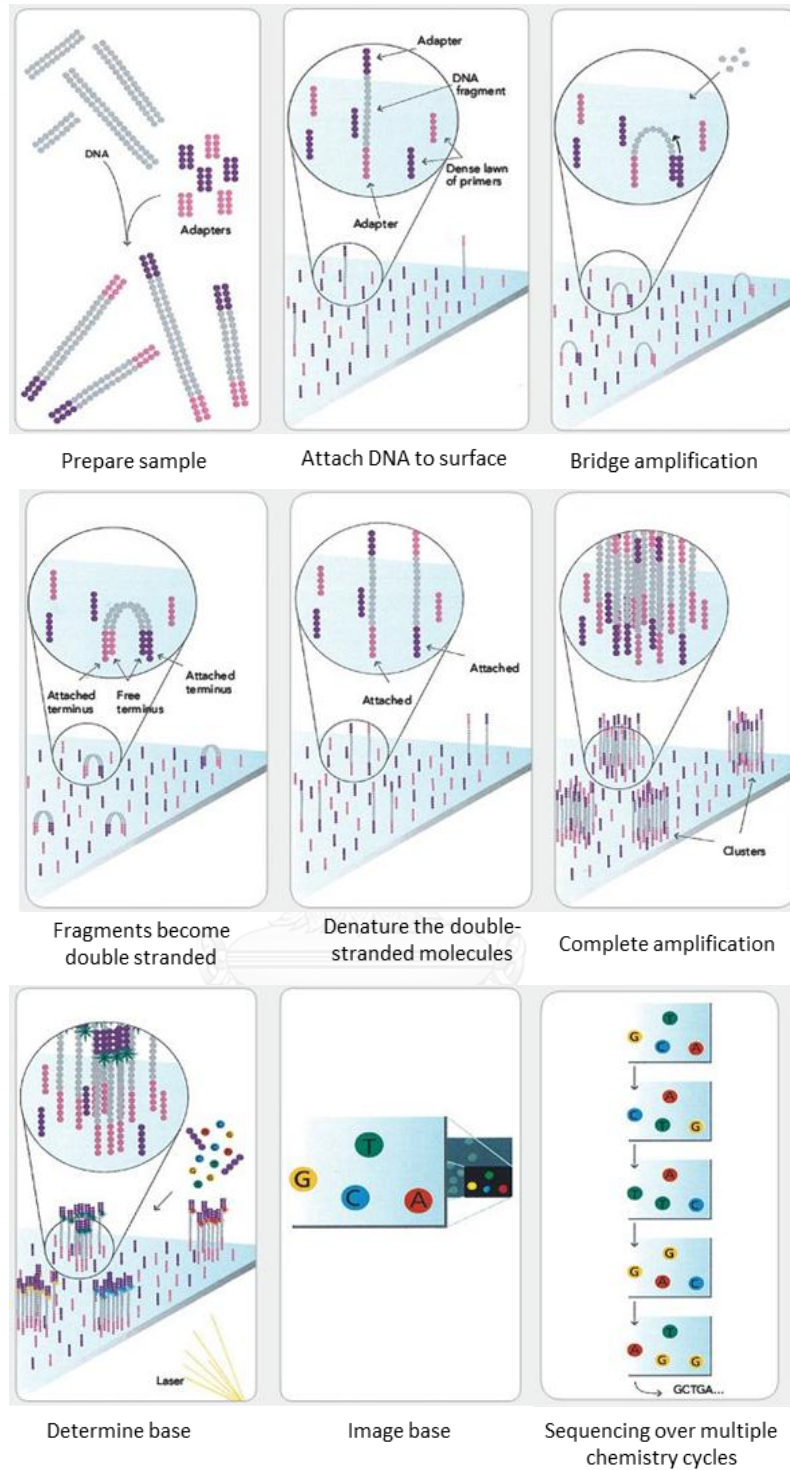


Figure 1.7 Next generation sequencing on Illumina platform with terminator-based method

1.6 miRNA expression analysis

Experimental analysis of miRNA expression is technically challenging because of their small size, sequence similarity among various members, low level, and tissue-specific. There are three main methods for determining and quantifying miRNA expression: Northern blot, real-time RT-PCR and microarray.

1.6.1 Northern blot

Northern blotting is an electrophoretic method for separating RNA molecules by size, shape, and/or electrical charge and individual RNA sequences were detected using radioactive or chemiluminescent-labeled oligonucleotides called probes (Alwine et al., 1977; Kevil et al., 1997; Valoczi et al., 2004). A benefit of Northern blotting is that it allows for not only detection but also determination of miRNA size. However, the Northern blotting method requires a large amount of RNA relative to other measurement methods and stringent hybridization of oligonucleotides to enable detection of molecules as small as miRNAs (Lu et al., 2005). Because of the hybridization limitations, modifications of oligonucleotides, called locked nucleic acid (LNA), have been shown to increase the sensitivity of Northern blotting without decreasing specificity (Valoczi et al., 2004). Nevertheless, because of its limitation, Northern blotting is less frequently used compared to alternative methods for detection and quantification on miRNA.

1.6.2 Real-time RT-PCR

Currently, there are three methods of quantitative PCR for miRNAs quantitation. One of the advantages of the real-time RT-PCR detection is that it can verify miRNAs that are expressed at low levels, but it is limited by high cost. The first method is that primer-extension (PE), real-time PCR method (Raymond et al., 2005). The PE-qPCR assay involved two steps (Figure 1.8, A). In the first step, cDNA was constructed from RNA template using gene specific primer (GSP) to convert the RNA template into cDNA, to add a universal PCR binding site at the end of the cDNA molecule and to extend the length of the cDNA to determine by qPCR. In the second step, the full-length cDNA was quantified by real-time PCR using a combination of LNA miRNA-specific reverse

primer (LNA-R primer) and universal primer. Amplification of cDNA was monitored in the real-time PCR reaction by SYBR green fluorescence.

The second method is to use real-time PCR by specific stem-loop primers for quantifying both the precursor and mature miRNAs (Kramer, 2011; Schmittgen et al., 2008). It included two steps: reverse transcription (RT) and real time PCR (Figure 1.8, B). First, the stem-loop RT primer is hybridized to a miRNA molecule and then reverse transcribed using reverse transcriptase. Next, the RT products are quantified using TaqMan probe or specific-miRNA primer. The assays method was specific for mature miRNAs and discriminated among related miRNAs that differ. Furthermore, they are not affected by genomic DNA contamination.

The third methods is that total RNA is polyadenylated by poly (A) polymerase and then cDNA was synthesized by an poly (T) RT adapter and reverse transcriptase using the 3' end of total RNA as templates (Shi and Chiang, 2005) (Figure 1.8, C). The cDNAs of miRNAs were amplified using miRNA-specific forward primer and reverse primer complementary to poly (T) RT adapter.

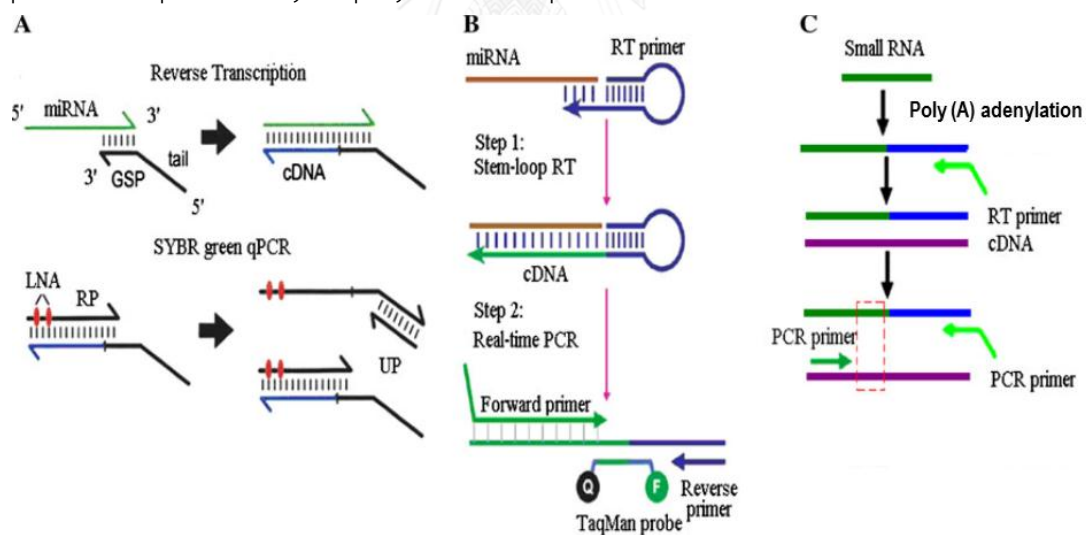


Figure 1.8 Principle of miRNA expression analysis by RT-PCR methods. (A) Primer-extension RT-PCR, (B) stem-loop RT-PCR and (C) poly A-tailed RT-PCR (Huang et al., 2011)

1.6.3 Microarray

MiRNA microarray technology is actually based on nucleic acid hybridization between target molecules and their corresponding complementary probes. First report of miRNA expression profiling by microarray was in human and mouse tissues (Liu et al., 2004). The low molecular weight of total RNA is labeled with radioisotope or fluorescent. The oligonucleotide probes are immobilized onto glass slides through covalent crosslinking forming miRNA microarray. Then, the labeled-small RNA was hybridized with miRNA array, resulting in specific binding of the labeled miRNAs to the corresponding probes. Subsequently, each kind of miRNA and its quantities can be evaluated by analyzing the signal intensity. Because miRNA is small; therefore, optimization of hybridization condition for specific binding is difficult. The recent microarray analysis is more sensitive and specific using miChip platform based on LNA-modified probe (Wang and Wang, 2006).

1.7 miRNA target identification

The best characterized for miRNA-target recognition sequences are seven-nucleotide seed binding sites, which are nucleotide 2 to 8 from the 5' end of the miRNA (Bartel, 2009). Moreover, miRNAs can also effectively repress the expression of their targets through "G-bulged sites", which include a G-bulge at position 5-6 of the seed-complementary region (Chi et al., 2012). Finding regulatory targets for plant miRNAs is relatively easy because they show nearly perfect complementarity to target mRNAs. In contrast, the computational prediction of miRNA target genes in animals is very difficult, mainly because of the lack of known miRNA target genes and their specificity target sites (Enright et al., 2003).

However, there are certain characteristics of the interaction between miRNAs and target genes that are commonly used by current algorithms: (i) the complementarity between miRNAs and target sites, (ii) the conservation of miRNA target genes among different species, (iii) the thermal stability of miRNA/mRNA duplex, (iv) no complicated secondary structure at miRNA target sites, (v) the ability of miRNA 5' end to bind to the target gene stronger than that of the 3' end. During the last decade, several bioinformatic tools have been developed to predict miRNA targets

such as miRanda, TargetScan, RNAhybrid, DIANA-microT, Pictar and rna22 (Alexiou et al., 2009; Witkos et al., 2011).

miRanda was the first bioinformatic software for prediction miRNA target genes (Enright et al., 2003). miRanda screened 3'UTRs, mainly based on sequence matching, miRNA and mRNA duplex thermal stability and conservation of the target site. TargetScan software predicts mammalian miRNA target genes based on the thermodynamic model of RNA interaction and sequence alignment analysis to predict conserved miRNA binding sites among different species (Lewis et al., 2003). Another software, RNAhybrid was developed based on analyzing the secondary structure of the miRNA/mRNA duplex (Rehmsmeier et al., 2004). This software can quickly and accurately calculate the hybridization free energy of small RNA fragment hybridized to large RNA fragment.

1.8 Current knowledge on miRNA in shrimp

In 2011, miRNAs were firstly discovered in hemocyte of shrimp, *M. japonicus* by sequencing small RNA recombinant plasmids. Thirty-five miRNAs including 15 miRNAs exhibited high homology to the known miRNA from other arthropods and other novel miRNAs were identified. Moreover, expression of 22 miRNAs were determined upon WSSV infection (Ruan et al., 2011). Small RNA of WSSV-infected shrimp at different time post-infection (0, 6, 24 and 48 h) were identified by next generation sequencing. From 63 host miRNAs identified, 48 of which were conserved in other animals representing 43 distinct miRNAs. Northern blot analysis identified 31 differentially expressed miRNAs. In response to virus infection, 25 of them were up-regulated and 6 of them were down-regulated. The TargetScan and miRanda algorithms were used to analyzed target genes of these differentially expressed miRNAs and immune-related genes were predicted as their miRNA targets (Huang et al., 2012).

The phagocytosis, apoptosis and phenoloxidase, are key immune reactions of shrimp immunity. Following activation or inhibition of these reactions in *M. japonicus*, the small RNA were sequenced and 24 miRNAs were seem to take great effects on phagocytosis, apoptosis or the pro-phenoloxidase system. The changes in expression level of these miRNAs were confirmed by Northern blots. Among the 24 innate

immunity-associated miRNAs, 21 miRNAs were conserved in animals, suggesting that these miRNAs might share the similar or the same functions when compared with other species. From degradome sequencing and prediction of target genes, miRNAs might regulated different target genes that involved in phagocytosis, apoptosis or prophenoloxidase system (Yang et al., 2012).

Upon infection, host expressed miRNAs for regulating the expression of host and viral genes to promote host antiviral responses, likewise, viruses generate microRNAs (miRNAs) to control the expression of host and viral genes to facilitate the infection. Recently, the viral miRNAs from white spot syndrome virus (WSSV) were characterized in *M. japonicus* in vivo. From small RNA sequencing, total of 89 putative WSSV miRNAs were identified. As revealed by miRNA microarray analysis and Northern blotting, the expression of viral miRNAs was tissue specific. The results showed that viral miRNA WSSV-miR-N24 could target the shrimp caspase 8 gene, and this miRNA repressed the apoptosis of shrimp hemocytes in vivo. As a result, the number of WSSV copies in shrimp was significantly increased as compared with the control (Huang et al., 2014).

1.9 Purpose of the thesis

In order to gain more insight into miRNA that involve in antiviral mechanisms in crustaceans, we applied small RNA sequencing using next generation sequencing to identify miRNAs in the hemocytes of WSSV-challenged *P. monodon* at the early and late phases of the infection. Moreover, miRNA expression profile that response to WSSV infection in *P. monodon* hemocyte was analyzed by Northern blot and stem-loop real-time RT-PCR. Immune-related target genes of miRNAs were predicted using in-house software using *P. monodon* EST database as a reference database and secondary structure with the thermal stability of miRNA/mRNA duplex was predicted using RNAhybrid software.

CHAPTER II

MATERIALS AND METHODS

2.1 Materials

2.1.1 Equipments

-20°C Freezer (Whirlpool)
2100 Bioanalyzer (Agilent Technologies)
-80°C Freezer (Thermo Electron Corporation)
96-well cell culture cluster, flat bottom with lid (Costar)
ÄKTA Prime Plus FPLC Purification System (GE Healthcare)
Autoclave model # MLS-3750 (SANYO E&E Europe (UK Branch) (UK Co.)
Automatic micropipette P10, P20, P100, P200 and P1000 (Gilson Medical Electrical)
Avanti J-30I high performance centrifuge (Beckman coulter)
Balance PB303-s (Mettler Teledo)
Biophotometer (Eppendorf)
C1000™ Thermal Cycler (Bio-Rad)
Centrifuge 5804R (Eppendorf)
Centrifuge Avanti™ J-301 (Beckman Coulter)
Centrivap Concentrator (LABCONCO)
Force mini centrifuge (Select BioProducts)
Gel Documentation System (GeneCam FLEX1, Syngene)
GelMate2000 (Toyobo)
Gene pulser (Bio-Rad)
Incubator 30°C (Heraeus)
Incubator 37°C (Memmert)
Innova 4080 incubator shaker (New Brunswick Scientific)
Laminar Airflow Biological Safety Cabinets ClassII Model NU-440-400E (NuAire, Inc., USA)
Maxtaform™ Grids, 75 mesh, 3.05mm O.D., Copper (Spi supplies)

Maxtaform™ Grids, 75 mesh, 3.05mm O.D., Nickel (Ted pella)
Microcentrifuge tube 0.6 ml and 1.5 ml (Axygen®Scientific, USA)
MicroPulser™ electroporator (Bio-Rad)
Minicentrifuge (Costar, USA)
Mini-PROTEAN® 3 Cell (Bio-Rad)
Minipulser electroporation system (Bio-Rad)
MiSeq sequencer (Illumina)
MS 3 vortex mixer (IKA)
NanoDrop 2000 UV-Vis Spectrophotometer (Thermo scientific)
Nipro disposable syringes (Nissho)
Optima™L-100 XP Ultracentrifuge (Beckman Coulter)
Orbital shaker SO3 (Stuart Scientific, Great Britain)
PCR Mastercycler (Eppendorf AG, Germany)
PCR thin wall microcentrifuge tubes 0.2 ml (Axygen®Scientific, USA)
PD-10 column (GE Healthcare)
pH-meter pH 900 (Precisa, USA)
Pipette tips 10, 100 and 1000 µl (Axygen®Scientific, USA)
Power supply, Power PAC3000 (Bio-Rad Laboratories, USA)
Quant® 2.0 fluorometer (Life technologies)
Refrigerated incubator shaker (New Brunswick Scientific, USA)
Refrigerated microcentrifuge MIKRO 22R (Hettich Zentrifugen, Germany)
Sonicator (Bandelin Sonoplus, Germany)
SpectraMax M5 Multi-Mode Microplate Reader (Molecular Devices)
Touch mixer Model#232 (Fisher Scientific)
Trans-Blot®SD (Bio-Rad Laboratories)
Transmission electron microscope (Hitachi - Science & Technology – H 7650)
Tri-sodium citrate (Sigma)
Water bath (Mettler)
Whatman® 3 MM Chromatography paper (Whatman International Ltd., England)

2.1.2 Chemicals and Reagents

100 mM dATP, dCTP, dGTP and dTTP (Promega)

Absolute alcohol, C₂H₅OH (Hayman)

Acid-phenol: Chloroform (Ambion, Life technologies)

Acrylamide, C₃H₅NO (Merck)

Agar powder, Bacteriological (Hi-media)

Agarose, low EEO, Molecular Biology Grade (Research Organics)

Amersham™ Hybond™ Blotting Membranes (GE Healthcare)

Ammonium persulfate, (NH₄)₂S₂O₈ (Bio-Rad)

Anti-digoxigenin-AP (Roche)

Blocking reagent (Roche)

Boric acid, BH₃O₃ (Merck)

Bromophenol blue (Merck)

Chloroform, CHCl₃ (Merck)

CL-XPosure™ Film (5×7 inches) (Thermo scientific)

CSPD (Roche)

Developer solution (Kodak Scientific)

Diethyl pyrocarbonate (DEPC), C₆H₁₀O₅ (Sigma)

DIG Easy Hyb buffer (Roche)

Dithiothreitol, DTT (Life technologies)

Ethidium bromide (Sigma)

Ethylene diamine tetraacetic acid disodium salt, EDTA (Ajax)

Fixer solution (Kodak Scientific)

GeneRuler™ 100bp DNA ladder (Fermentas)

GeneRuler™ 1kb DNA ladder (Fermentas)

Glycerol, C₃H₈O₃ (Ajax)

Glycine, USP Grade, NH₂CH₂COOH (Research organics)

Glycogen (Amresco)

Hydrochloric acid, HCl (Merck)

Isopropanol, C₃H₇OH (Merck)

Isopropyl- β -D-thiogalactoside (IPTG), $C_9H_{18}O_5S$ (USBiological)
 Maleic acid, $C_4H_4O_4$ (Ajax)
 miRNA marker (New England Biolabs)
 N, N, N', N'-tetramethylethylenediamine (TEMED) (BDH)
 N, N'-methylenebisacrylamide, $C_7H_{10}N_2O_2$ (USB)
 Novex® TBE Gels, 6%, 10 well (Life technologies)
 PhiX control library (Illumina)
 RNase inhibitor (New England Biolabs)
 Sodium acetate, CH_3COONa (Carlo Erba)
 Sodium chloride, NaCl (Ajax)
 Sodium citrate, $Na_3C_6H_5O_7$ (Carlo Erba)
 Sodium dodecyl sulfate, $C_{12}H_{25}O_4SNa$ (Vivantis)
 Sodium hydroxide, NaOH (Merck)
 TriReagent® (Molecular Research Center)
 Tris-(hydroxyl methyl)-aminomethane, $NH_2C(CH_2OH)_3$ (Vivantis)
 Tryptone type I (HIMEDIA)
 Tween™-20 (Fluka)
 Urea (Affy Metrix USB)
 Yeast extract powder (HIMEDIA)

2.1.3 Kits

DIG Oligonucleotide 3'-End Labeling Kit, 2nd generation (Roche)
 High Sensitivity DNA kit (Agilent)
 High-speed plasmid mini kit (Geneaid)
 Kapa library quantification kit (Kapa Bioscience)
 mirVana™ miRNA Isolation Kit (Ambion, Life technologies)
 MiSeq® Reagent Kit v3 (Illumina)
 Nucleospin® Extract II kit (Macherey-Nagel)
 Quant-iT™ RNA assay kit (Life technologies)
 RBC TA cloning vector (RBC Bioscience)
 RNA 6000 Nano kit (Agilent)

TruSeq® small RNA sample preparation kit (Illumina)

2.1.4 Enzymes

Poly-A-polymerase (New England Biolabs)

RiboLock RNase Inhibitor (Thermo scientific)

SsoFast EvaGreen Supermix (Bio-Rad)

SuperScript II reverse transcriptase (Invitrogen)

SuperScript III reverse transcriptase (Invitrogen)

T4 RNA ligase 2 deletion mutant (Epicentre)

Taq DNA polymerase (RBC Bioscience)

2.1.5 Antibiotics

Ampicillin (BioBasic)

2.1.6 Bacterial, yeast and virus strains

Escherichia coli strain XL-1-Blue

White spot syndrome virus (WSSV)

2.1.7 Software

Bio-Rad CFX Manager (Bio-Rad)

CLC Genomics Workbench (Qiagen)

MiSeq Reporter (Illumina)

2.2 Shrimp cultivation

The healthy black tiger shrimp (*Penaeus monodon*) size of about 15-20 grams body weight were purchased from farms. The black tiger shrimp were cultured in 3 groups of 20 individual per tank. Before the experiments, the shrimp were acclimatized in 15 ppt salinity, 28±4°C for at least one week.

2.3 WSSV-challenged *P. monodon*

The black tiger shrimp were injected at abdominal muscle with white spot syndrome virus (WSSV) with the dosage that causes 100% shrimp death within three days. WSSV stock was diluted for 10⁷ fold and 50 µl of diluted-WSSV was injected into shrimp. Hemolymph was collected at 0, 6 and 48 hours post-WSSV infection (hpi). The WSSV-infected shrimp and uninfected shrimp was checked for WSSV infection by

RT-PCR. A piece of gills collected from uninfected and WSSV-infected shrimp was homogenized in 200 μ l of lysis buffer (50 mM NaOH and 0.025% (w/v) SDS), heated at 100°C for 5 minutes and then chilled on ice for 2-3 minutes. The supernatant of gill lysate collected after centrifugation at 10,000 x g for 5 minutes at 4°C. Gill lysate was diluted (1:10) in sterile water and used as a template for PCR. The WSSV gene, VP28, was amplified using a forward primer: 5'-ATGCCATGCTATTTATTGTGATT-3' and a reverse primer: 5'-TAGCGGATCCCTCGGTCTCAGTGC-3'. The expected size of PCR product was 600 bp. The condition was pre-denatures at 94°C for 1 minute followed by 35 cycles of denaturation at 94°C for 30 seconds, annealing at 60°C for 30 seconds and extension at 72°C for 30 seconds, and final extension at 72°C for 7-10 minutes.

2.4 Hemocyte collection

Shrimp hemolymph was collected from the ventral sinus using 24G/1/2 inch needle fitted into a 1.0 ml syringe pre-loaded with 200 μ l of the cold anticoagulant (10% (w/v) trisodium citrate). The hemolymph was immediately centrifuged at 800 x g for 10 minutes at 4°C to separate the hemocyte. The hemocyte pellet was instantly frozen in the liquid nitrogen (N₂) until use.

2.5 Total RNA and total small RNA preparation

The hemocyte was collected at 0, 6 and 48 hours post WSSV-infected shrimp as described in the section 2.4. Total small RNA was isolated from hemocyte using mirVana™ miRNA Isolation Kit (Ambion, Life technologies). The hemocyte was removed from liquid nitrogen and Lysis/Binding Buffer was immediately added to least 1:10 ratio (w/v, add 1 ml Lysis/Binding Buffer for 0.1 g hemocyte). The hemocyte was immediately homogenized. After that 1/10 volume of the miRNA homogenate additive was added to hemocyte homogenate and mixed well by inversion for several times and kept on ice for 10 minutes. Then organic extraction was performed by adding an equal volume of acid-phenol: Chloroform to the homogenate followed by 1/10 volume of the miRNA homogenate additive and the mixture was vigorously shaken for 30-60 seconds. The mixture was centrifuged at 13,500 x g for 5 minutes at room temperature to separate the aqueous and organic phases. After centrifugation, the

upper aqueous phase was transferred to a fresh 1.5 ml microcentrifuge tube without disturbing the lower organic phase.

For total small RNA extraction, 1/3 volume of absolute ethanol was added to the aqueous phase and mixed thoroughly by inversion for several times. The lysate/ethanol mixture was applied to a filter cartridge and centrifuged at 10,000 x g for 15 seconds. After centrifugation, 2/3 volume of absolute ethanol was added to the filtrate (266 μ l absolute ethanol for 400 μ l filtrate) and mixed thoroughly by inversion. On the other hand, for total RNA extraction, 1.25 volumes of absolute ethanol was added to aqueous phase instead 1/3 volume of absolute ethanol and mixed by inversion.

Both of total small RNA and total RNA from previous step, 700 μ l of filtrate/ethanol mixture was passed through the new filter cartridge by centrifugation at 10,000 x g for 15 seconds. The flow-through was discarded. Then 700 μ l of miRNA wash solution 1 was added centrifuged at 10,000 x g for 10 seconds and flow-through was discarded. The filter was washed twice with 500 μ l of wash solution 2/3 and discarded flow-through. The residual fluid was removed from the filter by centrifugation at 10,000 x g for 1 minute. The filter cartridge was placed into a fresh collection tube. Then 50 μ l of pre-heated (95°C) elution solution was applied to the center of the filter and centrifuged at 10,000 x g for 1 minute. The eluate was applied again to the filter to maximize RNA recovery and then stored at -80°C until use. The quality and quantity of RNA were determined by spectrophotometric method (section 2.6).

2.6 RNA quantification by spectrophotometry

Total small RNA or total RNA concentration was determined by spectrophotometer. The spectrophotometer was read at 260 nm and 280 nm. The A_{260}/A_{280} ratio of 1.8-2.1 showed the high purity of RNA. The RNA concentration was calculated using the following equation:

$$C \text{ (mol/l)} = A_{260} (\epsilon \times l)$$

$$C \text{ (}\mu\text{l/ml)} = [A_{260} / (\epsilon \times l)] \times M \times 1000 = [(1000 \times M) / (\epsilon \times l)] \times A_{260}$$

Where: ϵ = extinction coefficient ($\text{L} \times \text{mol}^{-1} \times \text{cm}^{-1}$)

l = path length (cm): path length of modern spectrophotometers 1 cm

M = molecular weight (g/mol)

C = concentration ($\mu\text{l/ml}$)

For short nucleic acids (<200 nt), $(1000 \times M) / (\epsilon \times l) \sim 33$, the approximate concentration can be determined with the following formula:

Small RNA <200 nucleotide: $C (\mu\text{g/ml}) \sim 33 \times A_{260}$

Total RNA: $C (\mu\text{g/ml}) \sim 40 \times A_{260}$

2.7 Denaturing 15% polyacrylamide gel electrophoresis for RNA analysis

A denaturing 15% polyacrylamide gel with 8 M Urea was prepared. The 7.5 ml of acrylamide solution was prepared by dissolving 3.6 grams of urea in 750 μl of 10x TBE and 3.75 ml of 30% acrylamide/bis-acrylamide solution, the volume was adjusted to 7.5 ml with nuclease-free water and heated at 60°C to dissolve urea. The 75 μl of 10% APS and 4 μl of TEMED were added and the gel was immediately poured.

One microgram of total small RNA in DEPC-water was mixed with an equal volume of 2x RNA loading dye and heated for 20 minutes at 60 °C. Then the mixture was immediately placed on ice for at least 2 minutes. The denaturing 15% polyacrylamide gel was pre-electrophoresed at 100 volt for 10 minutes. Subsequently, the sample was loaded onto the gel and electrophoresed at 50 volts for 30 minutes then switched to 150 volts for 1.30 hours or until the dye front migrated to the bottom of the gel. Then the gel was stained with 0.5-1 $\mu\text{l/ml}$ ethidium bromide solution and RNA bands were visualized the RNA using UV transilluminator.

2.8 Identification miRNA involved in WSSV infection in *P. monodon*

2.8.1 Quality analysis of RNA and DNA by Bioanalyzer

In this experiment Agilent 2100 Bioanalyzer was used to analyze the quality as well as quantity of nucleic acid. For RNA fragment analysis, Agilent RNA 6000 Nano kit (Figure 2.1, A) was used to assess the RNA quality. First, the chip priming station (Figure 2.2, A) was set up. The fresh syringe was screwed into the chip priming station and the luer lock adapter was locked to the syringe. Then the base plate was adjusted to the C position. The syringe clip was released up to the top position.

The quality of the small RNA library was analyzed by Agilent High Sensitivity DNA kit (Figure 2.1, B). For this analysis, the expected size of small RNA library is 150 nucleotides. The size of the sample was used to determine whether it was small RNA library or the contaminated adapter. First, the chip priming station (Figure 2.2, B) was set up. The fresh syringe was screwed into the chip priming station and the luer lock adapter was locked to the syringe. Then the base plate was adjusted to the C position. The syringe clip was released up to the lowest position



Figure 2. 1 RNA 6000 nano chip (A) and high sensitivity DNA chip (B) on Agilent 2100 Bioanalyzer.

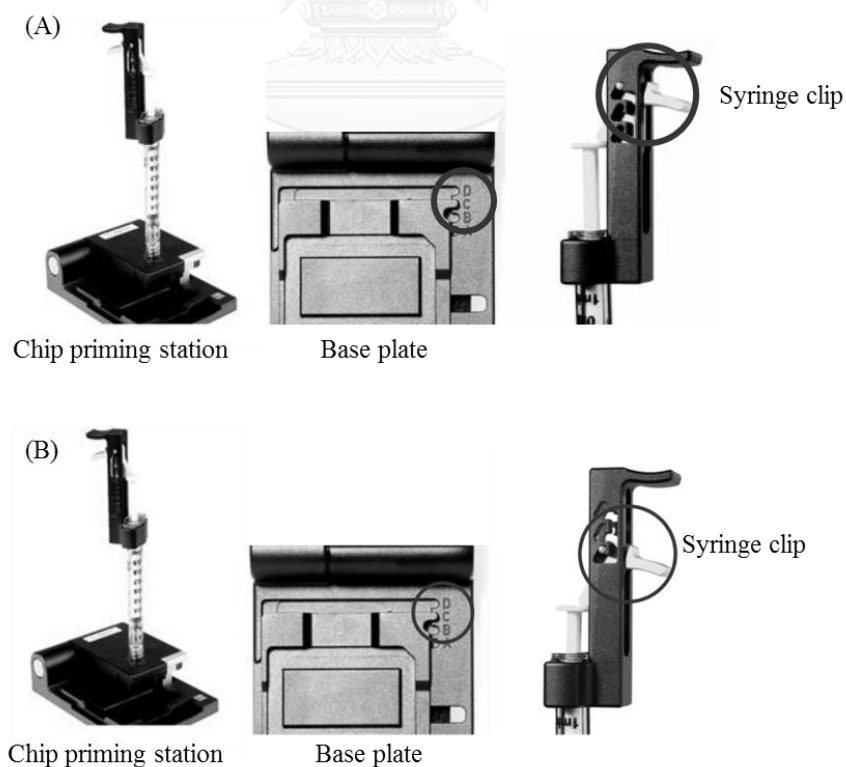


Figure 2. 2 Chip priming station for RNA 6000 nano chip (A) and high sensitivity DNA chip (B)

For small RNA analysis, the gel for Agilent RNA 6000 Nano kit was prepared by equilibration at room temperature for 30 minutes before use. Then 550 μl of Agilent RNA 6000 Nano gel matrix was passed through the filter in a microcentrifuge for 10 minutes at 1500 x g and stored at 4°C. The gel-dye mix prepared was used within one day. The 65 μl of filtered gel was mixed with 1 μl of RNA 6000 Nano dye and stored in the dark until use. After that, the new RNA Nano chip was placed on the chip priming station. The 9.0 μl gel-dye mixture were added into the bottom of the G well. The plunger of the syringe was pressed down for 30 seconds and released to the 1ml position. Then 9.0 μl of the gel-dye mixture were loaded into two G-labeled wells.

The RNA 6000 Nano marker 5 μl was loaded into the marked-well with the ladder symbol and each of the 12 sample wells. The samples and RNA ladder were heated at 70°C for 2 minutes and placed on ice immediately to minimize the secondary structure. Then 1 μl of the RNA ladder and each sample were pipetted into the well which marked with the ladder symbol and 12 sample wells, respectively. After that, RNA Nano chip loaded with ladder and RNA samples was shaken on the IKA vortex mixer for 60 seconds at 2,400 rpm. Finally, the RNA Nano chip was placed into the receptacle of Agilent 2100 Bioanalyzer and then started the analysis. Each RNA chip contained an interconnected set of microchannels that was used for separation of nucleic acid fragments based on their size as passed through it electrophoretically. The electrophoregram obtained was used for size and concentration determination.

The gel for Agilent High Sensitivity DNA reagents were prepared by equilibration at room temperature for 30 minutes before use. The gel-dye mix prepared was used within six weeks. The 15 μl of high sensitivity DNA dye was pipetted into high sensitivity DNA gel matrix and stored in the dark. The gel-dye mix was transferred to the top of spin filter and centrifuged at 2,240 x g for 10 minutes at room temperature. After that, the new high sensitivity DNA chip was placed on the chip priming station. The gel-dye mixed (9.0 μl) was added into the bottom of the G well. The plunger of the syringe was pressed down for 60 seconds and released to the 1ml position. Then 9.0 μl of the gel-dye mix was loaded into another three G-labeled wells.

The high sensitivity DNA marker, DNA ladder and samples were loaded into the well as same as RNA Nano chip. After that, high sensitivity DNA chip with loaded ladder

and DNA sample was shaken on the IKA vortex mixer for 60 seconds at 2,000 rpm. Finally, the high sensitivity DNA chip was analyzed by Agilent 2100 Bioanalyzer. The sample peaks should be appeared between the lower and upper markers.

From cDNA preparation of NGS for identify miRNA, the data obtained as a chromatogram of the electrophoretic profile. The distance was used to determined size of DNA as composed with that of ladder. The peak area determined amount of DNA in the gel.

2.8.2 RNA Quantitation using Quant® 2.0 fluorometer

Total RNA extracted from WSSV-infected shrimp hemocyte at 0, 6 and 48 hours was also quantified by Quant-iT™ RNA assay kit. The Quant® 2.0 fluorometer was calibrated with two RNA standards including 0 ng/μl and 10 ng/μl of *E.coli* rRNA standard. Quant-iT™ working solution was prepared by diluting Quant-iT™ reagent 1:200 in Quant-iT™ buffer. The 10 μl of two standards RNA and 1-20 μl of sample RNA was separately added into 190 μl of Quant-iT™ working solution. And then, the mixture was mixed by vortex for 2-3 seconds and incubated at room temperature for 2 minutes. The mixture-tubes were read in Qubit™ fluorometer on RNA concentration determination program. The concentration of RNA was expressed in μg/ml unit.

2.8.3 cDNA library construction

In order to perform next generation sequencing (NGS) of small RNA, cDNA libraries of small RNA from WSSV-infected hemocyte at 0, 6 and 48 hours were constructed using TruSeq® small RNA sample preparation kit following 3' and 5' adapter ligation, reverse transcription, PCR amplification and gel purification (Figure 2.3). Each small RNA library was separated by index sequence in the PCR amplification step. Because the optimum condition for NGS has not open established, various amount of total RNA or purified small RNA in a total volume of 5 μl was used (Table 2.1). The 3' adapter ligation was performed by mix 1 μl of RNA 3' Adapter (RA3) and 5 μl of total RNA or total small RNA in a pre-cooled nuclease-free 200 μl PCR tube. Then the reaction was incubated on the thermal cycler at 70°C for 2 minutes and immediately placed on ice. The master mix of 3' adapter ligation contained 2 μl of ligation buffer (HML), 1 μl of RNase inhibitor and 1 μl of T4 RNA ligase 2 deletion mutant

(Epicentre). Then 4 μl of master mix was added into the reaction tube and incubated at 28°C for 15 minutes. After that, 5' adapter was prepared, pre-heating 1.1 μl of RNA 5' Adapter (RA5) at 70°C for 2 minutes and then chilled on ice immediately and 1.1 μl of 10 mM ATP and 1.1 μl of T4 RNA Ligase were added into heated-RNA 5' adapter. To ligate 5' adapter to small RNA, mixture of RNA 5' adapter (3 μl) was added to 3' adapter ligation reaction and incubated at 28°C for 1 hour. The 5' and 3' adapter-ligated RNA was stored at -80°C.

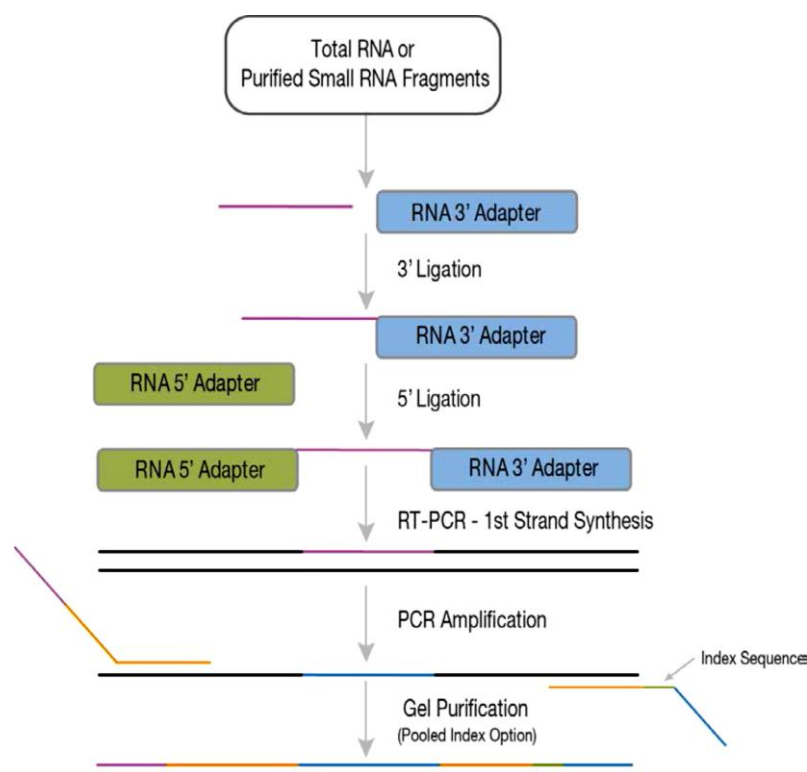


Figure 2. 3 Small RNA libraries preparation workflow using TruSeq® small RNA sample preparation kit

Table 2. 1 Amount of total RNA and total small RNA for cDNA preparation in NGS

No	RNA Type	Amount RNA (μg)
First trial	Total RNA	1
Second trial	Total small RNA	0.12
Third trial	Total small RNA	1

The reverse transcription was performed by mixing 6 μl of 5' and 3' adapter-ligated RNA with 1 μl of RNA RT primer, incubated at 70°C for 2 minutes, and placed on ice immediately. The reverse transcription reaction contained of 2 μl of

5X first strand buffer, 0.5 μ l of 12.5 mM dNTP mix, 1 μ l of 100 mM DTT, 1 μ l of RNase inhibitor and 1 μ l of SuperScript II reverse transcriptase. Then, the reaction was incubated at 50°C for 1 hour.

In this step the cDNA library was amplified by PCR in order to increase the copy number of cDNA library to the appropriate amount as well as to indexing each library with a specific PCR primer (RIPX). RIPX has unique sequences that help discriminating sample in the pooled cDNA libraries.

Each cDNA library was amplified by PCR. The PCR master mix (37.5 μ l) containing 8.5 μ l of ultrapure water, 25 μ l of PCR mix (PML), 2 μ l of RNA PCR primer (RP1) and 2 μ l of RNA PCR primer (RPIX) was added the above to transcription reaction. The PCR conditions were set on the thermal cycler accordingly: pre-heat lid to 100°C, 98°C for 30 seconds, 15 cycles of 98°C for 10 seconds, 60°C for 30 seconds and 72°C for 15 seconds, 72°C for 10 minutes and 4°C hold. The amplified cDNA libraries were stored at -20°C until use.

To purify cDNA of the corresponding mature miRNA, the PCR product was separated through 6% polyacrylamide gel electrophoresis (PAGE) in 1X TBE buffer (Tris-Borate-EDTA). The RNA ladders used for size selection were prepared by mixing 2 μ l of custom RNA ladder and 1 μ l of high resolution ladder with 2 μ l and 1 μ l of DNA loading dye, respectively. All amplified-cDNA was mixed with 10 μ l of DNA loading dye. After that, 2 μ l of custom RNA ladder mixture and high resolution ladder were loaded on the 6% PAGE gel into the wells flanking the samples. The gel was run for 60 minutes at 145 volts or until the blue front dye exit the gel. The gel was stained with 0.5 μ g/ml ethidium bromide for 2-3 minutes and viewed under a UV transilluminator. Then the cDNA whose size as between 145 and 160 bp was cut and placed into 0.5 ml gel breaker tube. The first expected product of 147 bp was mature miRNA (approximately 22 nucleotides) ligated with 5' and 3' adapters (125 nucleotides). The second, the expected size was 157 bp was mature miRNA with other regulatory small RNA molecules (approximately 32 nucleotides) called piwi-interacting RNAs ligated to 5' and 3' adapter (125 nucleotides). Then gel breaker tube with pieces of gel was centrifuged at 20,000 x g for 2 minutes. The small RNA library was eluted by 30-100 μ l of sterile water with shaking at room temperature for overnight and transferred to the

top of a 5 µm filter and centrifuged for 10 seconds at 600 x g. The small RNA library was concentrated using vacuum concentrator and stored at -80°C.

2.8.4 Small RNA library validation

2.8.4.1 Qualification of small RNA library by Bioanalyzer

The high sensitivity DNA kit (Agilent) was used for this analysis. The purified cDNA libraries were diluted to various concentration from 5-500 pg/µl and applied together with ladder to the sample wells of the high sensitivity DNA chip pre-priming with the synthetic gel. The chip was shaken on the vortex mixer then analyzed by bioanalyzer.

2.8.4.2 Small RNA library quantification by real-time PCR

Real-time PCR using Kapa library quantification kit (Kapa Bioscience) was performed in order to validate quality and quantity of small RNA libraries constructed before sequencing on the MiSeq instrument on the Illumina platform. First, 1 ml of Illumina GA Primer Premix (10x) was added to 5 ml bottle of KAPA SYBR® FAST qPCR Master Mix (2x). The small RNA library was diluted 1:1000 fold and the 10-fold series diluted DNA Standards were prepared. The PCR reaction was setup by mixing 6 µl of KAPA SYBR® FAST qPCR Master Mix containing Primer Premix, 2 µl of ultrapure water and 4 µl of diluted small RNA library or DNA Standard (1-6). The thermal cycler program was set as followed first-denaturation at 95°C for 5 minutes, and 35 cycles of denaturation at 95°C for 30 seconds and annealing at 60°C for 45 seconds.

2.9 Small RNA library sequencing on MiSeq instrument (Illumina)

2.9.1 Sample sheet creation

The TruSeq small RNA sample sheet was created by Illumina Experiment Manager (IEM) software. For this experiment, small RNA sequencing workflow was used for data analysis. The index number of each small RNA library at 0, 6 and 48 post-WSSV infection was set to comply with the RPIX primer from cDNA amplification. The sequencing read type was single read and the number of read cycles was set as 36 cycles. Moreover, the reference RNA databases such as *Drosophila melanogaster* were used for analyze contained RNA contaminants, RNA and mature miRNA.

2.9.2 Small RNA sequencing

For NGS on MiSeq, equal amount (2 nM) of each small RNA library was mixed and denatured following protocol for sequencing on the MiSeq protocol. First, fresh 0.2 N NaOH was prepared from 1.0 N NaOH stock. And then, 10 μ l of 0.2 N NaOH was mixed with 10 μ l of 2 nM pooled-small RNA library from WSSV-infected shrimp hemocyte at 0, 6 and 48 hours after infection and vigorously vortex. The mixture was incubated at room temperature for 5 minutes to denature small RNA library to single strand DNA. After that, 20 μ l of denatured small RNA library was combined with 980 μ l of pre-chilled HT1 to make the final concentration of the denatured small RNA library as 20 pM. The 20 pM denatured small RNA library was diluted to 7.5 pM in pre-chilled HT1 which in a final volume of 1 ml and immediately placed on ice. The 1 ml of the 7.5 pM denatured small RNA library was loaded into the MiSeq reagent cartridge. The flow cell and the reagent bottle were put into the MiSeq machine before loading the sample loaded cartridge and the machine and the program was started.

PhiX control library, adapter-ligated library, was used as a control for Illumina sequencing. It was recommended to combine PhiX library with small RNA library at 1% for most libraries, 5% for low diversity libraries and \geq 25% for older version of MiSeq software. In the first trial, the sequencing was not successful because the concentration of small RNA library was too low. For our next experiments, PhiX library was added to the pooled small RNA library to improve the sequencing result. Begin with 5 μ l of 4 nM PhiX library was combined with 5 μ l of 0.2 N NaOH and mixed by vortex. After that, the mixture was incubated for 5 minutes at room temperature. Denatured PhiX library 10 μ l was combined with pre-chilled HT1 990 μ l. Then 30 μ l of 20 pM denatured PhiX was mixed to 570 μ l denatured small RNA library so the concentration was 5% (v/v) and 1 ml was loaded to sample well on the cartridge.

2.10 Small RNA data analysis

After small RNA libraries of WSSV infected-shrimp hemocyte at 0, 6 and 48 hpi were sequenced on MiSeq instrument, the data was obtained in the FASTQ format which stored both a nucleotide sequences and its corresponding quality scores. The passing-filter read numbers of each small RNA library were analyzed by MiSeq Reporter

software. After that CLC Genomics Workbench software was used to exclude the 5' and 3' adapter from sequence raw reads. Then contaminated RNA including mRNA, rRNA and tRNA was searched and removed. After these processes, the remaining sequences were searched for known miRNA homolog against miRNA database, called miRBase (<http://www.mirbase.org/>) (Figure 2.4)

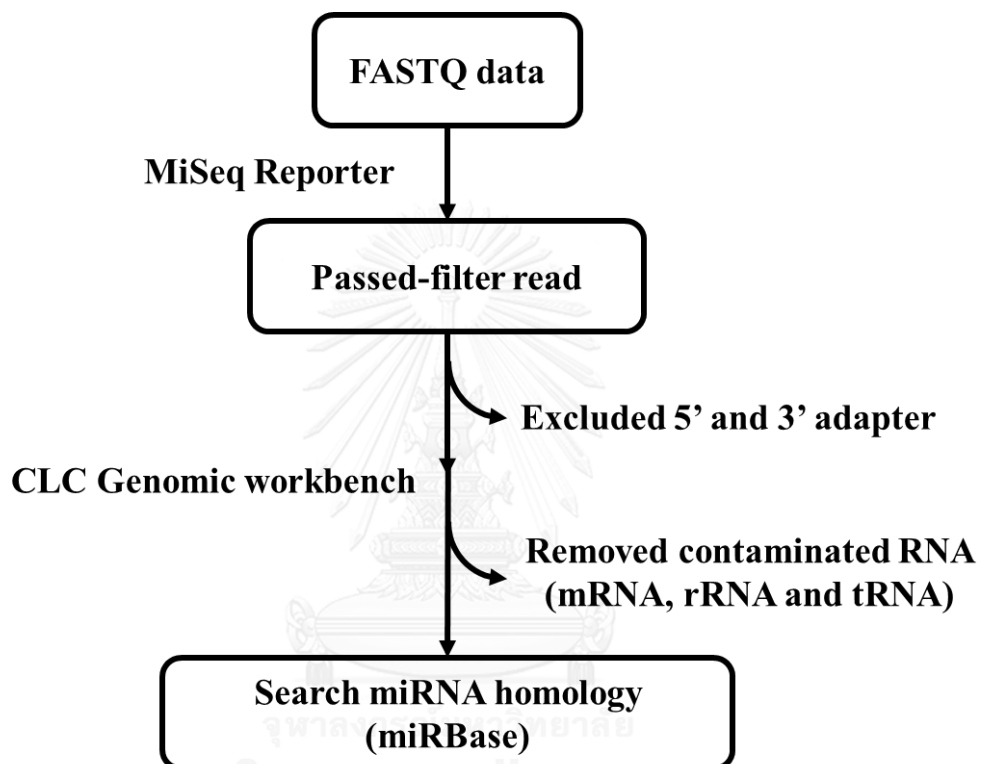


Figure 2. 4 Small RNA data analysis workflow

2.10.1 FASTQ format generation by MiSeq reporter software

Small RNA workflow analysis required reference databases for alignment and identification. Reference databases in FASTA file format were contaminant RNA, mature miRNA, small RNA sequence and reference genome. FASTQ file formats were generated by MiSeq reporter software and used as primary input for alignment. The files were written to the BaseCalls folder in the MiSeqAnalysis folder.

2.10.2 Small RNA sequence analysis by CLC Genomics workbench

After FASTQ data file generation by MiSeq reporter software, the small RNA sequences were imported to CLC Genomics workbench software. The small RNA

analysis was performed on the transcriptomic analysis part of the software. The 5' and 3' adapters were trimmed. The size of small RNA was selected between 18 to 26 nucleotides was selected. And then, the quality score was filtered at Q20 which had probability of wrong base call about 1 in 100. The remaining sequences were searched for the contaminant RNA by blastn program against nucleotide collection (nr) on NCBI databases to identify mRNA, tRNA and rRNA. The parameters were set as followed blastn against all organisms, expect score of 10, word size of 11, match of 2, mismatch of -3 and maximum number of hit sequences of 100. After all these processes, the known miRNAs were identified by against miRBase by using E-value cutoff of 10 and maximum number of hit was 100.

2.11 miRNA expression analysis

2.11.1 Northern blot analysis

miRNA expression after WSSV infection at 0, 6 and 48 hours in shrimp hemocyte was analyzed by Northern blot technique. There were three parts for detect miRNA expression including 3'-end labeling of oligonucleotide probe, hybridization and immunological detection.

2.11.1.1 Probe 3' end labeling with DIG-dUTP

The six oligonucleotide whose sequences are reverse complementary to interested miRNAs including; miR-190, miR-71-5p, miR-305-5p, miR-9a-5p, miR-275-3p, and let-7-5p were designed (Table 2.2). Also, oligonucleotide specific to U6, an internal control, was designed in Table 2.2. The oligonucleotide was labeled using DIG Oligonucleotide 3'-End Labeling Kit, 2nd generation (Roche). Then, 9 μ l of 100 pmol of each specific-miRNA oligonucleotide sequences was mixed with 4 μ l Reaction buffer, 4 μ l CoCl₂ solution, 1 μ l DIG-dUTP solution, 1 μ l dATP solution and 1 μ l 400 U Terminal transferase. The mixture was incubated at 37°C for 15 minutes and incubate on ice immediately. Then, 2 μ l 0.2 M EDTA (pH 8.0) was added to stop reaction and keep at -80°C until use. The labeling oligonucleotide efficiency was then determined. First, DIG-labeled oligonucleotide were diluted to final concentration of 100 to 1 fmol/ μ l. And then, the 1 μ l of diluted-DIG-labeled oligonucleotides and labeled control were spot onto nylon membrane. Then, the chemiluminescence detection was perform.

Table 2. 2 Sequences of specific-miRNA oligonucleotide probe for Northern blot analysis

Probe name	Sequence of specific-miRNA probe (5'-3')
miR-190_RC	CCAAGAATATCAAACATATCT
miR-71-5p_RC	TCCACTACCCATGTCTTTCA
miR-305-5p_RC	GCACCTGATGAAGTACAAT
miR-9a-5p_RC	CAGCTAGATCACCAAAGA
miR-275-3p_RC	GCTACATCAGGTACCTGA
let-7-5p_RC	CTATACAACCTACTACCTCA
U6_RC	AACGCTTCACGAATTTGCGT

2.11.1.2 Electrophoresis and blotting

Total small RNA after WSSV infection at 0, 6 and 48 hours (5 µg) were electrophoresed on 15% denaturing acrylamide gel as described in section 2.7. The miRNA marker (New England Biolabs) was used as a ladder and detected by DIG-labeled streptavidin. After the dye front reached the bottom of the gel, the gel was removed from slab and soaked in 1 x TBE. The nylon membrane and 2 sheets of thick filter papers were soaked in 1 x TBE in tank-blotting. Then, one sheet of filter paper was placed on the Trans-Blot® SD (Bio-rad), and eliminate air bubbles with pipette, followed by the nylon membrane, the gel, a sheet of filter paper, and finally the lid of the machine (Figure 2.5). Then, RNA on the gel was transferred at constant electricity of 100 mA for 1 hour. The nucleic acids were fixed onto the membrane by cross linking with UV-light on GS Gene Linker UV chamber (BIORAD) using the C-L 125 mJ program.



Figure 2. 5 Northern blot transfer cassette on the Trans-Blot® SD (Bio-Rad)

2.11.1.3 Hybridization

The membrane was soaked in pre-heated DIG Easy Hyb buffer at 37°C for 30 minutes. The labeled-oligonucleotide from section 2.11.1.1 was diluted in DIG Easy Hyb buffer (Roche) in ratio 1:1000. After that, the RNA-linked-membrane was hybridized to diluted labeled-oligonucleotide at 37°C for overnight. Then, post-hybridization was performed. The membrane was washed twice by post-hybridization buffer (2xSSC, 0.1% SDS) at 37°C for 15 minutes per time.

2.11.1.4 Immunological detection

Then, the membrane was washed in washing buffer containing 0.1 M Maleic acid, 0.15 M NaCl, 0.3% (v/v) Tween-20[®] pH 7.5 for 2 minutes at room temperature. The membrane was incubated in blocking solution containing 1% blocking reagent in maleic acid buffer (0.1 M maleic acid, 0.51 M NaCl pH 7.5) for 30 minutes. After that, the membrane was incubated in antibody solution (Anti-digoxigenin-AP:blocking solution 1:10000) for 30 minutes. The membrane was washed again with washing buffer twice for 15 minutes each. Then the membrane was equilibrated in detection buffer (0.1 M Tris-HCl, 0.1 M NaCl pH 9.5) for 5 minutes. Then, CSPD which is a chemiluminescent substrate for alkaline phosphatase was diluted 1:100 in detection buffer. The membrane was soaked in diluted-CSPD without air bubbles and incubated for 5 minutes. After that, excess-diluted CSPD was squeezed out and incubate at 37°C for 15 minute. Then, the membrane was exposed to the X-ray film. The film that exposed the membrane was washed in 1x Developer solution for 1 minute. Then, the film was washed again with water and 1x Fixer solution for 1 minute. The band of interested miRNA with expected sized 22 bp was determined.

2.11.2 Stem-loop quantitative RT-PCR

Due to limitation of Northern blot analysis, the temporal, miRNA expression was analyzed by stem-loop quantitative RT-PCR in shrimp hemocyte upon WSSV infection. Poly (A)-tailed quantitative RT-PCR was used to analyze U6 expression as internal control and stem-loop quantitative RT-PCR was used for specific-miRNA expression analysis.

2.11.2.1 Poly (A)-tailed quantitative RT-PCR of U6

2.11.2.1.1 Polyadenylation of total RNA

Total RNA of shrimp hemocyte after WSSV infection at 0, 6 and 48 hpi was used as a template for add adenyl base to 3' end of the RNA sequence. Five micrograms of total RNA was mixed with 5 µl of 10X polymerase reaction buffer, 5 µl of 10mM ATP, 1 µl of 40 U/µl of RNase inhibitor (NEB) and 1 µl of 5 U/µl poly-A-polymerase (NEB). Then the volume was adjusted by nuclease-free water to 50 µl. The polyadenylation reaction was started by incubation the mixture at 37°C for 30 minutes. Polyadenylated RNA was extracted from poly-A polymerase using acid/phenol chloroform. The 50 µl of nuclease-free water was added to the mixture for adjusted the final the volume to 100 µl and 100 µl (1:1) of acid-phenol chloroform was added. Then the sample was mixed by vortex for 30-60 seconds and centrifuged at 10,000xg for 5 minutes at room temperature. After the centrifugation, upper phase of the solution which contain poly-A-tailed RNA sample was collected. The ethanol precipitation was performed by mix upper phase with 0.5 µl of 20 mg/ml glycogen (Amresco) and 1/10 Vol of 3M Sodium acetate pH 5.2. Then the tube was mixed thoroughly by inversion and 1:2.5 Vol of pre-cooled absolute ethanol was added. The mixture was kept at -20°C for overnight. The RNA was pelleted by centrifugation at 14,000Xg for 10 minutes at 4°C and washed with 100 µl of pre-cool 80% Ethanol. The RNA pellet was air dried to remove the contaminated ethanol. Then the poly-A-tailed RNA was dissolved with 10 µl of nuclease-free water.

2.11.2.1.2 First strand cDNA synthesis of poly-A-tailed RNA

The first step of first strand cDNA synthesis was by mixing 1-2 µg of poly-A-tailed RNA with 1 µl of 50 µM CDS-3M primer; 5'-AAGCAGTGGTATCAACGCAGAGTGGCCGAGGCGGCCTTTTTTTTTTTTTTTTTTTTTTVN-3' and 1 µl of 10mM dNTPs mix. Then the mixture was adjusted the volume to 13 µl with nuclease-free water. The secondary structure form of the oligonucleotides was prevented by heating the mixture at 65°C for 5 minutes and chilled on the ice immediately. Then mastermix of the reverse transcription was prepared by mixing 4 µl of 5X First-strand buffer, 1 µl of 0.1 M Dithiothreitol (DTT), 1 µl of 40U/µl RiboLock RNase inhibitor (Thermo Scientific) and

1 μ l of 200U/ μ l SuperScript III reverse transcriptase (Invitrogen). Then, 7 μ l of first-strand cDNA synthesis mastermix was added to the mixture of poly-A-tail RNA and CDS-3M primer. The reaction was incubated 50°C for 30-60 minutes and terminated the enzyme reaction at 70°C for 15 minutes. Then the first-strand cDNA was stored at -20°C until use.

2.11.2.1.3 Quantitative RT-PCR of U6

The forward and reverse primers of U6 were designed. U6 Forward primer is 5'-CTCGCTTCGGCAGCACCA-3' and U6 reverse primer is 5'-AACGCTTCACGAATTTGCGT-3'. The quantitative real-time PCR of U6 was performed on CFX96 Touch Real-Time PCR Detection System (Bio-Rad). The reaction contained 5 μ l of SsoFast EvaGreen Supermix (Bio-Rad), 0.5 μ l of 10 μ M U6 forward primer, 0.5 μ l of 10 μ M U6 reverse primer and 1 μ l of undiluted cDNA from each reverse transcription reaction as template, each sample was run in triplicate. The thermal profile was 98°C for 2 minutes, follow by 40 cycles of 95°C for 5 seconds and 65°C for 30 seconds. Melt curve analysis was performed to determine the specificity of amplification reactions. The reactions were incubated at 95°C for 10 seconds and subsequently increase 0.5°C per 5 seconds from 55°C to 95°C.

2.11.2.2 Stem-loop quantitative RT-PCR of interested-miRNA

Real-time PCR is one of methods that analyze the gene expression using fluorescent molecule that reports an increase in the amount of DNA with a proportional increase in fluorescent signal. The amplified product was detected and measured as the reaction progresses.

2.11.2.2.1 Stem-loop primer design

Sixteen miRNAs were selected for miRNA expression analysis. They were miR-1-3p, miR-2a-3p, miR-7-5p, miR-9a-3p, miR-71-5p, miR-99a-3p, miR-100-5p, miR-184-3p, miR-190, miR-275-3p, miR-305-5p, miR-315, miR-317-3p, miR-750, miR-965 and bantam. According to Kramer, 2011, stem-loop reverse transcription (RT) primer, forward and reverse primers were designed (Table 2.3) adding 6 nucleotides (N₁-N₆) which reverse complementary with 3' end of interested miRNA to 3' end of stem-loop RT primer; 5'-GTCGTATCCAGTGCAGGGTCCGAGGTATTCGCACTGGATACGACACCCTT_N

$N_2N_3N_4N_5N_6-3'$. The forward primer was designed based on sequencing of 12-17 nucleotides from 5'-end of the interested miRNA which contained conserved sequences called "seed region". The melting temperature (T_m) of forward primer was adjusted to approximately $60^\circ\text{C}\pm 1^\circ\text{C}$ by adding randomly 3-7 nucleotides to 5'-end of selected sequenced. The reverse primer was universal reverse primer which can specifically bind to part of stem-loop RT primer.

2.11.2.2.2 cDNA synthesis for Stem-loop specific miRNA

The hemocyte collected from 3 individuals of WSSV-infected shrimp at 0, 6 and 48 hpi by centrifugation at 800xg for 10 minutes at 4°C and kept in liquid nitrogen until use. Total RNA from each shrimp was purified using mirVana miRNA Isolation Kit (Ambion) according to section 2.5. Equal amount of total RNA from each individual was pooled. First strand cDNA synthesis was performed using Superscript III Reverse Transcriptase (Invitrogen). In the reverse transcription reactions, 1.5 μg of pooled total RNA, 1 μl of 1 pmol/ μl Stem-loop specific miRNA RT primer, and 0.5 μl of 10 mM dNTPs mix were mixed and volume was adjusted to 6.5 μl with nuclease-free water. Then the mixture was heated to 65°C for 5 minutes, and incubated on ice immediately. Then, 2 μl of 5X First-strand Buffer, 0.5 μl of 0.1 M DTT, 0.5 μl of 40 U/ μl RiboLock RNase inhibitor (Thermo Scientific) and 0.5 μl of 200 U/ μl SuperScript III reverse transcriptase (Invitrogen) were added. The first strand cDNA synthesis reaction was incubated at 55°C for 1 hour and the reaction was stopped by heating at 70°C for 15 minutes. The specific stem-loop cDNA was stored at -20°C until use.

2.11.2.2.3 Stem-loop quantitative RT-PCR

The quantitative real-time PCR was performed using CFX96 Touch Real-Time PCR Detection System (Bio-Rad). The amplifications were performed in 10 μl reaction volume containing 5 μl of SsoFast EvaGreen Supermix (Bio-Rad), 0.5 μl of 10 μM specific miRNA forward primer, 0.5 μl of 10 μM universal reverse primer and 1 μl of 5 diluted cDNA from each stem-loop reverse transcription reaction as template and adjusted the reaction volume with sterile water, each sample was conducted in triplicate. The PCR condition was 98°C for 2 minutes, followed by 40 cycles of 95°C for 5 seconds and 60°C for 30 seconds. To determine the specificity of amplification of each primer, melt

curve analysis was performed after finishing the amplification as described previously to check specificity of amplification.

Table 2. 3 Primers used for quantitative stem-loop RT-PCR.

miRNA	Primer	Sequence (5'-3')
miR-1-3p	RT primer	GTCGTATCCAGTGCAGGGTCCGAGGTATTTCGCACTGGATACGACCCATAC
	Forward primer	GCGCCGCTGGAATGTAAAGAAG
miR-2a-3p	RT primer	GTCGTATCCAGTGCAGGGTCCGAGGTATTTCGCACTGGATACGACTCATCA
	Forward primer	CGGACGTATCACAGCCAGCTTTG
miR-7-5p	RT primer	GTCGTATCCAGTGCAGGGTCCGAGGTATTTCGCACTGGATACGACACTACC
	Forward primer	GCGGGGTGAAAGACATGGGTAG
miR-9a-3p	RT primer	GTCGTATCCAGTGCAGGGTCCGAGGTATTTCGCACTGGATACGACACAGCT
	Forward primer	GCGGGGTCTTTGGTGATCTAGCT
miR-71-5p	RT primer	GTCGTATCCAGTGCAGGGTCCGAGGTATTTCGCACTGGATACGACACTACC
	Forward primer	GCGGGGTGAAAGAGATGGGTGG
miR-99a-3p	RT primer	GTCGTATCCAGTGCAGGGTCCGAGGTATTTCGCACTGGATACGACGTGGGT
	Forward primer	GCCCTGCAAGCTCGATTCTATGG
miR-100-5p	RT primer	GTCGTATCCAGTGCAGGGTCCGAGGTATTTCGCACTGGATACGACCAAGTT
	Forward primer	GCCACGAACCCGTAGATCCG
miR-184-3p	RT primer	GTCGTATCCAGTGCAGGGTCCGAGGTATTTCGCACTGGATACGACACCCTT
	Forward primer	CCAGCATGGACGGAGAACTGA
miR-190	RT primer	GTCGTATCCAGTGCAGGGTCCGAGGTATTTCGCACTGGATACGACACCAAG
	Forward primer	GGCGGGCGCAGATATGTTTGATATTC
miR-275-3p	RT primer	GTCGTATCCAGTGCAGGGTCCGAGGTATTTCGCACTGGATACGACGCTACA
	Forward primer	CGGGGGTCAGGTACCTGATGTAG
miR-305-5p	RT primer	GTCGTATCCAGTGCAGGGTCCGAGGTATTTCGCACTGGATACGACGCACCT
	Forward primer	GCGCCGATTGTACTTCATCAGGT
miR-315	RT primer	GTCGTATCCAGTGCAGGGTCCGAGGTATTTCGCACTGGATACGACCTTCTG
	Forward primer	CGGGCGTTTTGATTGTTGCTCAG

Table 2. 3 Primers used for quantitative stem-loop RT-PCR (continue)

miRNA	Primer	Sequence (5'-3')
miR-317-3p	RT primer	GTCGTATCCAGTGCAGGGTCCGAGGTATTTCGCACTGGATACGACGGGATA
	Forward primer	GCACTCTGAACACAGCTGGTGG
miR-750	RT primer	GTCGTATCCAGTGCAGGGTCCGAGGTATTTCGCACTGGATACGACGCTGGA
	Forward primer	CGCCTGCCAGATCTAACTCTTCC
miR-965	RT primer	GTCGTATCCAGTGCAGGGTCCGAGGTATTTCGCACTGGATACGACGGGAA
	Forward primer	CGGGCGTAAGCGTATGGCTTTTC
bantam	RT primer	GTCGTATCCAGTGCAGGGTCCGAGGTATTTCGCACTGGATACGACCAGCTT
	Forward primer	GCCGCGTGAGATCATTTGTGAAAG
Universal reverse primer		CCAGTGCAGGGTCCGAGGTA

2.11.2.2.4 Data analysis for quantitative RT-PCR

Fluorescence signal was analyzed by the data analysis software of Bio-Rad CFX Manager. The cycle number that determines the exponential phase of amplification is called the threshold cycle, or C_T . The obtained C_T values were used to calculate the miRNA relative expression ratio (R).

PCR amplification efficiency, E, is calculated from the slope of the standard curve and expressed as the percentage of the efficiency or % efficiency (%E). The conversion of percentage efficiency to E used the following formula:

$$E = (\% \text{ Efficiency} * 0.01) + 1.$$

To determine the expression ratio of the sample, interested miRNA, the control, U6, a mathematical model described by Pfaffl according to the following equation was used:

$$\text{Relative expression ratios} = \frac{(E_{\text{target}})^{\Delta C_{T, \text{target (control-sample)}}}}{(E_{\text{ref}})^{\Delta C_{T, \text{ref (control-sample)}}}}$$

E_{target} is the real-time PCR efficiency of the interested miRNA transcript;

E_{ref} is the real-time PCR efficiency of the reference RNA transcript, U6;

$\Delta C_{T, \text{target}}$ is CT deviation of control (WSSV-injected at 0 hpi) – sample (WSSV-injected at 6, 48 hpi) of the interested miRNA transcript;

$\Delta C_{T, \text{ref}}$ is CT deviation of control (WSSV-injected at 0 hpi) – sample (WSSV-injected at 6, 48 hpi) of the reference RNA transcript, U6.

2.11.2.3 miRNAs and U6 recombinant plasmid construction

2.11.2.3.1 miRNAs and U6 amplification

To amplify miRNAs and U6, the PCR reaction was performed on C1000™ Thermal Cycler (Bio-Rad). The reaction was prepared in 0.2 ml tube and 50 µl of total volume. The amplification contained 5 µl of 10X reaction buffer, 1 µl of 10 mM forward primer, 1 µl of 10 mM reverse primer, 0.5 µl of 10 mM dNTP mix, 0.25 µl RBC Taq DNA polymerase (5 U/µl) and 1 µl of template, 2-fold diluted poly-A-tailed cDNA for U6 from section 2.11.2.1.2 and 5-fold diluted stem-loop cDNA for each interested miRNA from section 2.11.2.2.2. The PCR condition for U6 was 94°C for 2 minutes, follow by 35 cycles of 94°C for 30 seconds, 65°C for 30 seconds and 72°C for 30 seconds. The final extension of PCR condition was 72°C for 10 minutes and follow by 10°C for 10 minutes. For interested miRNAs the condition were 94°C for 2 minutes, follow by 35 cycles of 94°C for 30 seconds, 60°C for 30 seconds and 72°C for 30 seconds, 72°C for 10 minutes.

2.11.2.3.2 PCR product purification

The PCR product was extracted by PCR clean-up Macherey-Nagel (MN) Nucleospin® Extract II. Two volume of NTI was added to one volume of PCR product mixture. Then 700 µl of the NTI-PCR product mixture was loaded into Nucleospin® Gel and PCR clean-up column and centrifuged at 11,000Xg for 30 seconds. The membrane was washed 2 times with 700 µl of NT3 buffer and centrifuges at 11,000Xg for 30 seconds. To dry the membrane, the centrifugation was performed at 11,000Xg for 1 minute. The PCR product was eluted from the membrane using 20 µl of NE buffer.

2.11.2.3.3 Ligation of U6 and miRNA to TA vector

The purified PCR product of miRNA and U6 was ligated into TA vector using RBC TA cloning vector (RBC Bioscience). The amount of miRNA used was calculated following by the formula;

$$\text{Insert (ng)} = \frac{(\text{TA vector (ng)} \times \text{insert length (kb)})}{\text{TA vector length (kb)}} \times [\text{insert : TA vector ratio}]$$

For this experiment, the ratio of insert and TA vector was 5:1. The reaction was performed in volume 10 µl including; 50 ng TA vector, PCR product (miRNA or U6), 10X

Reaction buffer, T4 DNA ligase (400 U/ μ l). The mixture was incubated at 16°C for 3 hours.

2.11.2.3.4 Recombinant plasmid transformation

The ligation mixture was transformed into XL1-Blue *Escherichia coli* competent cell by electroporation method. The MicroPulser™ electroporator (Bio-rad) was set at 2.5 kV. The 2 μ l of ligation mixture was added into 40 μ l of XL1-Blue *E. coli* competent cell and incubated on ice for 1 minute. The competent-ligation mixture was transferred to the cold cuvette and put in the electroporator and then pulsed. The transform cell was immediately mixed by 1 ml of Lysogeny broth (LB). Then, the transformed cell was cultured at 37°C for 1 hour at 250 rpm. The recombinant cell was spread on LB agar plate containing ampicillin, X-gal, IPTG at final concentration 100 μ g/ml, 40 μ g/ml and 0.1 mM, respectively. The plate was incubated at 37°C for overnight (16–18 hours). The white colonies of transformant were selected

2.11.2.3.5 Recombinant plasmid extraction

The single colony of plasmid recombinant was cultured on LB broth at 37°C for 16-18 hours at 250 rpm. The interested-miRNA and U6 recombinant plasmid were extracted using Presto™ mini plasmid kit. The cultured cell was collected by centrifugation at 14,000xg for 1 minute. Then, 200 μ l of PD1 with RNaseA, 200 μ l of PD2 and 300 μ l of PD3 were added into cell, respectively. The mixture was centrifuged at 14,000xg for 5 minutes and the supernatant was transferred to PDH column followed by centrifugation at 14,000xg for 30 seconds. Then, PDH column was washed once with 400 μ l of W1 buffer and twice with 600 μ l of wash buffer followed centrifugation at 14,000xg for 3 minutes to dry the column. After that, the recombinant plasmid was eluted by adding 30 μ l of pre-heated (70°C) elution buffer and incubation at room temperature for 5 minutes and centrifugation at 14,000xg for 3 minutes. The miRNA and U6 recombinant plasmids were stored at -20°C and use as a template for standard curve construction in quantitative RT-PCR.

2.11.2.4 Determination of PCR efficiency

PCR efficiency of each miRNA amplified with specific primer was determined by standard curve method. Recombinant miRNA and U6 plasmid was used as templates

for standard curve construction. First, the copy number was calculated from concentration and size of recombinant plasmid following formula;

$$\text{Recombinant plasmid copy number} \left(\frac{\text{molecules}}{\mu\text{l}} \right) = \left[\frac{\text{(Recombinant plasmid concentration (g}/\mu\text{l))}}{\text{Plasmid length (nt)} \times 660} \right] \times (6.022 \times 10^{23})$$

The standard recombinant plasmid was 10-fold serial diluted from 10^7 molecules to 10^3 molecules. The amplification was performed in triplicate including a negative control, for each run. A calibration curve plotting C_T values against input quantities (log scale) was constructed for both reference (U6) and each miRNA. These PCR efficiencies were taken into account in relative quantitation.

2.12 miRNA Target prediction

To predict the gene targeted by miRNA, the software was developed by Dr. Kulwadee Somboonviwat from Software Engineering Program, International College, King Mongkut's Institute of Technology Ladkrabang. The inputs of the software were single miRNA and gene target database in the FASTA format. In the experiment, 60 miRNAs and expression sequence tag database (EST) of *P. monodon* were used as an input for miRNA and gene target database, respectively. This software will search for the location on mRNA targets that seed sequences (2-8 nucleotides from 5' end) of miRNA can bind perfect complementary. The percent complementary was calculated from number of nucleotide that perfect complementary to the target gene per total length of miRNA. The cutoff of percent complementary that are acceptable value was set at 65%. The screen of miRNA target software was shown in Figure 2.6.

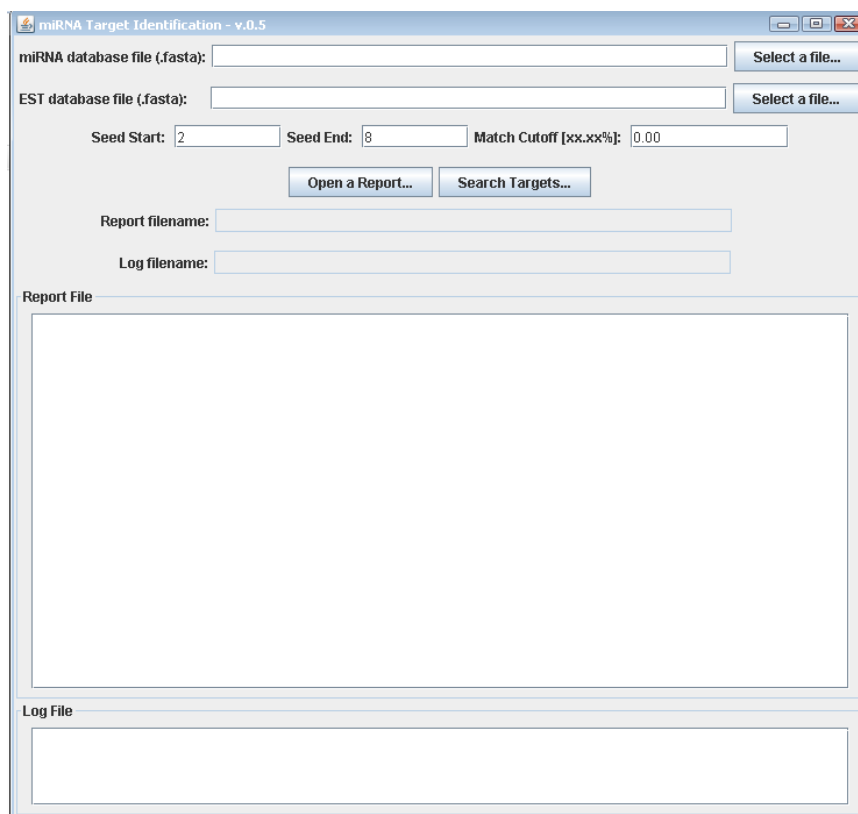


Figure 2. 6 miRNA target identification software

After miRNA target prediction, FASTA file of target gene was extracted and searched homology against NCBI database by using BLASTX algorithm to identify the target gene. The highest score with E-value cutoff was lower than 10^{-4} were selected. Then, the location of miRNA perfect complementary bind to target gene was characterized using ORF Finder software (<http://www.ncbi.nlm.nih.gov/gorf/gorf.html>). The target site of mRNA could be predict on 5' untranslated region (5' UTR), open reading frame (ORF) and 3' untranslated region (3' UTR).

Moreover, the structure of miRNA/mRNA duplex was predicted using RNAhybrid web tool (http://bibiserv2.cebitec.uni-bielefeld.de/rnahybrid?id=rnahybrid_view_submission). In the analysis of target sequence, a statistical analysis of minimum free energies (mfes) showing the spontaneous probability of miRNA/mRNA duplex (kcal/mol) was recorded. The less mfes, the more spontaneous miRNA/mRNA duplex could be formed. The input of RNAhybrid web tool contained miRNA sequence and target gene sequences in FASTA file.

CHAPTER III

RESULTS

3.1 Determination of WSSV infectivity in shrimp

To prepare sample for next generation sequencing, *Penaeus monodon* was infected with WSSV and the status of viral infection was monitored by detecting the expression of VP28 gene, which is a late gene of WSSV, in gills at 0, 6 and 48 hours post infection (hpi). The PCR result showed that VP28 gene was detected in gills of WSSV-challenged shrimp at 48 hpi, but were not at 0 and 6 hpi (Figure 3.1), indicating that shrimp were infected with WSSV.

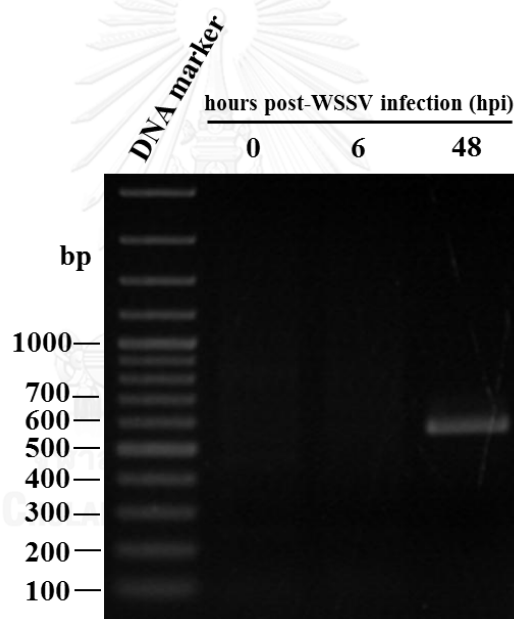


Figure 3. 1 Analysis of VP28 gene expression in gills of WSSV-infected shrimp at 0, 6 and 48 hours post-injection. DNA extracted from gills of WSSV-infected shrimp was used as a template for PCR. The VP28 gene of WSSV was amplified using a specific primer pair. The PCR products were run on 1.5% agarose gel electrophoresis and the gel was stained by ethidium bromide and visualized under UV light.

3.2 Total RNA and total small RNA preparation

Total RNA and total small RNA were extracted from hemocyte of WSSV-infected *P. monodon* at 0, 6 and 48 hpi using mirVana™ miRNA isolation kit. The quality of total

RNA and total small RNA sample were subsequently verified. The A_{260}/A_{280} ratio of the total RNA samples were 1.8-2.0 which was the expected ratio of the acceptable RNA quality. The total RNA and total small RNA samples were examined by electrophoresis on the denaturing acrylamide gel (Figure 3.2, A and B). The major discrete bands whose size ranged from 200 to 1,500 nucleotides were observed in the total RNA extract. For the total small RNA extract, the majority of bands are small RNAs whose size are lower than 500 nucleotides.

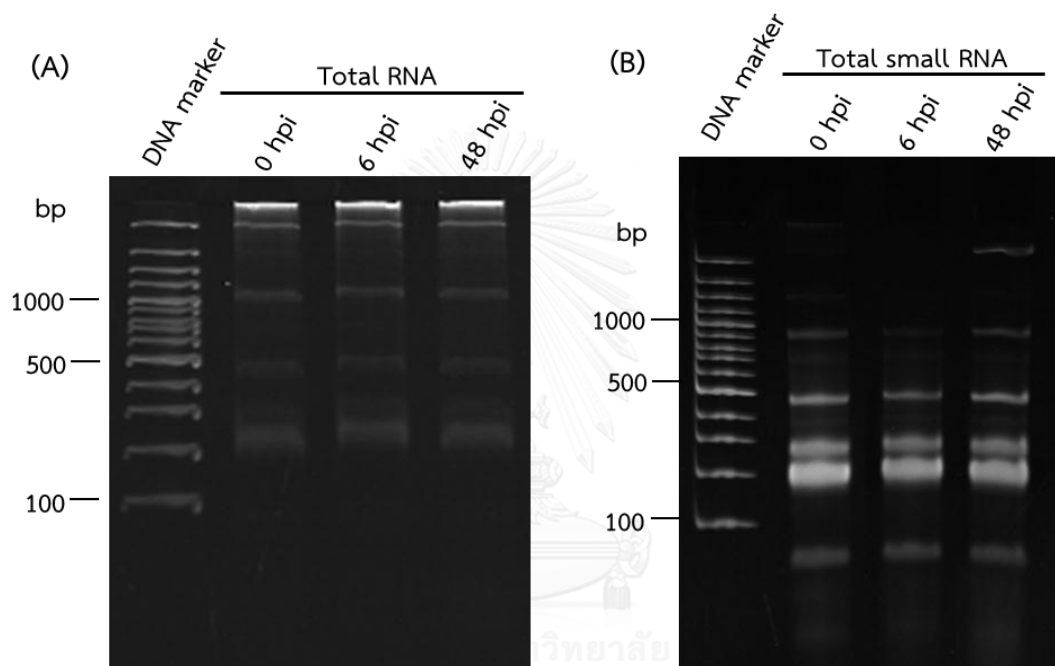


Figure 3. 2 Verification the quality of total RNA and total small RNA extracts by denaturing 15% acrylamide gel. Total RNA (A) and total small RNA (B) from hemocytes of WSSV-infected shrimp at 0, 6 and 48 hpi were electrophoresed on denaturing 15% acrylamide gel.

3.3 Identification of miRNA involved in WSSV infection in *P. monodon* by next generation sequencing

In this study, we applied next generation sequencing (NGS) for the identification of miRNA from WSSV-infected *P. monodon*. Small RNA libraries of WSSV-infected shrimp at 0, 6 and 48 hpi were prepared. Because there are no well-established shrimp small RNA-library preparation protocol for NGS, we have tried to prepare the small RNA-library for three times.

3.3.1 First preparation

3.3.1.1 Qualitative analysis of total RNA

For the first preparation, two sets of WSSV-infected shrimp hemocyte at 0, 6 and 48 hpi were collected. Each set was a pool of 3 individuals. The purified total RNA were analyzed for their quality by Bioanalyzer using the by Agilent RNA 6000 Nano kit. The obtained electropherogram that is a plot of migration time against fluorescence unit [FU], and the gel-like images of total RNA samples revealed a predominant band of 18S rRNA size of about 1.9 kb and some small RNA (Figure 3.3).

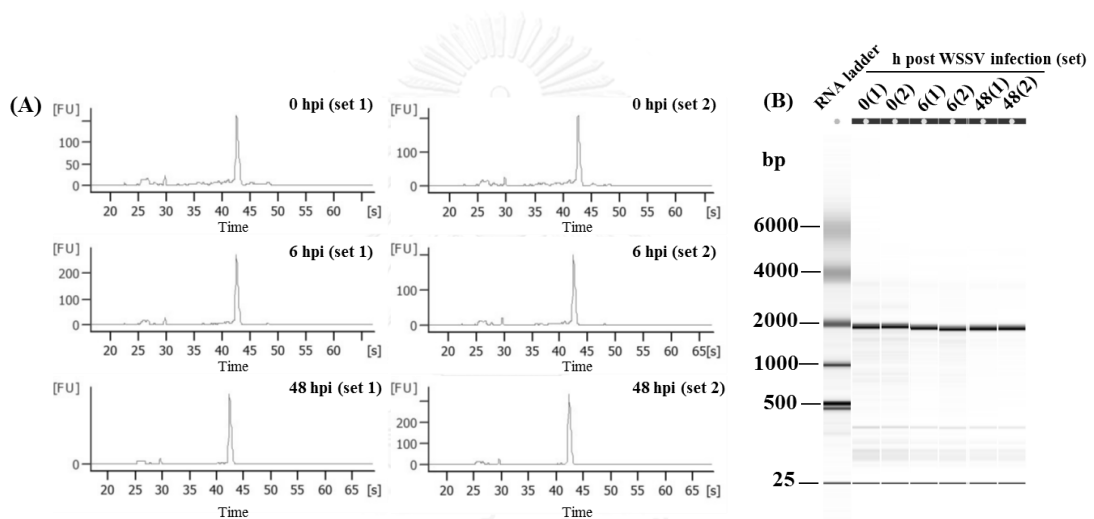


Figure 3.3 Analysis of total RNA quality by Bioanalyzer (1st preparation). Total RNA of WSSV infected shrimp at 0, 6 and 48 hpi were analyzed by Agilent RNA 6000 Nano kit on bioanalyzer instrument. Electropherogram (A) and gel- like image (B) displayed pattern of each total RNA sample.

3.3.1.2 Small RNA library preparation and validation

One μ g of the purified total RNA isolated from hemocyte of *P. monodon* after WSSV infection at 0, 6 and 48 hpi was used as the template for the small RNA libraries construction. The small RNA libraries were named miHcW0_1, miHcW6_1, and miHcW48_1, respectively. Two sets of each small RNA library were constructed. After 3' and 5' adaptor ligations, the 3', 5' adaptor-ligated RNA samples were

reverse-transcribed and cDNAs were then amplified by PCR. In the amplification step, RNA PCR primer indexes number 1 (RPI1), 2 (RPI2), 3 (RPI3), 4 (RPI4), 5 (RPI5), and 6 (RPI6) were used for labeling each small RNA library; miHcW0_1 (set 1), miHcW0_1 (set 2), miHcW6_1 (set 1), miHcW6_1 (set 2), miHcW48_1 (set 1) and miHcW48_1 (set 2), respectively. The amplified cDNA was separated on 6% polyacrylamide gel electrophoresis and cDNA with the expected size (150 nucleotides) was purified from the gel. All six small RNA libraries constructed were quantitatively and qualitatively analyzed by bioanalyzer using Agilent high sensitivity DNA kit. The results showed that the expected size of 150 nucleotides long fragments of small RNA libraries was not obtained (Figure 3.4). Moreover, quantitative real-time PCR was performed to determine the concentration of miHcW0_1 (sets 1 and 2) small RNA libraries. Only miHcW0_1 (sets 1 and 2) small RNA libraries were determined. The results indicated that the 3' and 5' adapters were successfully ligated to small RNA but the concentration of miHcW0_1 (sets 1; 0.0063 nM and set 2; 0.0070 nM) were not enough to sequencing on MiSeq instrument (Figure 3.5).

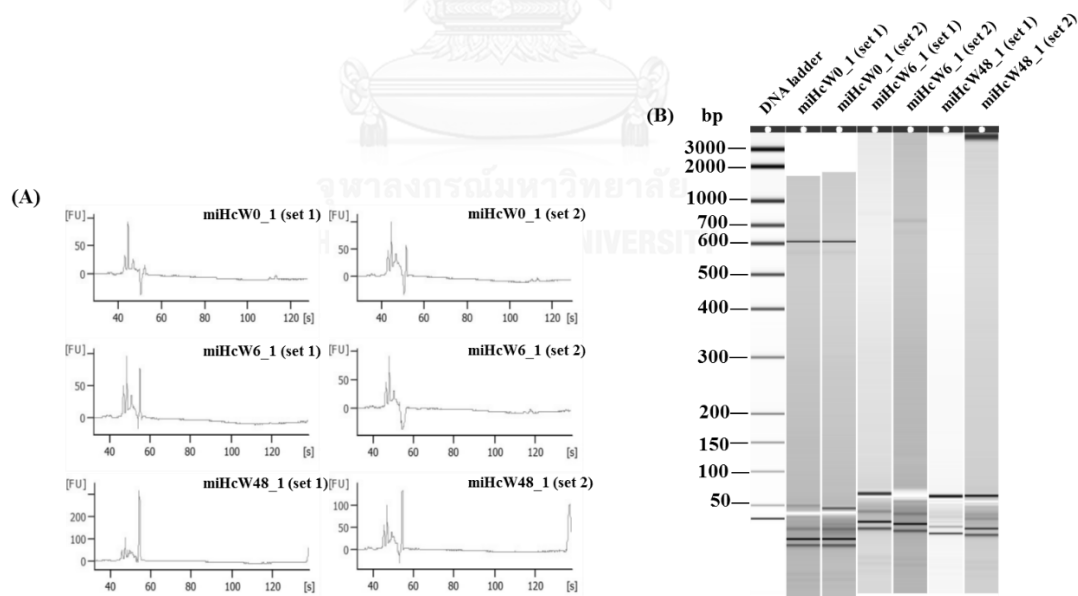


Figure 3. 4 Quantitative and qualitative analysis of small RNA libraries by bioanalyzer using Agilent high sensitivity DNA kit (1st preparation). Gel- like image (A) and electropherogram (B) of each small RNA library are shown.

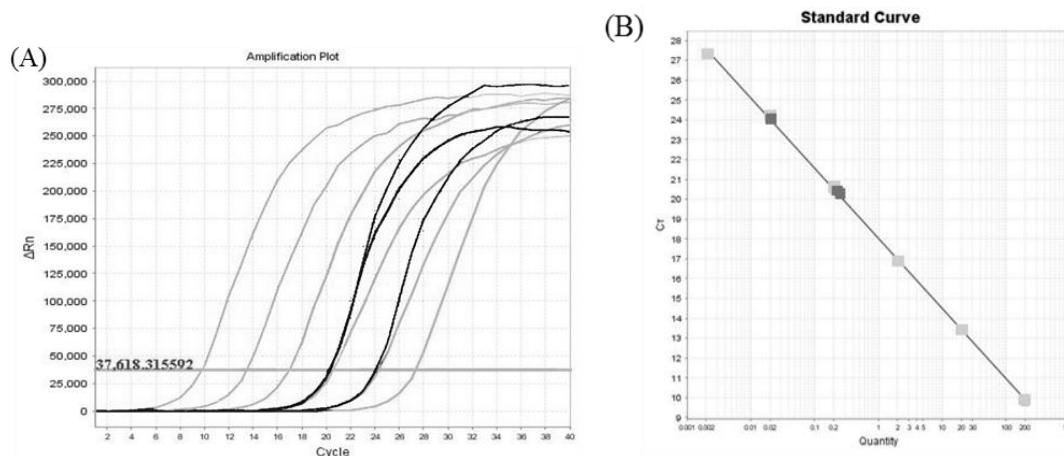


Figure 3. 5 Quantitative real-time PCR of miHcW0_1 small RNA library (sets 1 and 2). Small RNA library was quantitated using KAPA library quantification kit (Kapa Biosystems). Standard curve (A) and amplification curve (B) are shown. (dark grey line indicates sample, light grey indicates standard DNA)

3.3.2 Second preparation

Since the quality and the amount of starting RNA is critical to success of sequencing by NGS, the small RNA libraries preparation were modified by using total small RNA as template.

3.3.2.1 Quantitative and qualitative analyses of total small RNA

In the second preparation, we enriched the quantity of total small RNA by purification from total RNA using mirVana™ miRNA isolation kit. Total small RNAs were extracted from one hundred micrograms of hemocyte total RNA previously used in the first preparation and quantified by Qubit using Quant-iT™ RNA Assay Kit. Then, 120 ng of total small RNAs were used as a starting material to construct small RNA libraries. RNA PCR primer indexes number 10 (RPI10), 11 (RPI11) and 12 (RPI12) were used for amplification of miHcW0_2, miHcW6_2 and miHcW48_2 small RNA libraries. The amplified cDNA product of small RNA libraries were separated through 6% acrylamide gel. After EtBr staining, the band of small RNA libraries at the expected size was not clearly observed (Figure 3.6). However, the gel at the expected size (between 145 and 160 nucleotides) was cut and the cDNA of each small RNA library was eluted with water. After that, the amplified cDNAs were analyzed by bioanalyzer using high

sensitivity DNA kit. The Bioanalyzer 2100 analyzed data indicated that miHcW0_2, miHcW6_2, and miHcW48_2 libraries (0, 6 and 48 hpi) had expected size of about 152 nucleotides but the contaminated sequence of the adapter (120 nucleotides fragment) was found in miHcW0_2 (Figure 3.7). Using quantitative real-time PCR, all small RNA libraries could be amplified indicating the success of the 3' and 5' adapter ligation on small RNA. The concentration of three small RNA libraries, miHcW0_2, miHcW6_2 and miHcW48_2 calculated from real time PCR standard curve were 4.8, 1.67 and 4.57 nM, respectively (Figure 3.8).

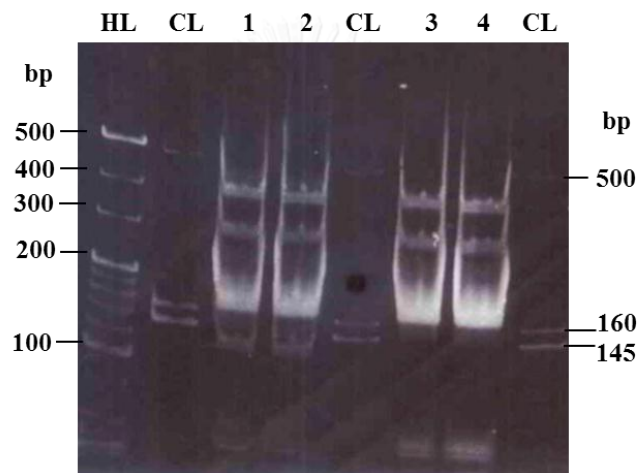


Figure 3. 6 Analysis of small RNA libraries constructed from total small RNA of WSSV-infected *Penaeus monodon* hemocyte at 0 and 6 hpi by 6% acrylamide gel electrophoresis

Lane HL : High resolution ladder

Lane CL : Custom ladder

Lane 1, 2 : miHcW0_2 small RNA library

Lane 3, 4 : miHcW6_2 small RNA library

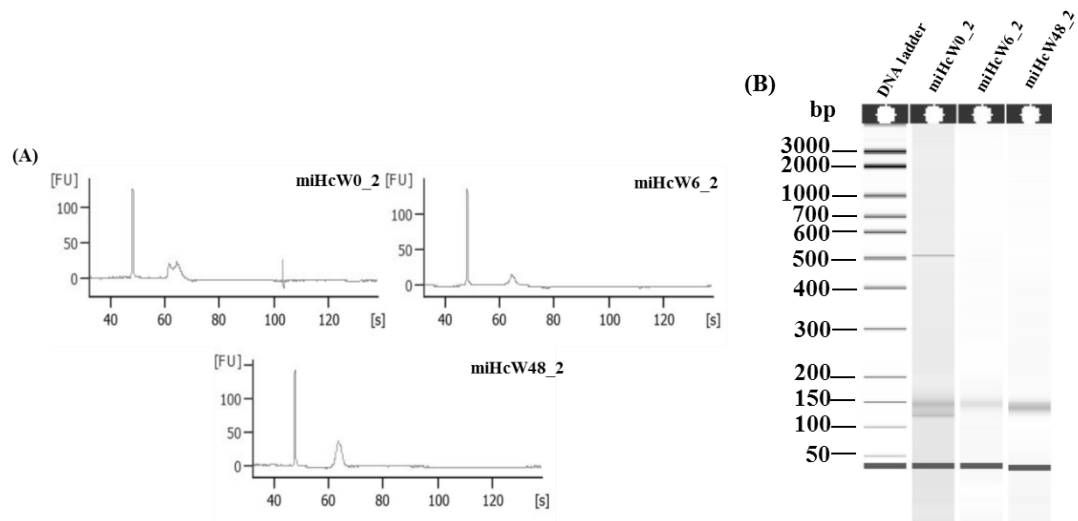


Figure 3. 7 Quantitative analysis of small RNA libraries using bioanalyzer (2nd preparation). The amplified products of small RNA libraries; miHcW0_2, miHcW6_2 and miHcW48_2, were electrophoresed on Agilent high sensitivity DNA kit. Gel- like image (A) and electropherogram (B) displayed pattern of each small RNA library.

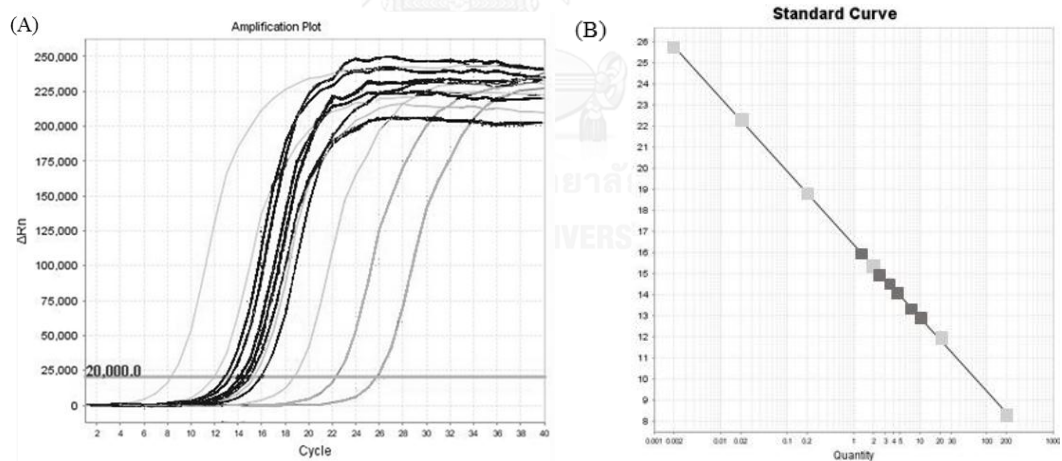


Figure 3. 8 Quantitative real time PCR analysis of small RNA libraries (2nd preparation) prepared from WSSV-infected shrimp hemocyte. The amplification curve (A) and standard curve (B) of standard DNA and small RNA library samples are shown. (dark grey indicates sample, light grey indicates standard DNA)

3.3.2.2 Small RNA sequencing

For the second preparation, all small RNA libraries at equal amount were pooled to make the final concentration of 2 nM in 5 μ l. After denaturation, the pooled small RNA libraries were diluted to final concentration of 2 pM and subjected to sequencing on MiSeq. Unfortunately, the samples could not be clustered. As a result, the machine could detect no signal of the hybridized small RNA libraries on the flow cell. The cause of unsuccessful clustering is that the concentration of denatured small RNA library was too low.

However, the same small RNA libraries was re-sequenced with modification. PhiX control library was added at the ratio of small RNA library: PhiX control library of 3:7. We hypothesized that if the PhiX control can clustering on the flow cell, our small RNA libraries would be clustered too. As expected, the sequencing was successful but the number of reads obtained was quite low. The number of raw read of small RNA libraries; miHcW0_2, miHcW6_2 and miHcW48_2, were 22,855, 9,561 and 35,329 reads, respectively. The sequences that pass the quality filter of the instrument were 11,837, 4,128 and 15,394 reads, respectively (Table 3.1). After 5' and 3' adapter trimming, the number of read of the remaining sequences were 5,748, 1,859 and 8,537 for miHcW0_2, miHcW6_2 and miHcW48_2, respectively. Size distribution analysis revealed that the average size of small RNA of each library was 20 nucleotides (Figure 3.9).

Table 3. 1 The number of raw reads and the passed filter (PF) reads of small RNA libraries after WSSV infection at 0, 6 and 48 hpi of the second small RNA preparation

Library	Counts		% PF
	Raw reads	PF reads	
miHcW0_2	22855	11837	51.79
miHcW6_2	9561	4128	43.18
miHcW48_2	35329	15394	43.57

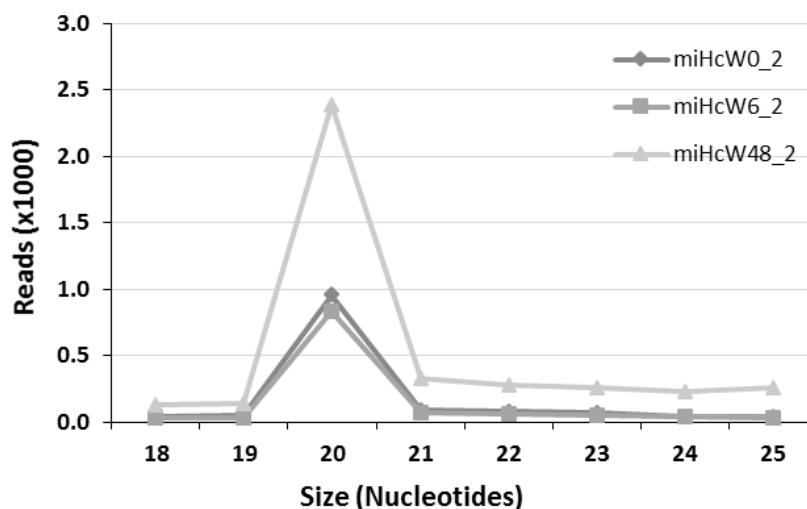


Figure 3. 9 Size distribution of small RNA libraries after 3' and 5' adapter trimming of small RNA sequencing in the second preparation.

The obtained small RNA sequences were analyzed by searching against NCBI database to remove any contaminated RNAs such as mRNA, rRNA, and mRNA. The remaining sequences (3,177 sequences) were searched against miRBase. 2,204 sequences out of 3,177 sequences were identified as miRNA homolog, the rest were identified as unknown small RNA. The sequences of miRNA homologs are summarized in Table 3.2.

Table 3.2 Nucleotide sequences and length of miRNA homologs that were identified in WSSV-infected shrimp hemocyte.

No	miRBase	Sequence	Length
1	miR-6241	TGGCAGTGTGGTTAGCTGGTTG	22
2	miR-6244	CCGGGCGTGGAAATCTCGGG	22
3	miR-305-3p	TATCACAGCCACCTTTGATGA	22
4	miR-6489-5p	TGGCAGTGTGGTTAGCTGGTTG	22
5	miR-100-5p	AACCCGTAGATCCGAACTTG	22
6	miR-184-5p	TGGACGGAGAACTGATAAGGGT	22
7	miR-182b-5p	TGGAATGTAAAGAAGTATGG	22
8	miR-4448	TGGCAGTGTGGTTAGCTGGTTG	22
9	miR-2373-3p	TTGTGACCGTTATAATGGGC	22
10	miR-309b-5p	TCACAACCTCCTTGAGTGAG	22
11	miR-471-5p	TGGCAGTGTGGTTAGCTGGTTG	22
12	miR-750	TGAAAGACATGGGTAGTGA	22
13	miR-9226	GTGAGCAAAGTTTCAGGTGTG	22
14	miR-99a-3p	CAAGCTCGATTCTATGGG	22
15	miR-6493-5p	CGTCCGGCAGGTTTTACCCC	22
16	let-7-3p	TGAGATCATTGTGAAAGCTG	22
17	miR1032	AACCCGTAGATCCGAACTTG	22
18	miR-2033-3p	TTGTGACCGTTATAATGGGC	22
19	miR-6237	TGGCAGTGTGGTTAGCTGGTTG	22
20	miR-9161	CCAGATCTAACTCTTCCAGCTC	22
21	miR-71-3p	GGAAAGGGACTTGAATT	22

3.3.3 Third preparation

Because a number of reads obtained in the second preparation was quite low; therefore, in the third preparation higher amount of total small RNA was used for small RNA library preparation.

3.3.3.1 Small RNA fragment analysis

In this preparation, total small RNA was prepared from the pool of 5 individuals of WSSV-infected *P. monodon* at various time 0, 6 and 48 hpi. Total small RNA samples about 1 µg (5 shrimps/time) prepared from WSSV-infected *P. monodon* at various times 0, 6 and 48 hpi were analyzed by bioanalyzer using Agilent RNA 6000 Nano kit. Electropherogram showed that RNA fragment size of all small RNA samples were lower than 25 nucleotides (Figure 3.10).

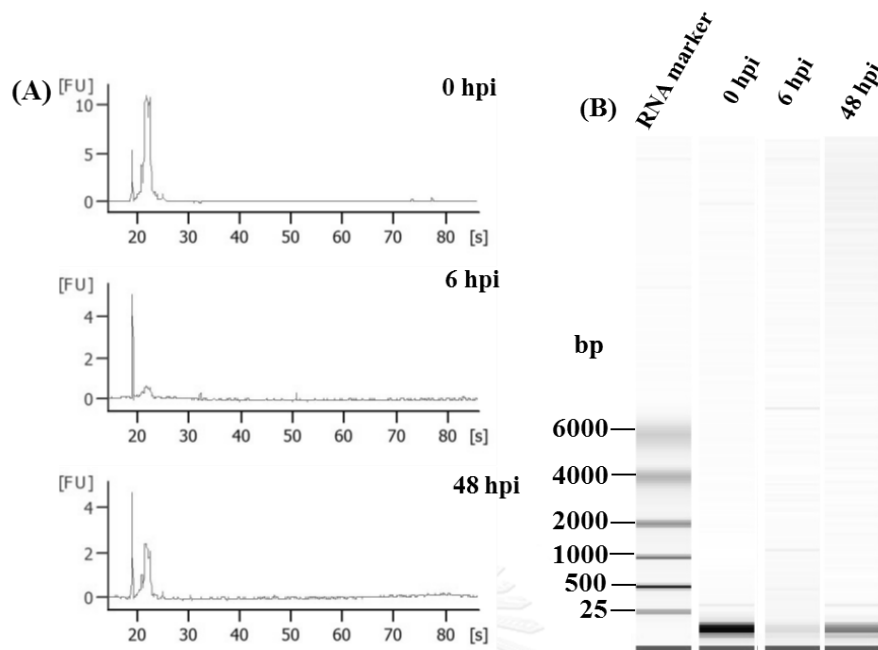


Figure 3. 10 Total small RNA extracted from WSSV-infected shrimp hemocyte at 0, 6, and 48 hpi by bioanalyzer using Agilent RNA 6000 Nano kit. The two-fold diluted small RNA samples were used for analysis. Gel-like image (A) and eletropherogram (B) of each total small RNA sample are shown.

3.3.3.2 Small RNA library preparation and validation

For the third preparation, about 1 μg of the quality-proven total small RNAs from the above section were used as template to construct small RNA libraries; miHcW0_3, miHcW6_3 and miHcW48_3. They were labeled with RNA PCR primer indexes number 1 (RPI1), 3 (RPI3) and 5 (RPI5), respectively. To obtain the concentrated purified small RNA library, following electrophoresis on 6% of polyacrylamide gel, the amplified cDNAs with corresponding size were eluted from the gel pieces with water and then concentrated by speed vacuum. Then, concentrated-small RNA libraries were quantified by bioanalyzer using a high sensitivity DNA kit. The result showed that all small RNA libraries have expected size of about 152 bp but the total amount was vary (Figure 3.11). The success of adapter ligation was confirmed by quantitative real-time PCR.

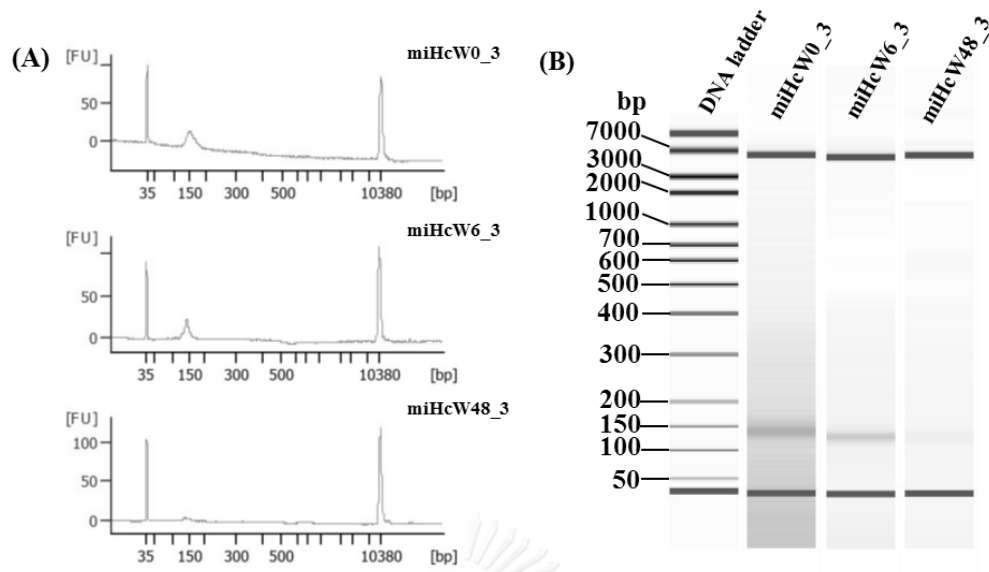


Figure 3. 11 Qualitative and quantitative analysis of small RNA libraries after amplification electrophoresed by Agilent high sensitivity DNA kit. Electropherogram (A) and gel- like image (B) displayed pattern of each small RNA library.

3.3.3.3 Small RNA sequencing

To ensure that the sequencing can pass the clustering step, the control library, PhiX, was mixed with 2 nM pooled small RNA libraries at the ratio PhiX: pooled libraries of 1:4 (v/v). After small RNA libraries were sequenced, the number of raw reads of small RNA libraries; miHcW0_3, miHcW6_3 and miHcW48_3 were 157,026, 196,468 and 107,556 reads, respectively. The sequences that passed the quality filter of the instrument were 128,408, 158,651 and 85,828 reads, respectively (Table 3.3). The 5' and 3' adapters were subsequently removed and trimmed, the number of reads of remaining sequences were 27,013, 34,179 and 26,209, respectively. Analysis of small RNA size distribution showed that, the average sizes of trimmed small RNA of all libraries were 20 nucleotides (Figure 3.12). Sequence analysis by searching against NCBI database, in average 95% were contaminated RNAs. Then, to characterize the shrimp miRNA homologs, the remaining small RNA sequences were compared to miRNA sequences deposited in miRBase 16.0. The percentage of matched miRNAs of miHcW0_3, miHcW6_3 and miHcW48_3 were 2.21, 3.04 and 0.45, respectively. The

remaining of small RNA sequences were unknown (Table 3.4). A total of 46 miRNA homologs were identified from hemocyte of WSSV-infected *P. monodon*. The sequence of miRNA homologs that were found in small RNA libraries are shown in Table 3.5.

Table 3. 3 The number of raw reads and pass filter (PF) reads of small RNA libraries of WSSV infection *P. monodon* hemocyte (3rd preparation)

Library	Counts		%PF
	Raw reads	PF reads	
miHcW0_3	157026	128408	81.77
miHcW6_3	196468	158651	80.75
miHcW48_3	107556	85828	79.80

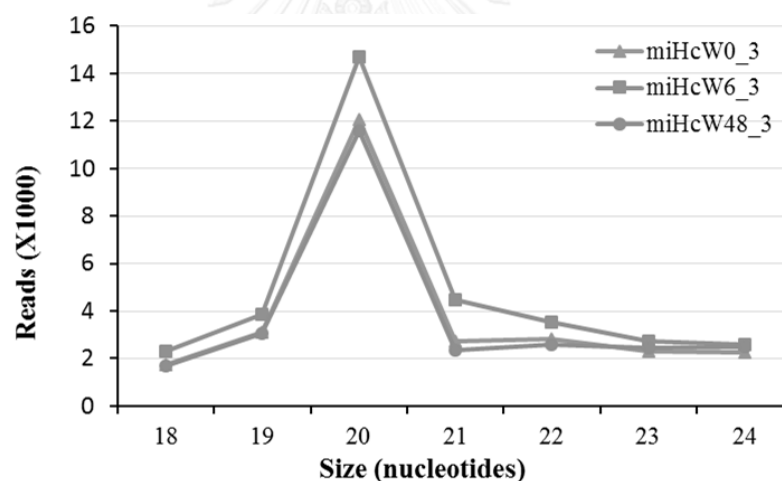


Figure 3. 12 Size distribution of small RNA libraries after 3' and 5' adapter trimming in the third preparation.

Table 3. 4 Summary of sequences identified from small RNA libraries of WSSV-infected shrimp hemocyte at 0, 6 and 48 hpi.

Group	No. of reads in miHcW0_3		No. of reads in miHcW6_3		No. of reads in miHcW48_3	
	Counts	% of Count	Counts	% of Count	Counts	% of Count
Raw reads	27013	100	34179	100	26209	100
microRNA homolog	596	2.21	1040	3.04	118	0.45
Contamination RNA	25611	94.81	32147	94.06	25193	96.12
Unknown small RNA	809	2.99	992	2.9	898	3.43

Table 3. 5 Nucleotide sequences and length of known miRNAs that were found in WSSV-infected shrimp hemocytes.

No	miRBase	Sequence	Length	No	miRBase	Sequence	Length
1	bantam	TGAGATCATTGTGAAAGCTG	20	24	miR-2b	TATCACAGCCACCTTTGATGA	21
2	let-7-3p	CTGTACAACCTGCTAACTTTC	21	25	miR-305-5p	ATTGTA CTTCATCAGGTGC	19
3	let-7-5p	TGAGGTAGTAGTTGTATAGTTTT	24	26	miR-307a-3p	TCACAACCTCCTTGAGTGAG	20
4	miR-1000-5p	ATATTGTCCCGTCACAGCAGT	21	27	miR-315	TTTTGATTGTTGCTCAGAAG	20
5	miR-100-5p	AACCCGTAGATCCGAACTTG	20	28	miR-316	TGTC TTTTTCTGCTTTGCTGCCG	23
6	miR-12-5p	TGAGTATTACATCAGGTACTGG	22	29	miR-317-3p	TGAACACAGCTGGTGGTATCCC	22
7	miR-1260	CGAATCCCACCCTGCCACC	20	30	miR-33a-5p	ATGCATTGTAGTTGCATTG	19
8	miR-1-3p	TGGAATGTAAAGAAGTATGG	20	31	miR-34-5p	TGGCAGTGTGGTTAGCTGGTTG	22
9	miR-184-3p	TGGACGGAGAACTGATAAGGGT	22	32	miR-6490	CGACCTCGAGTGGAGGGA	18
10	miR-190	AGATATGTTTGATATCTTGGT	22	33	miR-6493-3p	AGGGGGAAACCCGCTGAGC	20
11	miR-193	TACTGGCCTGCTAAGTCCC	19	34	miR-6493-5p	CGTCCGGCAGGTTTACCCC	20
12	miR-2001	TTGTGACCGTTATAATGGGC	20	35	miR-71-3p	ATCTCACTACCTTGCTTTTC	20
13	miR-252-5p	CTAAGTACTAGTGCCGCAGGA	21	36	miR-71-5p	TGAAAGACATGGGTAGTGA	19
14	miR-263a-5p	AATGGCACTGGAAGAATTCACG	22	37	miR-750	CCAGATCTAACTCTTCCAGC	20
15	miR-275-3p	TCAGGTACCTGATGTAGC	18	38	miR-7-5p	TGGAAGACTAGTGATTTTGTG	22
16	miR-2765	TTGGTAACTCCACCACCGTTG	21	39	miR-8-5p	CATCTTACCGGACAGCATTA	20
17	miR-276a-3p	TAGGAACTTCATACCGTGCT	20	40	miR-87-3p	GTGAGCAAAGTTTCAGGTGTG	21
18	miR-279	TGACTAGATCCACACTCATCC	21	41	miR-92b-3p	AATTGCACTAGTCCCGGCCT	20
19	miR-281-2-5p	AAGAGAGCTATCCGTCGACA	20	42	miR-965	TAAGCGTATGGCTTTTCCCC	20
20	miR-282-5p	TAGCCTCTCCTTGGCTTTGTC	21	43	miR-981	TTCGTTGTCGTCGAAACCTG	20
21	miR-2898	TACCCCGCATCTCCACCATG	20	44	miR-99a-3p	CAAGCTCGATTCTATGGG	18
22	miR-2a	CAGCCAGCTTTGATGAGCGT	20	45	miR-9a-5p	TCTTTGGTGATCTAGCTG	18
23	miR-2a-3p	TATCACAGCCAGCTTTGATGA	21	46	miR-9b	ATAAAGCTAGATTACCAAAGC	21

3.5 miRNA expression analysis

The expression of miRNAs after WSSV infection in *P. monodon* hemocyte at 0, 6 and 48 hpi were determined by Northern blot analysis and stem-loop real-time PCR analysis.

3.5.1 Northern blot analysis

3.5.1.1 Determination of labeling probe efficiency

In this section, six miRNAs such as miR-190, miR-71-5p, miR-305-5p, miR-9a-5p, miR-275-3p, and let-7-5p were selected for analysis. In order to determine the expression level of miRNA by Northern blot analysis, oligonucleotide probes specific to selected miRNAs and the control U6 were labeled at 3' end using DIG oligonucleotide 3'-end labeling kit, 2nd generation (section 2.11.1.1). The efficiency of probe labeling was determined by spotting them onto a nylon membrane and detecting the chemiluminescence signal on the X-ray film. According to the intensity detected, the efficiency of all miRNA probes were as good as the positive control indicating the successful of oligonucleotide probe labeling (Figure 3.13).

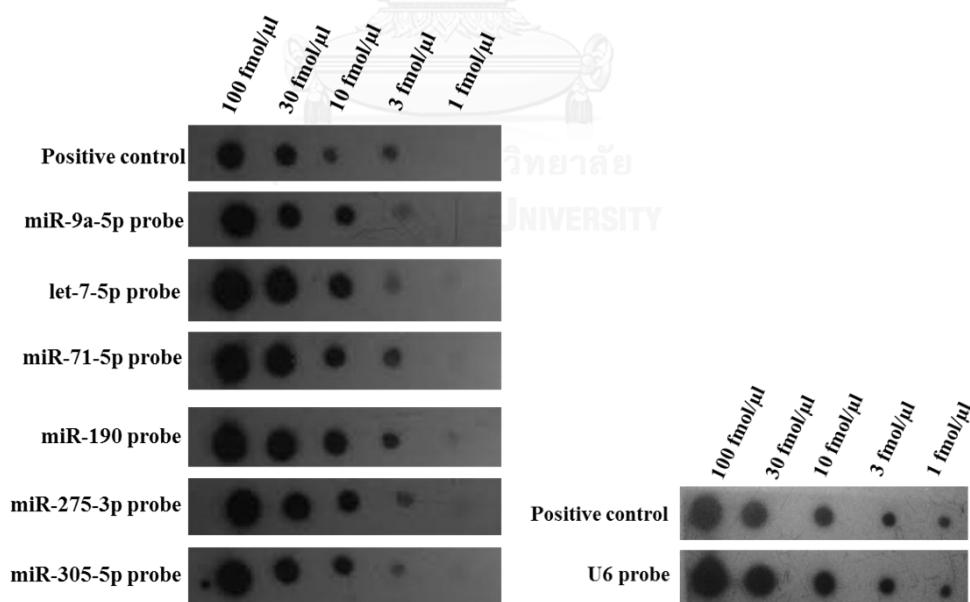


Figure 3. 13 Determination of oligonucleotide probe efficiency. Oligonucleotide probes specific to miR-190, miR71-5p, miR-305-5p, miR-9a-5p, miR-275-3p, and let-7-5p as well as the control U6, at concentration of 100, 30, 10, 3 and 1 fmol/μl were spotted on to a nylon

membrane and CSPD was added. The chemiluminescence was detected by DIG luminescent detection kit.

3.5.1.2 miRNA expression determined by Northern blot analysis

For miRNA expression analysis, 1.5 μ g of total small RNA from WSSV-infected shrimp hemocyte at 0, 6 and 48 hpi were electrophoresed on the denaturing 15% acrylamide gel and transferred onto nylon membrane. Each probe was separately hybridized with the fixed membrane and the chemiluminescence detection was performed. From six miRNAs examined, only let-7-5p and miR-71-5p were successfully detected with approximately 22 nucleotides length. The expression of U6, an internal control, had nearly equal expression level at all-time point (0, 6 and 48 hpi). The miR-71-5p and let-7-5p were expressed at high level at 0 and 6 hpi in the WSSV-infected shrimp and their expression was significantly decreased at 48 hpi (Figure 3.14).

Because the limitation of the sensitivity of detection and the amount of miRNA in the WSSV-infected shrimp hemocyte were too low, so the stem-loop real-time PCR analysis were instead performed.

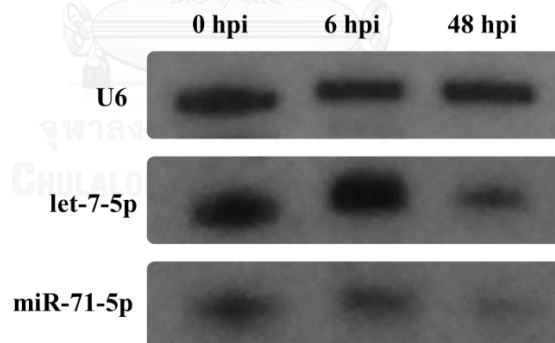


Figure 3. 14 Northern blot analysis of miRNAs, let-7-5p and miR-71-5p, in WSSV-infected *P. monodon*. Total small RNA of WSSV-infected shrimp at 0, 6 and 48 hpi (1.5 μ g) was separated on the denaturing 15% polyacrylamide gel and transferred onto nylon membrane. Membrane was hybridized with each probe at 37°C for overnight and then the chemiluminescence signal was detected by X-ray film exposure. U6 was used as an internal control.

3.5.2 miRNA expression analysis by stem-loop real-time PCR

To analyze the miRNA expression, U6 was amplified as an internal control of small RNA expression. The recombinant plasmid, U6 in TA vector, was constructed and used as a template to generate standard curve. Real-time PCR efficiency was calculated from the slope of plot (threshold cycle vs Log various known amount of ten-fold diluted plasmid template) (Figure 3.15, A). The PCR efficiency of U6 amplification was 103.6%. Dissociation curve of U6 showed the single peak of the expected melting temperature revealing that the specific product was amplified (Figure 3.15, B).

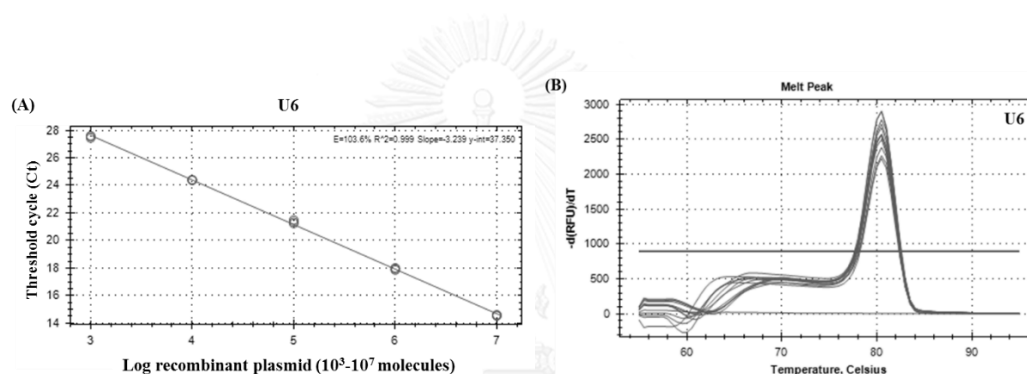


Figure 3. 15 Amplification efficiency curves of reference U6 recombinant plasmid (A). The dissociation curves of reference U6 from cDNA libraries after WSSV infection at 0, 6 and 48 hpi (B).

To verify the changes of expression level upon WSSV infection 16 selected miRNAs including miR-1-3p, miR-2a-3p, miR-7-5p, miR-9a-3p, miR-71-5p, miR-99a-3p, miR-100-5p, miR-184-3p, miR-190, miR-275-3p, miR-305-5p, miR-315, miR-317-3p, miR-750, miR-965 and bantam upon WSSV challenge, their expression levels in shrimp hemocyte at various time post-WSSV injection were evaluated by stem-loop quantitative real-time RT-PCR. In this study, U6 which was a non-coding small nuclear RNA was used as a reference gene. The cDNA of each specific RT-stem-loop miRNA prepared from total RNA of WSSV infected *P. monodon* hemocyte each time point (0, 6 and 48 hpi) were used as template.

First, the amplification efficiency of selected miRNAs was determined. A serial dilution of recombinant plasmid containing selected miRNA was used as a template

for standard curve construction. Real time PCR efficiency was calculated from the slope obtained from the curve plot of log dilutions of miRNA recombinant plasmid with threshold cycle (Ct) (Figure 3.16). The real time PCR efficiencies and melting temperature of each miRNA are shown in Table 3.6. The real time PCR efficiencies were unequal between miRNAs. Therefore, relative expression ratios of certain miRNA were calculated to correct differences in efficiency. The specificity of real time PCR results was assessed by dissociation curve analysis (Figure 3.17). The single peak at certain T_m was found in the dissociation curve indicating that a single product was amplified. The amplicon size of each miRNA PCR product was approximately 65 bp.

The expression ratios of miRNA at each time point after WSSV infection were calculated in relative to U6. Then, the fold change of the expression at each time point was calculated by normalizing to that of 0 hpi (Figure 3.18). The differentially expressed miRNAs upon WSSV infection were those have fold change higher than +1.5 or lower than -1.5. The results showed that the expression of 11 out of 16 miRNAs were altered following challenge. The expression level of miR-7-5p, miR-275-3p, miR-305-5p, miR-317-3p and bantam were unchanged both at 6 and 48 hpi. For miR-9a-5p, the expression was down-regulated at 6 hpi about 2.69 folds and recovered at 48 hpi to the same level as 0 hpi. The expression of miR-2a-3p, miR-71-5p, miR-99a-3p, miR-184-3p, miR-190 and miR-965 were unchanged at 6 hpi but decreased at 48hpi for 1.76, 1.61, 1.78, 3.12, 1.92 and 1.82 folds, respectively. For miR-100-5p, the expression was up-regulated 1.67 folds at 6 hpi but down-regulated 2.34 folds at 48 hpi. The expression of miR-1-3p was decreased 1.59 folds at 6 hpi but increased about 1.54 folds at 48 hpi. However, the interesting miR-315 expression was dramatically increased approximately 2.01 and 5.99 folds at 6 and 48 hpi, respectively. Another interesting miRNA was miR-750, the expression was sharply down-regulated for 11.78 and 9.63 folds at 6 and 48 hpi, respectively. The fold change results were summarized (Table 3.6).

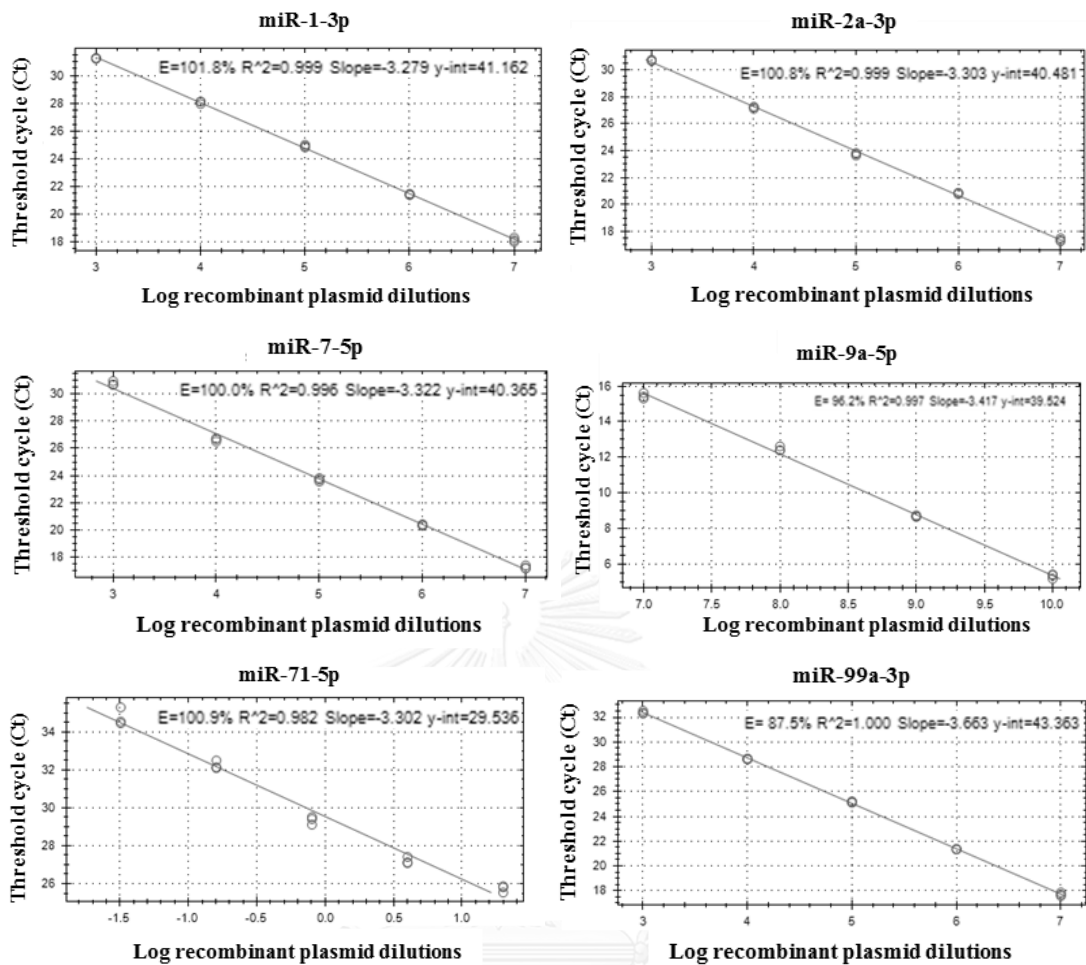


Figure 3. 16 Standard curves of miRNAs determined by stem-loop real-time RT-PCR; ten folds diluted-recombinant plasmid (10^3 to 10^7 molecules) of 16 miRNAs including miR-1-3p, miR-2a-3p, miR-7-5p, miR-9a-3p, miR-71-5p, miR-99a-3p, miR-100-5p, miR-184-3p, miR-190, miR-275-3p, miR-305-5p, miR-315, miR-317-3p, miR-750, miR-965 and bantam were amplified and analyzed on Bio-Rad CFX96 Real-time system.

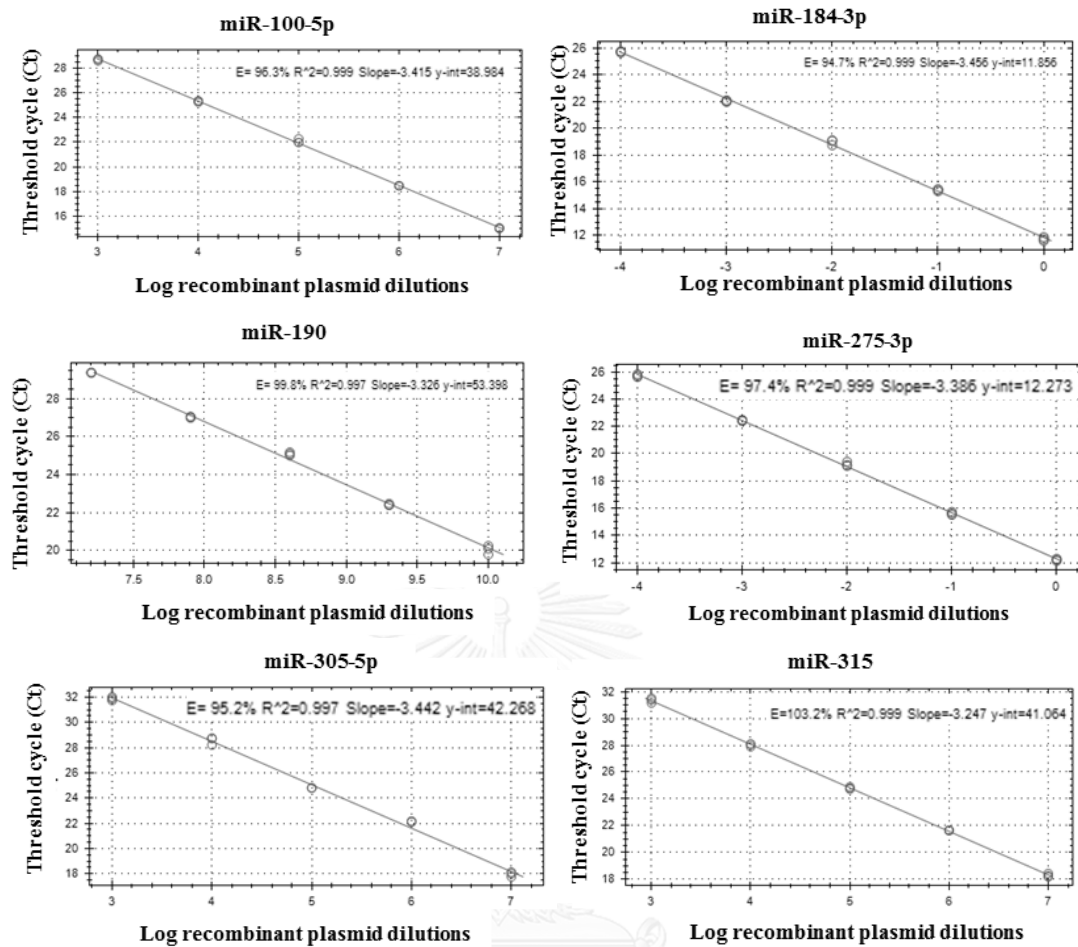


Figure 3.16 Standard curves of miRNAs determined by stem-loop real-time RT-PCR; ten folds diluted-recombinant plasmid (10^3 to 10^7 molecules) of 16 miRNAs including miR-1-3p, miR-2a-3p, miR-7-5p, miR-9a-3p, miR-71-5p, miR-99a-3p, miR-100-5p, miR-184-3p, miR-190, miR-275-3p, miR-305-5p, miR-315, miR-317-3p, miR-750, miR-965 and bantam were amplified and analyzed on Bio-Rad CFX96 Real-time system (continue).

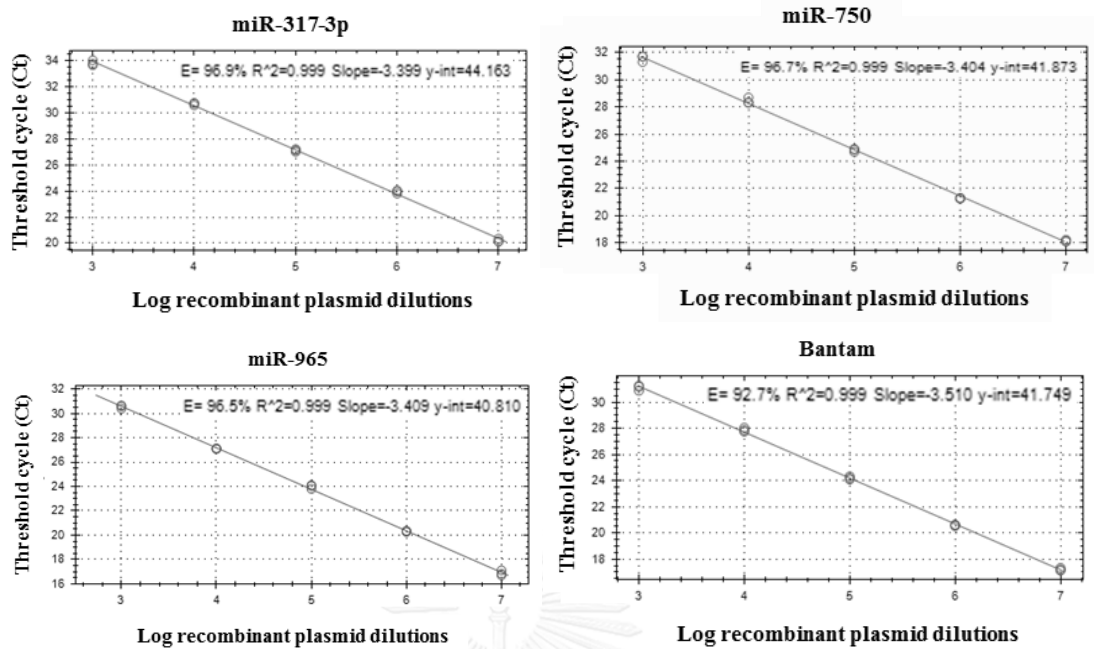


Figure 3.16 Standard curves of miRNAs determined by stem-loop real-time RT-PCR; ten folds diluted-recombinant plasmid (10^3 to 10^7 molecules) of 16 miRNAs including miR-1-3p, miR-2a-3p, miR-7-5p, miR-9a-3p, miR-71-5p, miR-99a-3p, miR-100-5p, miR-184-3p, miR-190, miR-275-3p, miR-305-5p, miR-315, miR-317-3p, miR-750, miR-965 and bantam were amplified and analyzed on Bio-Rad CFX96 Real-time system (continue).

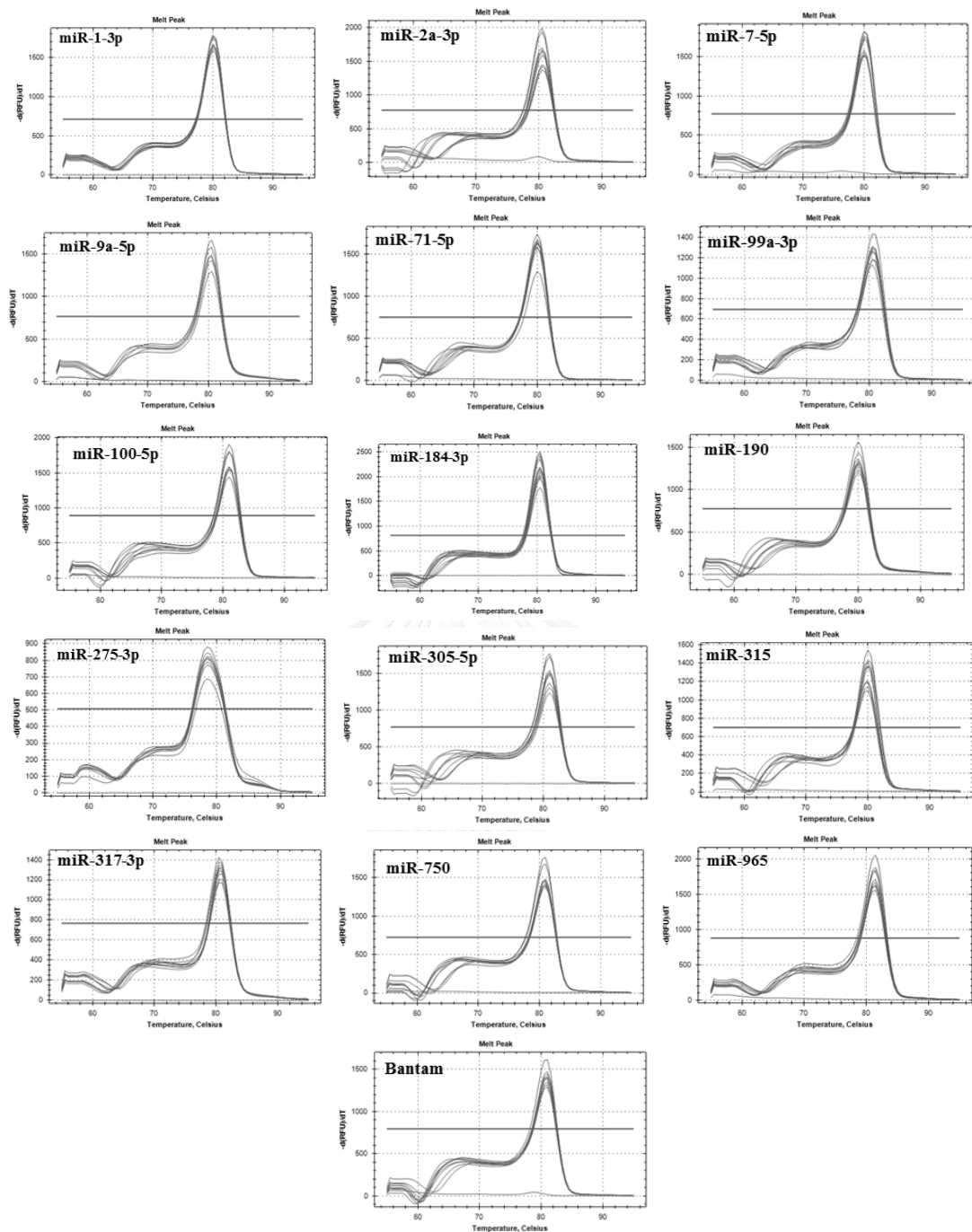


Figure 3. 17 The dissociation curves of miRNAs; miR-1-3p, miR-2a-3p, miR-7-5p, miR-9a-3p, miR-71-5p, miR-99a-3p, miR-100-5p, miR-184-3p, miR-190, miR-275-3p, miR-305-5p, miR-315, miR-317-3p, miR-750, miR-965 and bantam

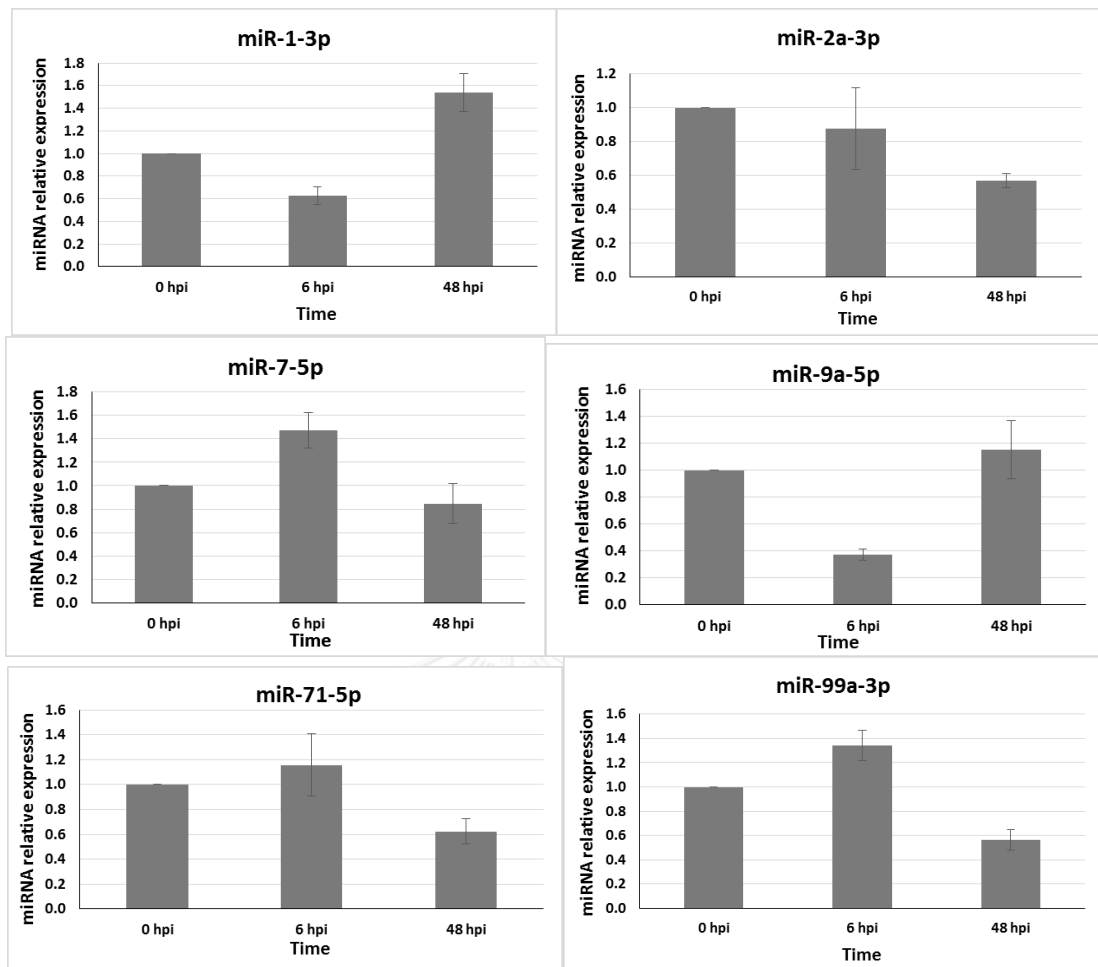


Figure 3. 18 Relative expression analysis of miRNAs in response to WSSV infection. Relative expression of miRNA transcript levels were determined in WSSV-infected *P. monodon* hemocyte by real-time RT-PCR, standardized against U6 as the internal reference, at 0, 6 and 48 hpi.

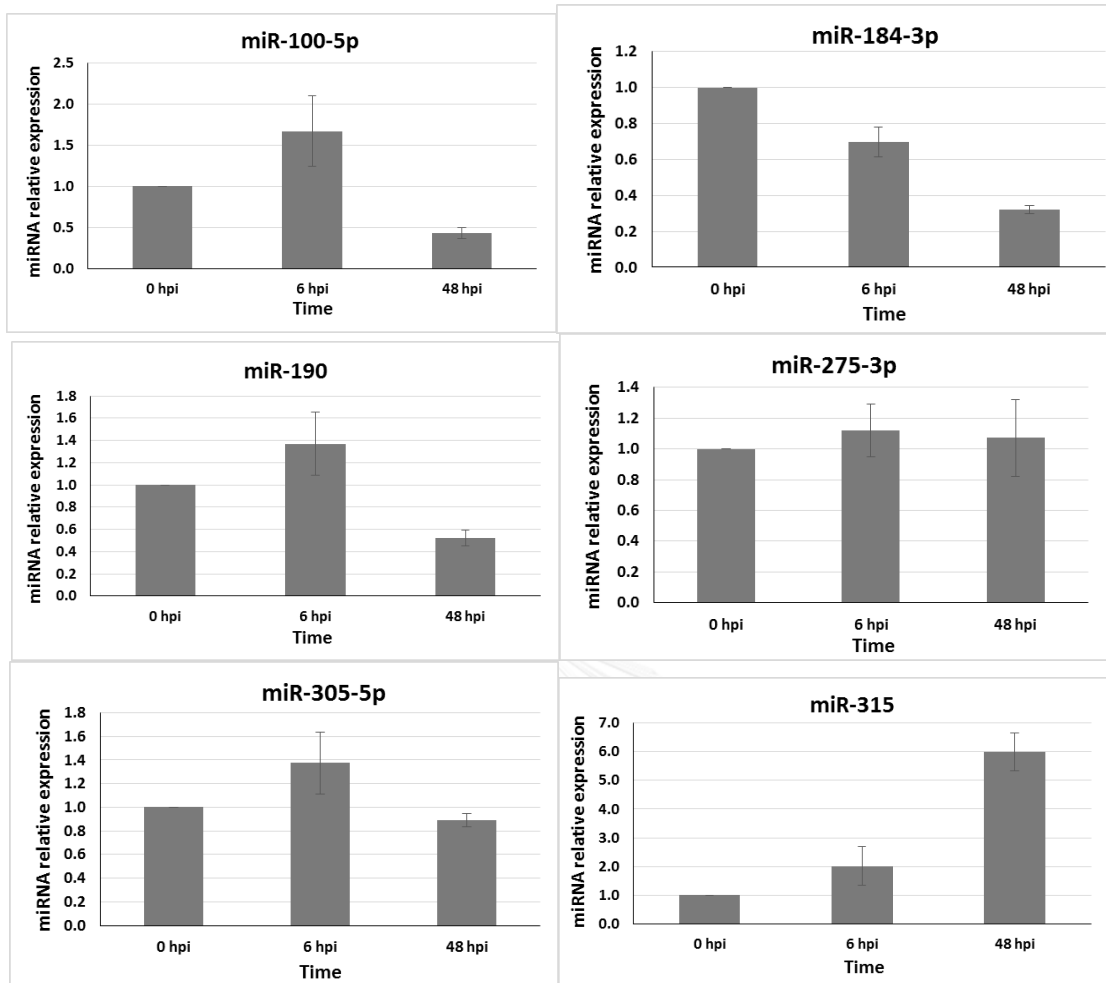


Figure 3.18 Relative expression analysis of miRNAs in response to WSSV infection. Relative expression of miRNA transcript levels were determined in WSSV-infected *P. monodon* hemocyte by real-time RT-PCR, standardized against U6 as the internal reference, at 0, 6 and 48 hpi (continue).

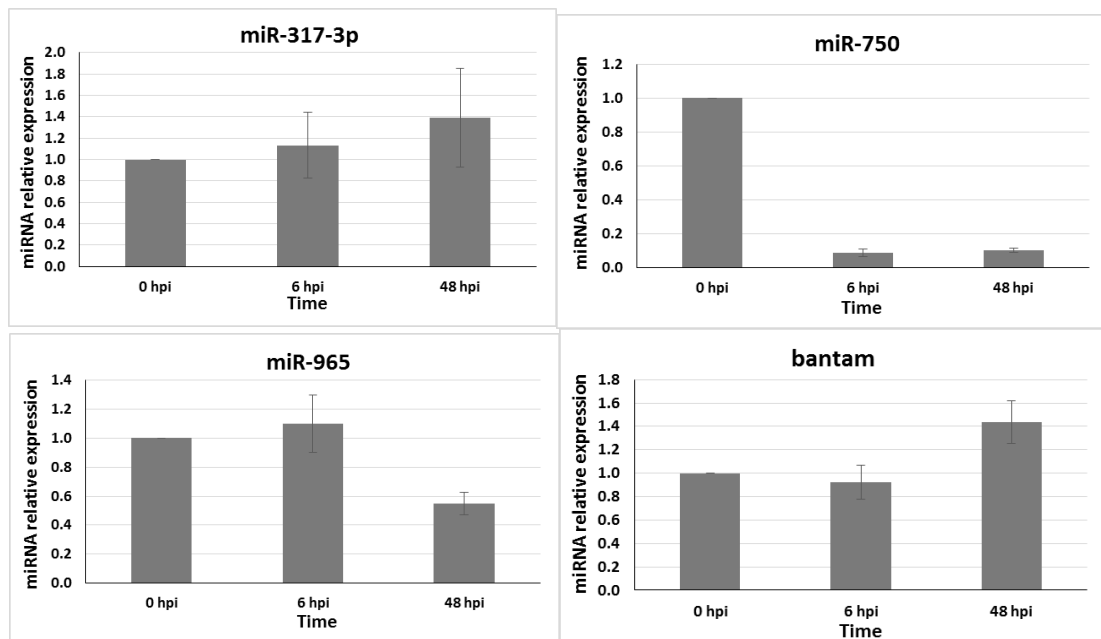


Figure 3.18 Relative expression analysis of miRNAs in response to WSSV infection. Relative expression of miRNA transcript levels were determined in WSSV-infected *P. monodon* hemocyte by real-time RT-PCR, standardized against U6 as the internal reference, at 0, 6 and 48 hpi (continue).

Table 3. 6 The PCR efficiency for each amplified miRNA, melting temperature and fold-change of expression upon WSSV infection at 6 and 48 hpi of each miRNA.

Sample	PCR efficiency	Melting temperature (°C)	Fold change of expression*	
			6hpi	48hpi
miR-7-5p	2.000	80.5	+1.48	-1.18
miR-275-3p	1.974	78.5	+1.12	+1.07
miR-305-5p	1.952	81.0	+1.38	-1.12
miR-317-3p	1.969	81.0	+1.13	+1.39
bantam	1.927	81.0	-1.08	+1.44
miR-9a-5p	1.947	80.5	-2.69	+1.15
miR-2a-3p	2.008	80.5	-1.14	-1.76
miR-71-5p	2.009	79.5	+1.16	-1.61
miR-99a-3p	1.875	80.5	+1.34	-1.78
miR-184-3p	1.962	80.0	-1.43	-3.12
miR-190	1.998	80.0	+1.37	-1.92
miR-965	1.965	81.5	+1.11	-1.82
miR-100-5p	1.963	81.0	+1.67	-2.34
miR-1-3p	2.018	80.0	-1.59	+1.54
miR-315	2.032	80.5	+2.09	+5.99
miR-750	1.967	81.0	-11.78	-9.63
U6	2.036	80.5	ND	ND

*Fold change in miRNA expression at 6 and 48 hpi in relative to at 0 hpi

+ means the up-regulation of the miRNA expression in relative to the expression level at 0 hpi

- means the down-regulation of the miRNA expression in relative to the expression level at 0 hpi

ND is not determined

3.6 miRNA target prediction

The data of the target mRNA of each miRNA identified could provide clues for miRNA function. In this study, bioinformatics analysis was performed against *P. monodon* EST sequencing databases.

Nowadays, the genome sequence of the shrimp is not available, so the *P. monodon* EST databases were used for mRNA target prediction. Because of the prediction program available on the internet is not applicable for the analyses using

EST sequences, this miRNA target prediction program was developed by Dr. Kulwadee Somboonviwat. The criteria use for this prediction were seed sequence (2-8 nucleotides from 5' end) of miRNA should perfect complementary to mRNA at any different regions; open reading frame (ORF), 3' untranslated region (3' UTR) and 5' untranslated region (5' UTR), and the overall complementary of miRNA to target mRNA should not lower than 65%. Also, the RNAhybrid software (<http://bibiserv.techfak.uni-bielefeld.de/rnahybrid/>) was used to analyze the structure of the miRNA-target mRNA hybrid and calculate the minimum free energy (mfe) of obtained structure (Table 3.8). The low mfe (<-20 kcal/mol) indicates likely spontaneous occurring of the uncomplicated secondary structure. The predicted target mRNAs of the identified *P. monodon* miRNAs were identified as shown in Table 3.7.



Table 3.7 miRNA targets of the identified *Penaeus monodon* miRNAs predicted against *P. monodon* EST and transcriptome databases

Function mRNA target	Target gene	miRNA (Target site)
Other immune molecules	Chitinase	miR-2898 (ORF)
	Autophagy-related protein 2-like protein	miR-275-3p (ORF), miR-92b-3p (ORF), miR-9a-5p (5'UTR, ORF)
	Beclin 1-associated autophagy-related key regulator	miR-750 (-), miR-9a-5p (-)
	Beclin-1-like protein	miR-1032 (ORF), miR-307a-3p (ORF, 3'UTR)
	Cj-cadherin	miR-2a (ORF, 3'UTR), miR-981 (ORF),
	Cadherin-23-like	miR-981 (ORF)
	Cadherin	miR-2001 (ORF), miR-9161 (ORF), miR-275-3p (ORF)
Proteinase/proteinase inhibitor	Serine proteinase inhibitor 7	miR-184-5p (ORF), miR-9a-5p (ORF)
	Kunitz-type serine protease inhibitor	bantam (3'UTR), miR-307a-3p (ORF), miR-6493-3p (5'UTR), miR-276a-3p (ORF)
	Serine protease snake	miR-6493-3p (ORF)
	Serine protease	miR-92b-3p (ORF), miR-1032 (ORF), miR-316 (ORF), bantam (ORF)
	Cathepsin C	miR-275-3p (ORF)
	Cathepsin D	bantam (3'UTR), miR-307a-3p (ORF), miR-9161 (3'UTR), miR-1260 (ORF)
	Alpha-2-macroglobulin isoform 3	miR-6237 (ORF)
Blood clotting system	Proclotting enzyme-like	miR-2a (-), miR-2a-3p (-), miR-2b (-)
Apoptotic tumor-related protein	Programmed cell death protein 2-like	miR-1000-5p (ORF)
	Programmed cell death protein	miR-184-5p (5'UTR)
	Cell death protein	miR-1000-5p (ORF), miR-184-5p (5'UTR)
	Cell death protein CED-3	miR-307a-3p (ORF)
	Caspase 2, apoptosis-related cysteine protease	miR-9a-5p (ORF)
	Apoptosis regulatory protein Siva	let-7-3p (ORF)
	Apoptosis-inducing factor, mitochondrion-associated	bantam (ORF), miR-2001 (ORF)
	Apoptotic chromatin condensation inducer in the nucleus	miR-316 (ORF), miR-9a-5p (ORF)
	Inhibitor of apoptosis protein	miR-6489-5p (ORF)

Table 3.7 miRNA targets of the identified *Penaeus monodon* miRNAs predicted against *P. monodon* EST and transcriptome databases (continue)

Function mRNA target	Target gene	miRNA (Target site)
ProPO system	Clip domain serine proteinase 2	miR-1260 (ORF), miR-2a (ORF)
	Prophenoloxidase-activating enzyme 1a	miR-315 (5'UTR)
Antimicrobial peptides	Crustin Pm4 antimicrobial peptide	miR-2a (ORF)
	Anti-lipopolysaccharide factor isoform 6	miR-315 (ORF)
	Anti-lipopolysaccharide factor isoform 3	miR-6489-5p (ORF)
	Penaeidin 3b antimicrobial peptide	miR-6493-5p (5'UTR), miR-981 (ORF)
	Lysozyme-like protein 1	miR-965 (ORF)
Signaling transduction	Calcium and integrin-binding protein 1	miR-9161 (3'UTR)
	Integrin alpha-8-like	miR-317-3p (5'UTR)
	Integrin	miR-317-3p (ORF), miR-92b-3p (5'UTR)
	Integrin-alpha FG-GAP repeat-containing protein 2-like	miR-34-5p (ORF)
	Inhibitor of Bruton tyrosine kinase	miR-9a-5p (ORF)
	Membrane-associated tyrosine- and threonine-specific cdc2-inhibitory kinase-like	miR-71-5p (ORF)
	Tyrosine-protein kinase	miR-8-5p (3'UTR), miR-981 (5'UTR)
	Leucine-rich repeat serine/threonine-protein kinase 1	miR-307a-3p (ORF), miR-981 (5'UTR), miR-6241 (ORF)
	Serine/threonine-protein kinase-like	miR-87-3p (ORF), miR-276a-3p (5'UTR), miR-33a-5p (5'UTR), bantam (ORF), miR-9a-5p (ORF), miR-1000-5p (ORF), miR-276a-3p (ORF)
	Serine/threonine-protein kinase	miR-981 (ORF), miR-2a-3p (3'UTR), let-7-5p (ORF), miR-305-5p (ORF), miR-4448 (ORF), miR-9a-5p (3'UTR)
	STE20-like serine/threonine-protein kinase	let-7-3p (3'UTR)
	Serine/threonine-protein phosphatase regulatory subunit gamma	bantam (ORF), miR-2001 (3'UTR)
	Major serine/threonine-protein phosphatase PP2A-2 catalytic subunit	miR-2a-3p (3'UTR)

Table 3.7 miRNA targets of the identified *Penaeus monodon* miRNAs predicted against *P. monodon* EST and transcriptome databases (continue)

Function mRNA target	Target gene	miRNA (Target site)
Heat-shock protein	cAMP-dependent protein kinase catalytic subunit	miR-275-3p (ORF)
	Activator of 90 kDa heat shock protein ATPase homolog 1	let-7-3p (ORF)
	HEAT repeat-containing protein	miR-2a-3p (3'UTR), miR-2b (3'UTR)
	HEAT repeat-containing protein-like	miR-282-5p (ORF)
	70kD heat shock-like protein	miR-6241 (ORF)
	Heat shock protein 70b	miR-471-5p (5'UTR, ORF), miR-99a-3p (5'UTR), miR-1-3p (3'UTR), miR-9a-5p (ORF)
	Heat shock protein	miR-9a-5p (ORF)
	Heat shock protein 40	miR-71-5p (3'UTR)
	Heat shock protein 67B2	miR-317-3p (ORF), miR-6237 (3'UTR), miR-6244 (ORF), miR-965 (ORF)
	DnaJ homolog dnj-2 precursor	miR-282-5p (ORF)
Oxidative stress	Thioredoxin	miR-71-3p (ORF)
	Thioredoxin domain-containing protein-like isoform	miR-2373-3p (ORF), miR-2a-3p (ORF), miR-2b (3'UTR)
	Glutathione peroxidase	miR-276a-3p (ORF), miR-9161 (5'UTR)
	Glutathione S-transferase	miR-6244 (ORF)
	Copper/zinc superoxide dismutase	miR-33a-5p (3'UTR)

Table 3. 8 Prediction of miRNA-target mRNA duplex structure using RNAhybrid software

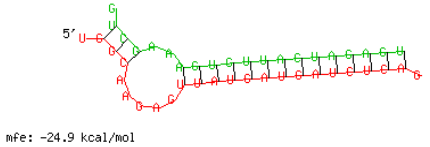
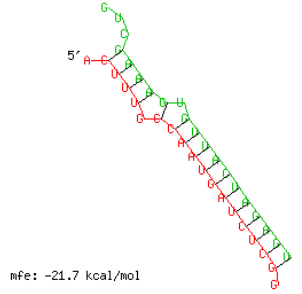
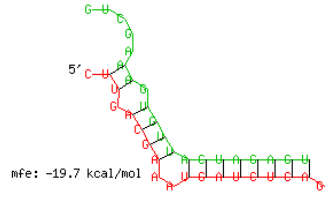
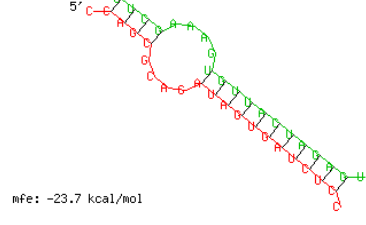
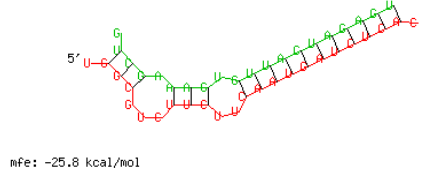
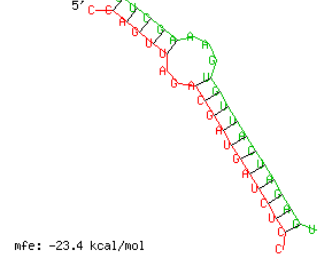
No	miRNA	Target gene	mfe (kcal/mol)	miRNA / target duplex
1	bantam	Apoptosis-inducing factor, mitochondrion-associated	-24.9	 <p>mfe: -24.9 kcal/mol</p>
2	bantam	Cathepsin D	-21.7	 <p>mfe: -21.7 kcal/mol</p>
3	bantam	Kunitz-type serine protease inhibitor	-19.7	 <p>mfe: -19.7 kcal/mol</p>
4	bantam	Serine protease	-23.7	 <p>mfe: -23.7 kcal/mol</p>
5	bantam	Serine/ threonine-protein kinase-like	-25.8	 <p>mfe: -25.8 kcal/mol</p>
6	bantam	Serine/threonine-protein phosphatase regulatory subunit gamma	-23.4	 <p>mfe: -23.4 kcal/mol</p>

Table 3. 8 Prediction of miRNA-target mRNA duplex structure using RNAhybrid software (continue)

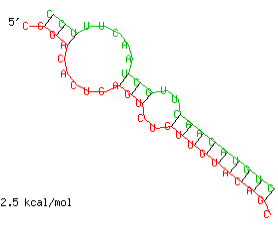
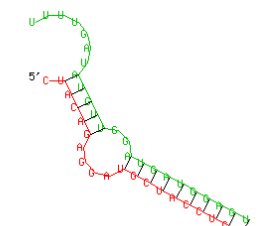
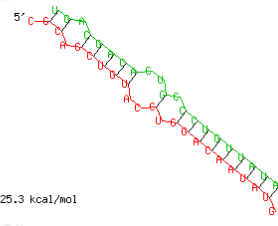
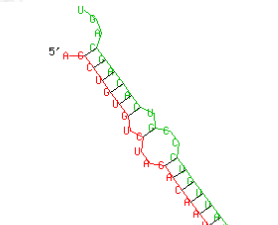
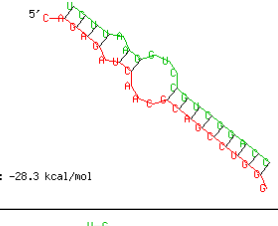
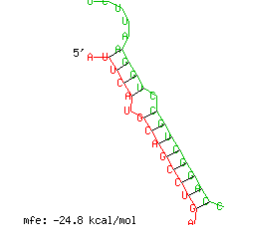
No	miRNA	Target gene	nfe (kcal/mol)	Structure interaction between miRNA and their target
7	let-7-3p	Apoptosis regulatory protein Siva	-22.5	 <p>nfe: -22.5 kcal/mol</p>
8	let-7-5p	Serine/threonine-protein kinase	-24.9	 <p>nfe: -24.9 kcal/mol</p>
9	miR-1000-5p	Cell death protein	-25.3	 <p>nfe: -25.3 kcal/mol</p>
10	miR-1000-5p	Serine/threonine-protein kinase-like	-23.7	 <p>nfe: -23.7 kcal/mol</p>
11	miR-1032	Beclin-1-like protein	-28.3	 <p>nfe: -28.3 kcal/mol</p>
12	miR-1032	Serine protease	-24.8	 <p>nfe: -24.8 kcal/mol</p>

Table 3. 8 Prediction of miRNA-target mRNA duplex structure using RNAhybrid software (continue)

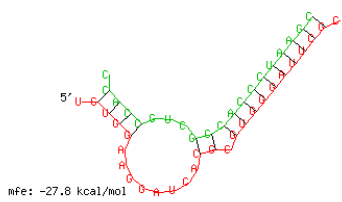
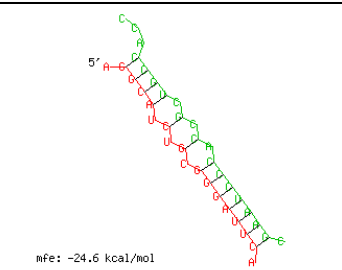
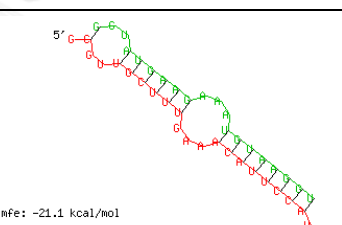
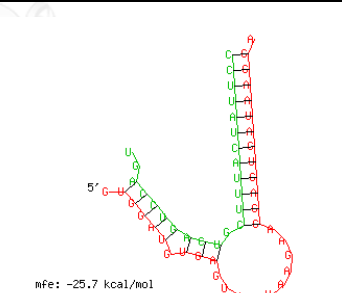
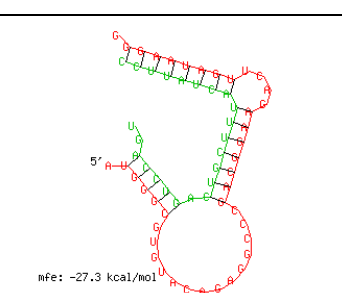
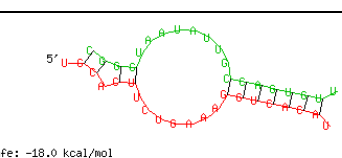
No	miRNA	Target gene	nfe (kcal/mol)	Structure interaction between miRNA and their target
13	miR-1260	Cathepsin D	-27.8	 <p>nfe: -27.8 kcal/mol</p>
14	miR-1260	Clp domain serine proteinase 2	-24.6	 <p>nfe: -24.6 kcal/mol</p>
15	miR-1-3p	Heat shock protein 70b	-21.1	 <p>nfe: -21.1 kcal/mol</p>
16	miR-184-5p	Cell death protein	-25.7	 <p>nfe: -25.7 kcal/mol</p>
17	miR-184-5p	Serine proteinase inhibitor 7	-27.3	 <p>nfe: -27.3 kcal/mol</p>
18	miR-2001	Apoptosis-inducing factor, mitochondrion-associated	-18.0	 <p>nfe: -18.0 kcal/mol</p>

Table 3. 8 Prediction of miRNA-target mRNA duplex structure using RNAhybrid software (continue)

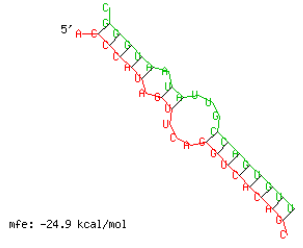
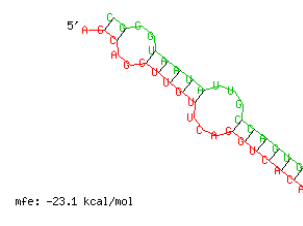
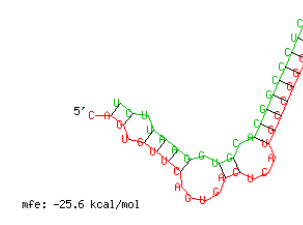
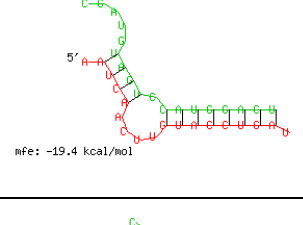
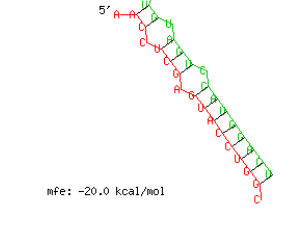
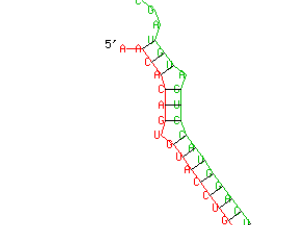
No	miRNA	Target gene	mfe (kcal/mol)	Structure interaction between miRNA and their target
19	miR-2001	Cadherin	-24.9	 <p>mfe: -24.9 kcal/mol</p>
20	miR-2001	Serine/threonine-protein phosphatase regulatory subunit gamma	-23.1	 <p>mfe: -23.1 kcal/mol</p>
21	miR-2373-3p	Thioredoxin domain-containing protein-like isoform	-25.6	 <p>mfe: -25.6 kcal/mol</p>
22	miR-275-3p	Autophagy-related protein 2-like protein	-19.4	 <p>mfe: -19.4 kcal/mol</p>
23	miR-275-3p	Cadherin	-20.0	 <p>mfe: -20.0 kcal/mol</p>
24	miR-275-3p	cAMP-dependent protein kinase	-23.8	 <p>mfe: -23.8 kcal/mol</p>

Table 3. 8 Prediction of miRNA-target mRNA duplex structure using RNAhybrid software (continue)

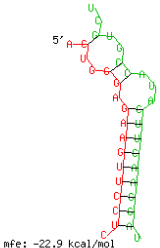
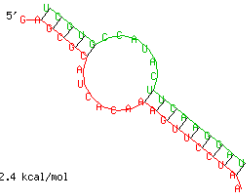
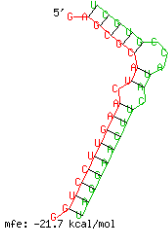
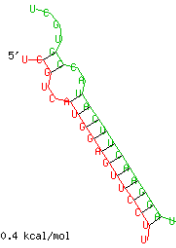
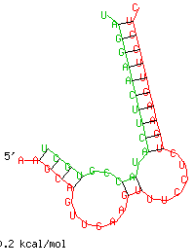
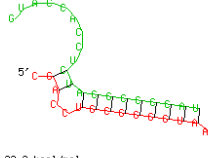
No	miRNA	Target gene	mfe (kcal/mol)	Structure interaction between miRNA and their target
25	miR-276a-3p	Glutathione peroxidase	-22.9	 mfe: -22.9 kcal/mol
26	miR-276a-3p	Serine/threonine-protein kinase-like	-22.4	 mfe: -22.4 kcal/mol
27	miR-276a-3p	Serine/threonine-protein kinase-like	-21.7	 mfe: -21.7 kcal/mol
28	miR-276a-3p	Serine/threonine-protein kinase-like	-20.4	 mfe: -20.4 kcal/mol
29	miR-276a-3p	Kunitz-type serine protease inhibitor	-20.2	 mfe: -20.2 kcal/mol
30	miR-2898	Chitinase	-23.2	 mfe: -23.2 kcal/mol

Table 3. 8 Prediction of miRNA-target mRNA duplex structure using RNAhybrid software (continue)

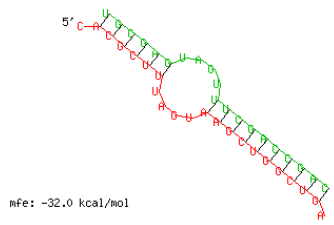
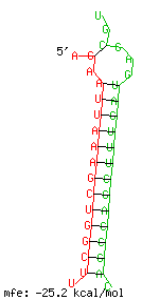
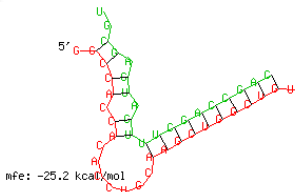
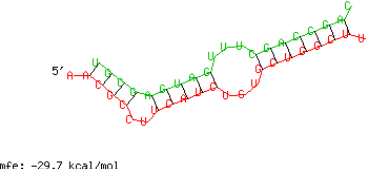
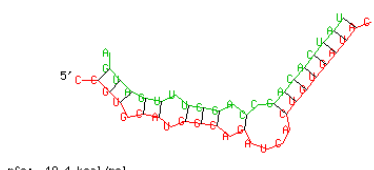
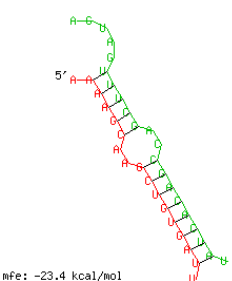
No	miRNA	Target gene	ΔH_{fe} (kcal/mol)	Structure interaction between miRNA and their target
31	miR-2a	Cadherin	-32.0	 <p>ΔH_{fe}: -32.0 kcal/mol</p>
32	miR-2a	Clip domain serine proteinase 2	-25.2	 <p>ΔH_{fe}: -25.2 kcal/mol</p>
33	miR-2a	Crustin Pm4 antimicrobial peptide	-25.2	 <p>ΔH_{fe}: -25.2 kcal/mol</p>
34	miR-2a	Proclotting enzyme	-29.7	 <p>ΔH_{fe}: -29.7 kcal/mol</p>
35	miR-2a-3p	Proclotting enzyme	-19.4	 <p>ΔH_{fe}: -19.4 kcal/mol</p>
36	miR-2a-3p	Serine/threonine-protein kinase	-23.4	 <p>ΔH_{fe}: -23.4 kcal/mol</p>

Table 3. 8 Prediction of miRNA-target mRNA duplex structure using RNAhybrid software (continue)

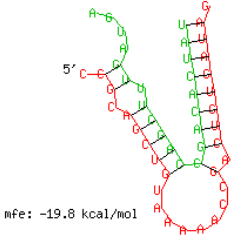
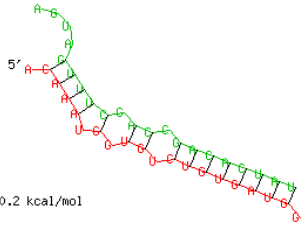
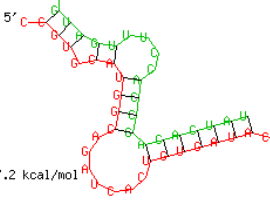
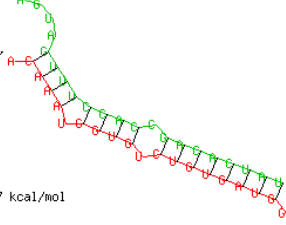
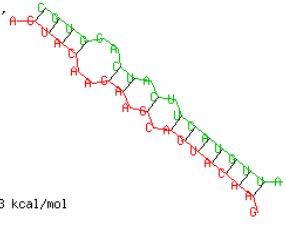
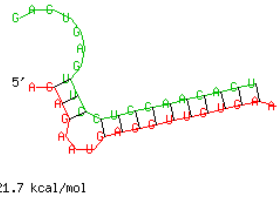
No	miRNA	Target gene	mfe (kcal/mo)	Structure interaction between miRNA and their target
37	miR-2a-3p	Major serine/threonine-protein phosphatase PP2A-2 catalytic subunit	-19.8	 <p>mfe: -19.8 kcal/mol</p>
38	miR-2a-3p	Thioredoxin domain-containing protein-like isoform	-20.2	 <p>mfe: -20.2 kcal/mol</p>
39	miR-2b	Proclotting enzyme	-17.2	 <p>mfe: -17.2 kcal/mol</p>
40	miR-2b	Thioredoxin domain-containing protein-like isoform	-24.7	 <p>mfe: -24.7 kcal/mol</p>
41	miR-305-5p	Serine/threonine-protein kinase	-18.3	 <p>mfe: -18.3 kcal/mol</p>
42	miR-307a-3p	Beclin-1-like protein	-21.7	 <p>mfe: -21.7 kcal/mol</p>

Table 3. 8 Prediction of miRNA-target mRNA duplex structure using RNAhybrid software (continue)

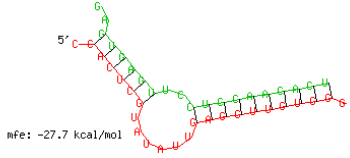
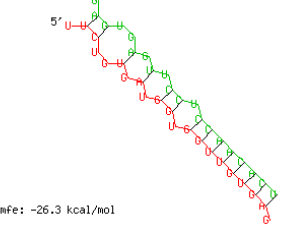
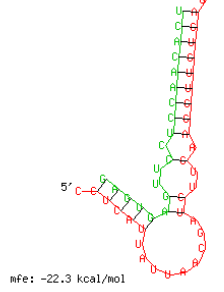
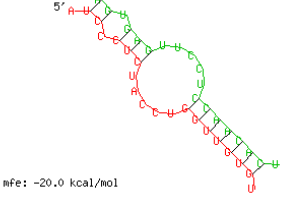
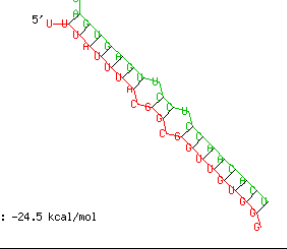
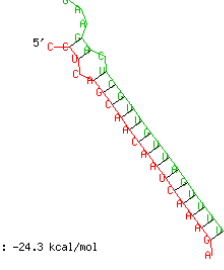
No	miRNA	Target gene	mfe (kcal/mol)	Structure interaction between miRNA and their target
43	miR-307a-3p	Beclin-1-like protein	-27.7	
44	miR-307a-3p	Cathepsin D	-26.3	
45	miR-307a-3p	Cell death protein CED-3	-22.3	
46	miR-307a-3p	Leucine-rich repeat serine/threonine-protein kinase 1	-20.0	
47	miR-307a-3p	Kunitz-type serine protease inhibitor	-24.5	
48	miR-315	Anti-lipopolysaccharide factor isoform 6	-24.3	

Table 3. 8 Prediction of miRNA-target mRNA duplex structure using RNAhybrid software (continue)

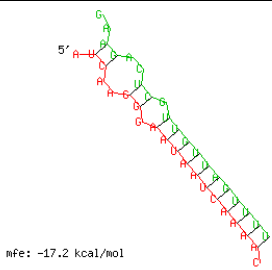
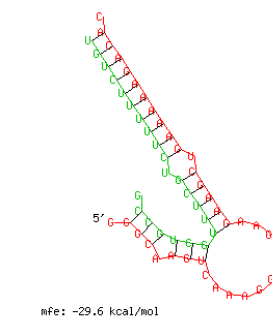
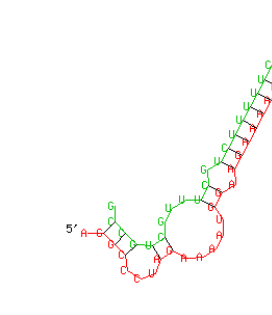
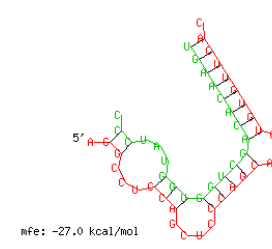
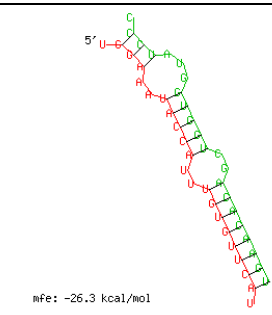
No	miRNA	Target gene	nfe (kcal/mol)	Structure interaction between miRNA and their target
49	miR-315	Prophenoloxidase-activating enzyme 1a	-17.2	 <p>nFe: -17.2 kcal/mol</p>
50	miR-316	Apoptotic chromatin condensation inducer in the nucleus	-29.6	 <p>nFe: -29.6 kcal/mol</p>
51	miR-316	Serine protease	-24.4	 <p>nFe: -24.4 kcal/mol</p>
52	miR-317-3p	Heat shock protein 67B2	-27.0	 <p>nFe: -27.0 kcal/mol</p>
53	miR-317-3p	Integrin	-26.3	 <p>nFe: -26.3 kcal/mol</p>

Table 3. 8 Prediction of miRNA-target mRNA duplex structure using RNAhybrid software (continue)

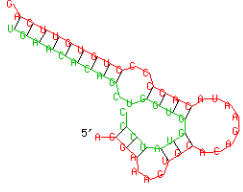
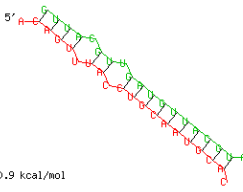
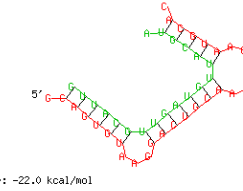
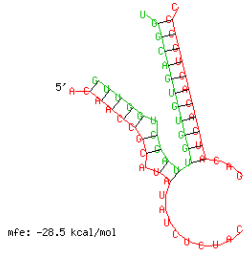
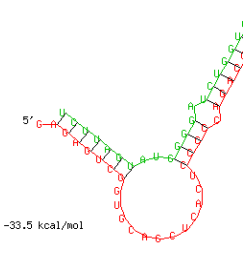
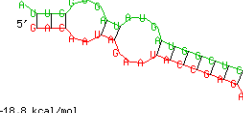
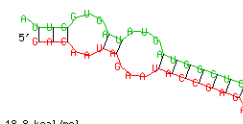
No	miRNA	Target gene	nfe (kcal/mol)	Structure interaction between miRNA and their target
54	miR-317-3p	Integrin	-25.3	 <p>nfe: -25.3 kcal/mol</p>
55	miR-33a-5p	Copper/zinc superoxide dismutase	-20.9	 <p>nfe: -20.9 kcal/mol</p>
56	miR-33a-5p	Serine/threonine-protein kinase-like	-22.0	 <p>nfe: -22.0 kcal/mol</p>
57	miR-34-5p	Integrin	-28.5	 <p>nfe: -28.5 kcal/mol</p>
58	miR-4448	Serine/threonine-protein kinase	-33.5	 <p>nfe: -33.5 kcal/mol</p>
59	miR-471-5p	Heat shock protein 70b	-18.8	 <p>nfe: -18.8 kcal/mol</p>
60	miR-471-5p	Heat shock protein 70b	-18.8	 <p>nfe: -18.8 kcal/mol</p>

Table 3. 8 Prediction of miRNA-target mRNA duplex structure using RNAhybrid software (continue)

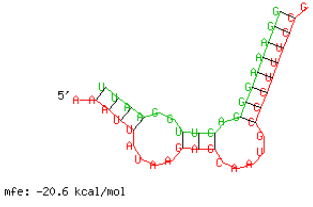
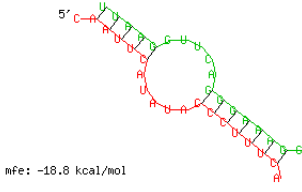
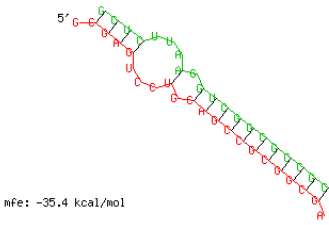
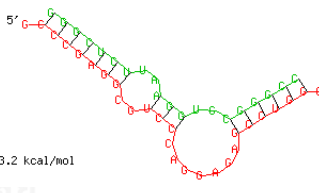
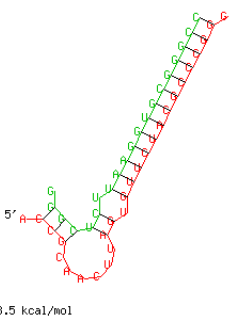
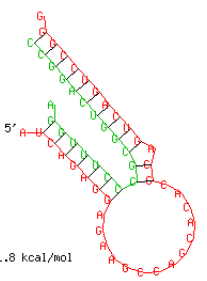
No	miRNA	Target gene	nfe (kcal/mol)	Structure interaction between miRNA and their target
61	miR-6237	Alpha-2-macroglobulin	-20.6	
62	miR-6237	Heat shock protein 67B2	-18.8	
63	miR-6241	Leucine-rich repeat serine/threonine-protein kinase 1	-35.4	
64	miR-6244	Glutathione S-transferase	-33.2	
65	miR-6244	Heat shock protein 67B2	-33.5	
66	miR-6489-5p	Anti-lipopolysaccharide factor isoform 3	-31.8	

Table 3. 8 Prediction of miRNA-target mRNA duplex structure using RNAhybrid software (continue)

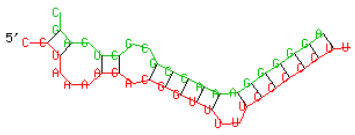
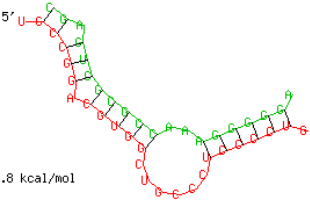
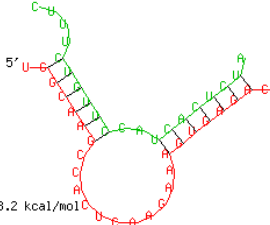
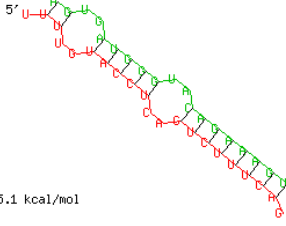
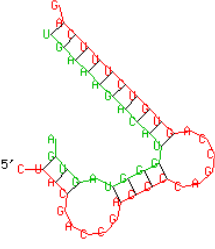
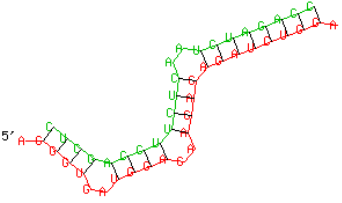
No	miRNA	Target gene	ΔG (kcal/mol)	Structure interaction between miRNA and their target
67	miR-6493-3p	Kunitz-type serine protease inhibitor	-26.6	 <p>mfe: -26.6 kcal/mol</p>
68	miR-6493-5p	Penaeidin 3b antimicrobial peptide	-26.8	 <p>mfe: -26.8 kcal/mol</p>
69	miR-71-3p	Thioredoxin	-18.2	 <p>mfe: -18.2 kcal/mol</p>
70	miR-71-5p	Heat shock protein 40	-25.1	 <p>mfe: -25.1 kcal/mol</p>
71	miR-71-5p	Membrane-associated tyrosine- and threonine-specific cdc2-inhibitory kinase-like	-24.1	 <p>mfe: -24.1 kcal/mol</p>
72	miR-750	Beclin 1-associated autophagy-related key regulator	-28.9	 <p>mfe: -28.9 kcal/mol</p>

Table 3. 8 Prediction of miRNA-target mRNA duplex structure using RNAhybrid software (continue)

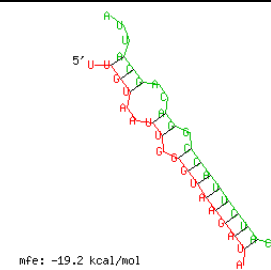
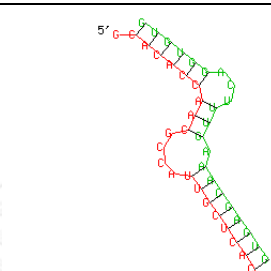
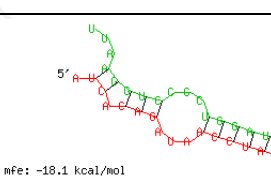
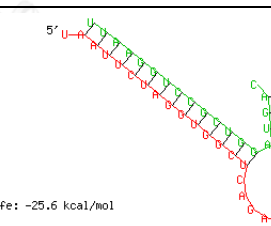
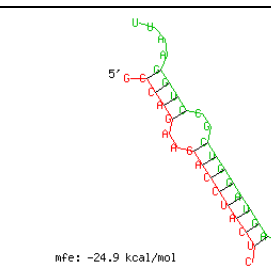
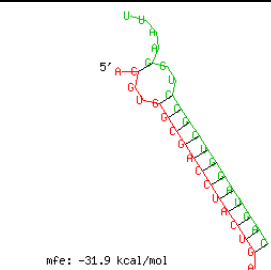
No	miRNA	Target gene	nfe (kcal/mol)	Structure interaction between miRNA and their target
73	miR-8-5p	Tyrosine-protein kinase	-19.2	 <p>nfe: -19.2 kcal/mol</p>
74	miR-87-3p	Serine/threonine-protein kinase-like	-25.7	 <p>nfe: -25.7 kcal/mol</p>
75	miR-9161	Integrin	-18.1	 <p>nfe: -18.1 kcal/mol</p>
76	miR-9161	Cathepsin D	-25.6	 <p>nfe: -25.6 kcal/mol</p>
77	miR-9161	Cadherin	-24.9	 <p>nfe: -24.9 kcal/mol</p>
78	miR-9161	Glutathione peroxidase	-31.9	 <p>nfe: -31.9 kcal/mol</p>

Table 3. 8 Prediction of miRNA-target mRNA duplex structure using RNAhybrid software (continue)

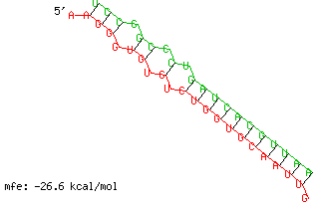
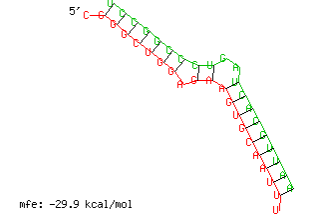
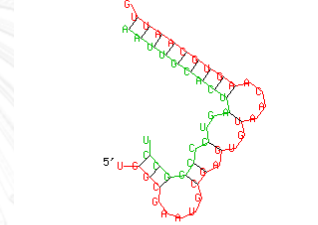
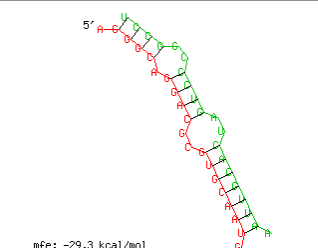
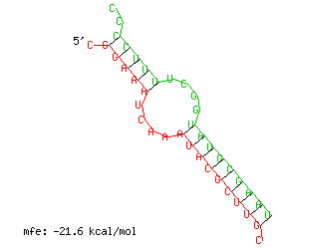
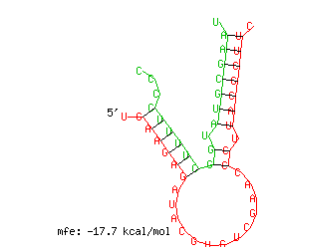
No	miRNA	Target gene	mfe (kcal/mol)	Structure interaction between miRNA and their target
79	miR-92b-3p	Autophagy-related protein 2-like protein	-26.6	 <p>mfe: -26.6 kcal/mol</p>
80	miR-92b-3p	Autophagy-related protein 2-like protein	-29.9	 <p>mfe: -29.9 kcal/mol</p>
81	miR-92b-3p	Integrin	-21.7	 <p>mfe: -21.7 kcal/mol</p>
82	miR-92b-3p	Serine protease	-29.3	 <p>mfe: -29.3 kcal/mol</p>
83	miR-965	Heat shock protein 67B2	-21.6	 <p>mfe: -21.6 kcal/mol</p>
84	miR-965	Lysozyme-like protein 1	-17.7	 <p>mfe: -17.7 kcal/mol</p>

Table 3. 8 Prediction of miRNA-target mRNA duplex structure using RNAhybrid software (continue)

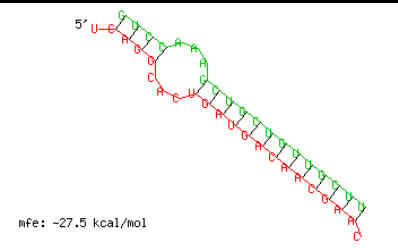
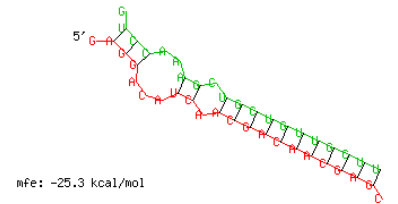
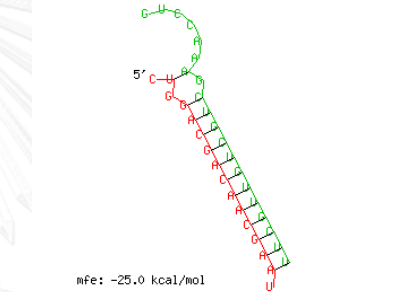
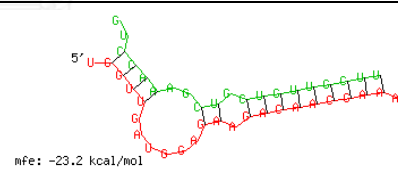
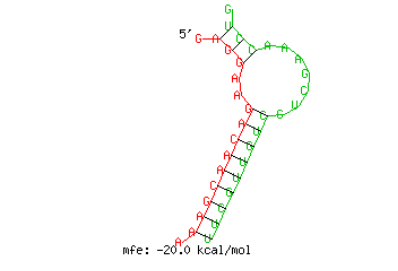
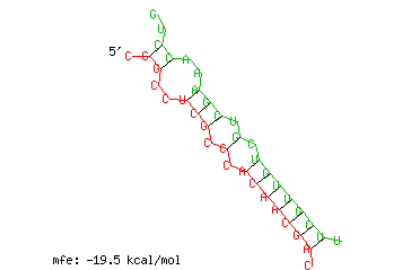
No	miRNA	Target gene	nfe (kcal/mol)	Structure interaction between miRNA and their target
85	miR-981	Cadherin	-27.5	 <p>nfe: -27.5 kcal/mol</p>
86	miR-981	Cadherin	-25.3	 <p>nfe: -25.3 kcal/mol</p>
87	miR-981	Serine/threonine-protein kinase	-25.0	 <p>nfe: -25.0 kcal/mol</p>
88	miR-981	Penaeidin 3b antimicrobial peptide	-23.2	 <p>nfe: -23.2 kcal/mol</p>
89	miR-981	Leucine-rich repeat serine/threonine-protein kinase 1	-20.0	 <p>nfe: -20.0 kcal/mol</p>
90	miR-981	Serine/threonine-protein kinase	-19.5	 <p>nfe: -19.5 kcal/mol</p>

Table 3. 8 Prediction of miRNA-target mRNA duplex structure using RNAhybrid software (continue)

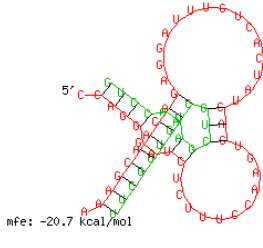
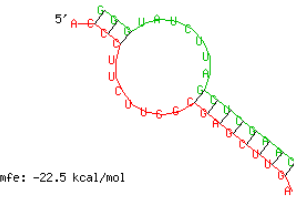
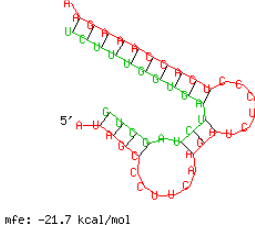
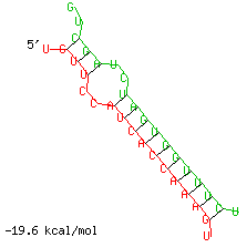
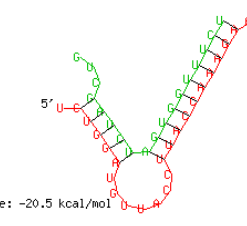
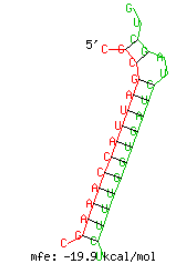
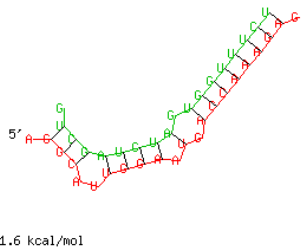
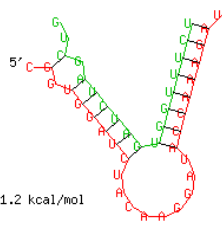
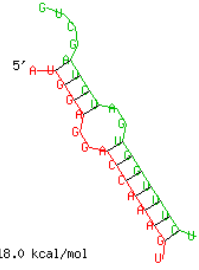
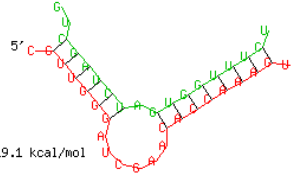
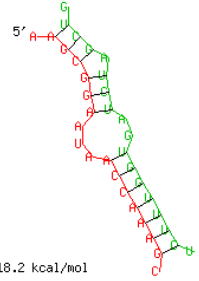
No	miRNA	Target gene	nfe (kcal/mol)	Structure interaction between miRNA and their target
91	miR-981	Tyrosine-protein kinase	-20.7	
92	miR-99a-3p	Heat shock protein 70b	-22.5	
93	miR-9a-5p	Apoptotic chromatin condensation inducer in the nucleus	-21.7	
94	miR-9a-5p	Autophagy-related protein 2-like protein	-19.6	
95	miR-9a-5p	Beclin 1-associated autophagy-related key regulator	-20.5	
96	miR-9a-5p	Caspase 2	-19.9	

Table 3. 8 Prediction of miRNA-target mRNA duplex structure using RNAhybrid software (continue)

No	miRNA	Target gene	nfe (kcal/mol)	Structure interaction between miRNA and their target
97	miR-9a-5p	Heat shock protein	-21.6	 <p>mfe: -21.6 kcal/mol</p>
98	miR-9a-5p	Heat shock protein 70	-21.2	 <p>mfe: -21.2 kcal/mol</p>
99	miR-9a-5p	Serine/threonine-protein kinase	-18.0	 <p>mfe: -18.0 kcal/mol</p>
100	miR-9a-5p	Serine/threonine-protein kinase	-19.1	 <p>mfe: -19.1 kcal/mol</p>
101	miR-9a-5p	Serine proteinase inhibitor 7	-18.2	 <p>mfe: -18.2 kcal/mol</p>

CHAPTER IV

DISCUSSIONS

In the recent years, there is growing evidence that miRNAs are involved in regulating genes of host and pathogenic viruses upon viral infection. The role of miRNAs in viral pathogenesis has been deeply studied in mammalian systems in which virus induced cellular miRNAs and virus-encoded miRNAs have been shown to influence the outcome of virus infection and regulation of the cellular responses (Cullen, 2011; Jopling et al., 2006; Pfeffer et al., 2004). The reports have revealed that after viral infection, (i) host miRNAs regulate their own transcripts as well as viral mRNAs to control viral infection (Hussain and Asgari, 2010; Jayachandran et al., 2013; Mehrabadi et al., 2013; Zhang et al., 2014a) (ii) viral miRNAs regulate both cellular and viral transcripts using host miRNA machinery to facilitate viral replication (Hussain et al., 2008; Hussain et al., 2012; Singh et al., 2012; Singh et al., 2014). In crustaceans, there were few studies investigating miRNAs that play essential roles in viral infection.

The black tiger shrimp *Penaeus monodon* is one of the main successfully species cultured worldwide. White spot syndrome disease is the major cause of the production loss. To fight against WSSV, shrimp rely on several immune effectors and pathways including proteins/genes, signaling pathways, apoptosis and RNA interference pathway (RNAi) (Liu et al., 2009a). RNA interference is one of many pathways that regulate the gene expression by the regulators siRNA or miRNA.

Several methods such as forward genetic experiment, cDNA sequencing and next generation sequencing, have been used for miRNA identification (Ambros and Lee, 2004; Friedlander et al., 2008; Lee et al., 1993). To date, next generation sequencing (NGS) technologies are quickly becoming the method of choice because it needs significantly low amount of starting material and gives more accurate and reliable sequencing result. Without the available shrimp genome sequences, our study applied next generation sequencing of small RNA libraries prepared from WSSV-infected *P. monodon* hemocyte and bioinformatic analysis to identify *P. monodon* miRNAs that are involved in antiviral response. To conduct NGS of shrimp small RNAs, we have tried

to construct small RNA libraries using 1 µg total RNA as recommended in the standard protocol. Unexpectedly, the sequencing could not be complete because the amount of cDNA is not enough for clustering on the flow cell. This problem was accomplished by small RNA enrichment and the addition of the PhiX control library to the sequencing in the second and the third trials. However, the number of raw reads obtained from the next-generation sequencing per run 1,686,108 reads and 2,186,083 reads for the second and the third trials, respectively, were extremely low when compared to miRNAs identified from WSSV-infected *Marsupenaeus japonicus* in lymphoid organ (~35 million reads) (Huang et al., 2012) and hemocyte (~9-12 million reads) (Yang et al., 2012). It should be noted that other than technical problem, the different in number of raw reads depended on the tissue used for the analysis. Sequence analysis from both trials identified a total of sixty miRNA homologs from hemocyte of WSSV-infected *P. monodon*. The percentage of miRNA homologs from WSSV-infected *P. monodon* hemocyte was approximately only 0.5-3% of raw reads, on the other hand, the percent of miRNA homologs in lymphoid organ of *M. japonicus* were about 70% of raw reads (Huang et al., 2012). This results indicated that our raw data contain high proportion of degraded contaminated RNAs such as mRNA, rRNA and tRNA. Because of the low ratio of miRNAs homologs, the miRNA expression profile in *P. monodon* hemocyte that response to WSSV could not be analyzed from NGS result. Therefore, the expression of miRNAs were further studied.

From sixty miRNA homologs identified from hemocyte of WSSV-infected *P. monodon* by searching against miRBase, some miRNA homologs were conserved and have been identified in various species. For examples, the most conserved miRNAs such as miR-1-3p, miR-263a-5p, miR-34-5p and miR-8-5p, have been found in *Drosophila melanogaster* (fruitfly) (Aravin et al., 2003; Lai et al., 2003; Ruby et al., 2007; Sempere et al., 2003; Stark et al., 2007), *Bombyx mori* (silkworm) (He et al., 2008; Liu et al., 2010; Tong et al., 2006; Yu et al., 2008), *Apis mellifera* (honey bee) (Chen et al., 2010; Weaver et al., 2007), *Mus musculus* (mouse) (Ahn et al., 2010; Chiang et al., 2010; Dostie et al., 2003; Lagos-Quintana et al., 2002; Landgraf et al., 2007; Zhu et al., 2010), *Homo sapiens* (human) (Dostie et al., 2003; Koh et al., 2010; Landgraf et al., 2007; Lim et al., 2003a; Lui et al., 2007), *Caenorhabditis elegans* (roundworm) (Ambros et al.,

2003; Grad et al., 2003; Kato et al., 2009; Lagos-Quintana et al., 2001; Lau et al., 2001; Lee and Ambros, 2001; Lim et al., 2003b; Ruby et al., 2006; Warf et al., 2011; Zisoulis et al., 2010) and *Daphnia pulex* (Wheeler et al., 2009). Moreover, miR-100-5p, miR-12-5p, miR-33a-5p, miR-7-5p, miR-9a-5p and miR-193 which found in *P. monodon* have been identified in several species whose data available in miRBase except in *C. elegans*. Some miRNAs including miR-252-3p, miR-2a-3p, miR-307a-3p, miR-92b-3p, bantam, miR-275-3p, miR-276a-3p, miR-279, miR-305-5p, miR-317-3p, miR-71-5p and miR-965, have been found only in arthropod (Aravin et al., 2003; Chen et al., 2010; He et al., 2008; Lai et al., 2003; Liu et al., 2010; Ruby et al., 2007; Sempere et al., 2003; Stark et al., 2007; Tong et al., 2006; Weaver et al., 2007; Wheeler et al., 2009; Yu et al., 2008). Two miRNAs, miR-99a-3p and miR-1260, were previous identified in vertebrates, *M. musculus* and *H. sapiens*. Moreover, other three miRNAs; miR-6489-5p, miR-6493-3p and miR-6493-5p, were the homologs of known miRNAs of *M. japonicus* in miRBase (Huang et al., 2012). In the current study, only miRNA homologs were reported. The remaining unknown sequences will be further predicted against *P. monodon* EST database and WSSV genome to identify either novel host miRNAs or WSSV miRNAs by computational prediction techniques (Chiang et al., 2010; Leclercq et al., 2013).

There are three main methods for validating small RNAs identified by high-throughput approaches and quantifying miRNA expression level including Northern blot (Alwine et al., 1977; Kevil et al., 1997; Valoczi et al., 2004), PCR (Raymond et al., 2005; Schmittgen et al., 2008; Shi and Chiang, 2005) and microarray (Liu et al., 2004; Wang and Wang, 2006). After sequence analysis and miRNA homologs identification, the miRNA expression level in hemocyte of WSSV-challenged *P. monodon* was determined. Although, Northern blot analysis is less sensitive than other methods, it can demonstrate the size of mature miRNAs and pre-miRNAs products and quantitate the expression level of miRNAs (Kim et al., 2010; Varallyay et al., 2008). The most popular probe-labeling protocol used for Northern blot analysis is based on incorporation of radioisotope (^{32}P). However, isotope labeling is often inconvenient and hazardous. A safer methods of non-isotopic labeling with dioxigenin were used to detect small RNAs (Holtke and Kessler, 1990; Ramkissoon et al., 2006).

However, the modification of nucleotide, called locked nucleic acid (LNA), increase the sensitivity of the non-isotopic northern blot analysis (Valoczi et al., 2004). LNA-modified oligonucleotides have been shown to exhibit improved thermal stability when hybridized to their target molecules (Braasch and Corey, 2001). By the reason of high cost of LNA, the unmodified nucleotides were used as a probes in ours study. Because of the limitation of DIG-labeled oligonucleotide probe sensitivity and very low level of miRNA expression, only two miRNAs, miR-71-5p and let-7-5p, could be detected. Our results showed that in hemocyte of WSSV-infected *P. monodon*, expression of miR-71-5p and let-7-5p did not change at 6 hpi but down-regulated at 48 hpi. On contrary, after WSSV infection in *M. japonicus*, Northern blot analysis revealed that the expression of miR-71 and let-7 in lymphoid organ was up-regulated after WSSV infection at 6, 24 and 48 hours (Huang et al., 2012).

As stated before that Northern blot analysis has limitation in the detection of miRNA expression, stem-loop real-time PCR was used instead. The stem-loop quantitative RT-PCR is an accurate and sensitive detection for quantitating the miRNA expression level (Chen et al., 2005a). The result of miR-71-5p expression analysis from Northern blot and stem-loop real-time PCR was coincident. However, stem-loop real-time RCR of let-7-5p was not performed.

Stem-loop real-time PCR analysis of 16 miRNAs from *P. monodon* hemocyte revealed that 11 of them are differentially expressed upon WSSV infection. Previous reports indicated that expression of miRNAs in different tissues are diverse (Huang et al., 2014). According to our report, the expression of miR-7-5p in WSSV-infected *P. monodon* hemocyte was stable at 0, 6 and 48 hpi, but in *M. japonicus* lymphoid organ, the expression of miR-7 was reduced after WSSV infection at 6, 24 and 48 hours. The expression of miR-275 was increased upon WSSV infection in *M. japonicus* lymphoid organ at 0-48 hours, but did not change in the hemocyte of WSSV-challenged *P. monodon*. In hemocyte, *P. monodon* miR-100 expression was up-regulated at 6 hpi but decreased at 48 hpi, whereas; miR-100 of WSSV-infected *M. japonicus* lymphoid organ constantly expressed at 0-24 hpi but increased at 48 hpi. For miR-965, the expression level was down-regulated at 48 hpi in WSSV-infected *P. monodon* hemocyte but in *M. japonicus* lymphoid organ, the expression of miR-965 did not

change after WSSV infection from 0-48 hours. However, in *M. japonicus*, mjn-miR-444 (miR-184-3p) expressed in hemocyte of WSSV-infected shrimp was down-regulated at 36 hpi and 72 hpi (Ruan et al., 2011), respectively, our result shared similar pattern of miR-184-3p expression but differ in time response. This might be cause by the different WSSV dosage used for infection.

Two out of 11 differentially expressed miRNAs identified such as miR-315 and miR-750, were highly responded to WSSV infection. As observed in WSSV-infected *M. japonicus* lymphoid organ, the expression of miR-315 from hemocyte were extremely up-regulated at late phase of WSSV infection (Huang et al., 2012). In giant freshwater prawn, *Macrobrachium rosenbergii*, tissue distribution analysis showed that miR-750 was highly expressed in hepatopancreas but its expression in hepatopancreas did not altered after Infectious hypodermal and hematopoietic necrosis (IHHNV) challenge (Tan et al., 2013). On other the hand, miR-750 expression level was dramatically down-regulated after WSSV infection in *P.monodon* hemocyte.

In order to characterize functions of miRNAs identified in *P. monodon* in antiviral response against WSSV infection, the target mRNAs of each miRNA were predicted. Because *P. monodon* genome sequence is not available, the *P. monodon* EST database was used in this analysis. Currently, very few freeware for miRNA target analysis are available and some of those are not compatible to our reference database, so our group developed a new platform for *P. monodon* miRNA target identification. To analyze the putative target mRNA for the identified miRNAs, the following criteria such as; the complementarity between miRNAs and target sites, the thermal stability of miRNA/mRNA duplex, no complicated secondary structure at miRNA target sites, were taken into consideration (Alexiou et al., 2009; Witkos et al., 2011). Our in-house program predicted the target mRNA base on the perfect complementary match of miRNA seed sequence to the target mRNAs. Most of the miRNA prediction algorithm are limited to browse the 3'UTR of mRNAs. However, 3'UTR is not the only binding region for miRNAs, there are also sites located in 5'UTR or even within coding DNA sequence of mRNAs (Akbari Moqadam et al., 2013; Forman and Coller, 2010; Moretti et al., 2010; Wei et al., 2011). From the miRNA target prediction, the analyzed miRNAs were found to target on all three regions of the mRNA including 3'UTR, ORF and 5'UTR.

Moreover, perfect seed base-pairing is not always an essential factor for miRNA-mRNA binding; mismatch of seed sequence miRNA against mRNA may also happen (Chi et al., 2012; Shin et al., 2010; Wei et al., 2011). As a result, the percentage of false-positive and false-negative finding is substantial in the miRNA target discovery. Therefore, miRNA-target interactions should be experimentally confirmed using *in vitro* miRNA reporter assay (Watanabe et al., 2006) and *in vivo* silencing or enhancing of miRNA in shrimp (Huang et al., 2014).

In fact, a single gene can be regulated by multiple miRNAs, and likewise, a single miRNA might target more than one mRNA. In *C. elegans*, the regulation of miR-71 was involved in lifespan according to the signaling from gonad, the nervous system and the intestine (Boulias and Horvitz, 2012). The 3'UTR of miR-71 target gene was predicted against *Litopenaeus vannamei* EST by TargetScan and miRanda algorithms, and was identified as serine protease (Huang et al., 2012). Moreover, inhibition or activation of innate immune reaction in *M. japonicus* revealed that miR-71 in hemocyte was involved in regulation of apoptosis, phagocytosis and phenoloxidase pathways (Yang et al., 2012). From our results, miR-71-5p might regulate heat-shock protein 40 (Hsp40) which co-operates with Hsp70 to facilitate protein folding of nascent protein (Li et al., 2009) and tyrosine kinase the key enzyme in signaling pathway. In the A549, human lung adenocarcinoma epithelial cell line, the expression level of Hsp70 and Hsp40 were up-regulated during CELO avian adenovirus replication (Glotzer et al., 2000). Hsp40 was also shown to be crucial for enhancement of HIV-1 gene expression and replication (Kumar and Mitra, 2005). Down-regulation of miR-71-5p at 48 hpi in WSSV-infected *P. monodon* hemocyte, implied that the expression of its target Hsp40 might up-regulated at late phase of WSSV infection to activate of WSSV replication.

The target prediction of miRNA targets, heat shock protein 70 (Hsp70) from *P. monodon* EST database was regulated by miR-1-3p. Hsp70 plays a role in the host stress response by acting as a molecular chaperone which is critical for protein folding, membrane translocation, and degradation of misfolded proteins. During viral infection, viruses also need cellular chaperones for their own protein folding processes and Hsp70 is the major inducible heat shock protein frequently recruited by virus (Lahaye

et al., 2012). The up-regulation of the Hsp70 induced by WSSV infection was also observed in mudcrab hemolymph (Liu et al., 2011). Moreover, the increasing of Hsp70 expression could enhance the resistance of *P. clarkii* to WSSV infection (Wu et al., 2014). In WSSV-infected *L. vannamei*, the expression of Hsp70 mRNA level was up-regulated from 6-12 hpi and gradually down-regulated at 24 and 48 hpi (Li et al., 2014). From our result, the decrease at 6 hpi and increase at 48 hpi in miR-1-3p expression level implied that miR-1-3p might be important to Hsp70 regulation during WSSV infection.

In *Spiroplasma eriocheiris* infected *P. clarkii*, miR-184 was up-regulated after the infection and targeted Notch signaling pathway gene (Ou et al., 2013). In *D. melanogaster*, miR-184 expression pattern changed during the development of embryo, especially in the central nervous system (Li et al., 2011). The alpha-2-macroglobulin and transferrin gene in *L. vannamei* were targeted by miR-184 (Yang et al., 2012). According to our in-house software prediction, miR-184-5p targeted immune-related genes such as program cell-death protein, a protein required for apoptosis (Liu et al., 2014), and serine protease inhibitor 7 (*PmSERPIN7*). *PmSERPIN7* shared similarity approximately 94% to serine protease inhibitor in *F. chinensis* (*FcSERPIN*) (Homvises et al., 2010). Amino acid sequence analysis indicated that *FcSERPIN* may have inhibitory activity against prophenoloxidase activating proteinase (PAP) and clotting enzyme which were the important immune-related protein in shrimp (Liu et al., 2009b). We speculated that the decrease in miR-184-5p expression at 48 hours after WSSV infection, might cause an increase in the expression of *PmSERPIN7* and program cell death. These could help shrimp to defend against invading WSSV.

Previous report in *D. melanogaster* showed that miR-315 inhibited Axin and Notum, thereby regulating Wingless pathway (Silver et al., 2007). Moreover, in *P. clarkii*, phosphoenolpyruvate carboxylkinase (PEPCK) in insulin signaling pathway was regulated by miR-315 (Ou et al., 2013). From our prediction, the target gene of miR-315 in *P. monodon* was anti-lipopolysaccharide isoform 6 (*ALFPm6*) and prophenoloxidase-activating enzyme 1a (*PmPPAE1*). These miR-315 target genes are important immune effectors against pathogen infections in shrimp (Charoensapsri et al., 2009; Ponprateep et al., 2012). Upon challenge with WSSV, the *ALFPm6* transcript

expression levels in hemocyte highly increased at 12 hpi, and then decreasing rapidly at 24 hpi before being up-regulated again at 48 hpi (Ponprateep et al., 2012). In contrast, the expression level of miR-315 was extremely up-regulated after WSSV infection, *ALFPm6* which is its putative target should be gradually down-regulated. This contradiction of miRNA and target gene expression revealed that *ALFPm6* gene expression might be controlled by other signaling pathway.

Prophenoloxidase activating system serves an important roles in innate immune responses. The pattern-recognition receptor (PRRs) recognized the structure of pathogens which activated serine proteinase cascade to trigger the melanization. The *PmPPAE1* in hemocyte was highly decreased after bacterial infection at 0-24 hpi and recovered to the higher level at 48 hpi (Charoensapsri et al., 2009). Also, it has been reported that proPO system play role in fighting against WSSV infection (Amparyup et al., 2012). The increasing of miR-315 expression at 48 hpi post-WSSV infection might suppress the expression of *PmPPAE1* transcript to control proPO activation at the late phase of WSSV infection.

Autophagy is an evolutionarily conserved process that is responsible for the removal of damaged organelles and long-lived proteins for recycling. Moreover, it is also a process that enables cells to cope with stresses including pathogen infection. Accumulative evidence showed that some viruses suppress this pathway for their survival, while others enhance or exploit this pathway to benefit their replication (Sir and Ou, 2010). From our prediction, Beclin 1 associated autophagy-related key regulator is Beclin1-binding protein. Binding of Beclin1-associated autophagy-related key regulator to Beclin1 promote autophagy (Kang et al., 2011). The decrease in miR-750 expression level implied that upon WSSV infection autophagy process might be activated as a result of viral degradation.

Lysozyme plays a role as a bio-defense molecule in the innate immunity against the invasion of bacterial pathogens by catalyzing the hydrolysis peptidoglycan in the bacterial cell walls (Qasba and Kumar, 1997). The miR-965 was predicted to target i-type lysozyme-like protein 1, so it might be important in bacterial and viral immune response.

In *Bombyx mori*, *Bm-ase* gene that is involved in the nervous system and peripheral nervous system, myogenesis, blood corpuscles formation, sex determination, midgut development in metazoans was regulated by miR-9a (Song et al., 2013). In our prediction, miR-9a-5p could regulate caspase 2 gene. Apoptosis, a cell suicide program that is used to remove damaged cells, plays important roles in immune system by preventing the virus invasion (Everett and McFadden, 1999). The caspase is the key enzyme in activated apoptosis pathway. So, the down regulation of miR-9a-5p expression at 6 hpi might implied that apoptosis pathway was activated by increasing of caspase 2 level causing the reduction of WSSV infection.

So far, most studies on miRNAs have focused on the development of organism. But there are some research reported that miRNAs also function in immune system. In *M. sexta*, microRNAs were identified and predicted to target mRNA of pattern recognition protein, pro-phenoloxidase, antimicrobial peptide, and conserved intracellular signal transduction (Toll, IMD, JAK-STAT, MAPK-JNK-p38, and small interfering RNA pathways) (Zhang et al., 2014b). Moreover, miRNAs in *M. japonicus* were characterized to be involved in innate immunity, including the cell-based immunity (mainly apoptosis and phagocytosis) and the humoral immunity (such as pro-phenoloxidase system) (Yang et al., 2012). In our study, miRNAs that are involved in shrimp immune responses were identified (Figure 4.1). The identified immune-related target genes were proteinase or proteinase inhibitor, blood clotting system, apoptosis-related protein, pro-phenoloxidase system, antimicrobial peptide, signal transduction, heat shock protein and oxidative stress. The information obtained strongly indicated that miRNAs play essential role in shrimp immunity against viral infection.

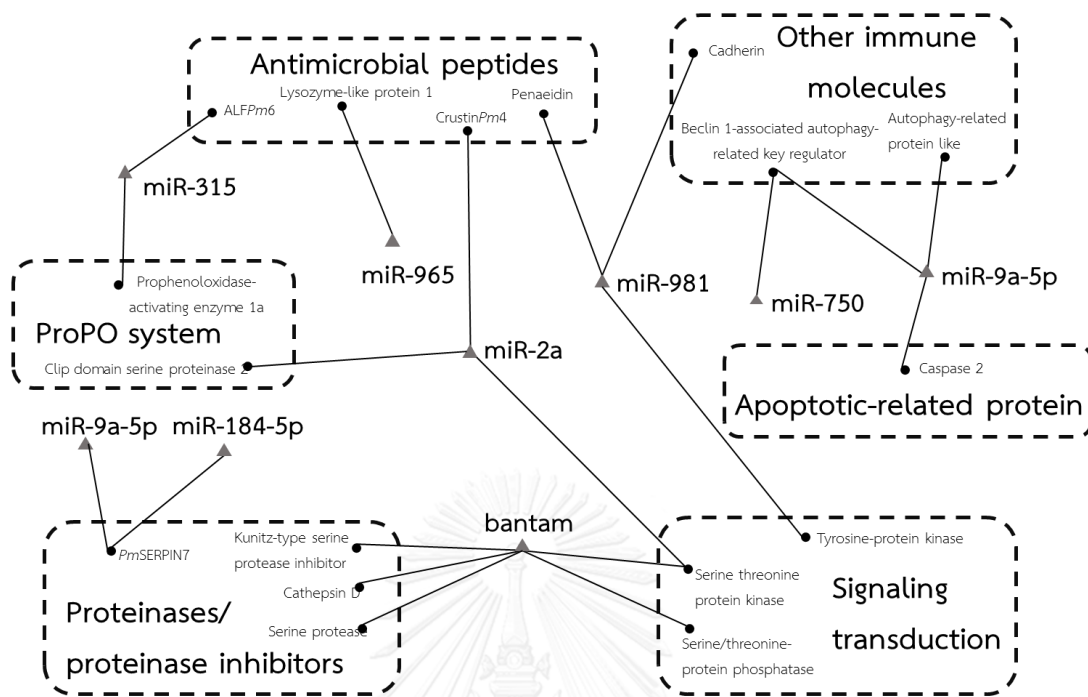


Figure 4. 1 Predicted interactions between miRNAs and mRNAs involved in shrimp immune responses.

REFERENCES

- Ahn, H.W., R.D. Morin, H. Zhao, R.A. Harris, C. Coarfa, Z.J. Chen, A. Milosavljevic, M.A. Marra, and A. Rajkovic. 2010. MicroRNA transcriptome in the newborn mouse ovaries determined by massive parallel sequencing. *Molecular human reproduction*. 16:463-471.
- Akbari Moqadam, F., R. Pieters, and M.L. den Boer. 2013. The hunting of targets: challenge in miRNA research. *Leukemia*. 27:16-23.
- Alexiou, P., M. Maragkakis, G.L. Papadopoulos, M. Reczko, and A.G. Hatzigeorgiou. 2009. Lost in translation: an assessment and perspective for computational microRNA target identification. *Bioinformatics*. 25:3049-3055.
- Alwine, J.C., D.J. Kemp, and G.R. Stark. 1977. Method for detection of specific RNAs in agarose gels by transfer to diazobenzyloxymethyl-paper and hybridization with DNA probes. *Proceedings of the National Academy of Sciences of the United States of America*. 74:5350-5354.
- Ambros, V. 2003. MicroRNA pathways in flies and worms: growth, death, fat, stress, and timing. *Cell*. 113:673-676.
- Ambros, V., and R.C. Lee. 2004. Identification of microRNAs and other tiny noncoding RNAs by cDNA cloning. *Methods in molecular biology*. 265:131-158.
- Ambros, V., R.C. Lee, A. Lavanway, P.T. Williams, and D. Jewell. 2003. MicroRNAs and other tiny endogenous RNAs in *C. elegans*. *Current biology : CB*. 13:807-818.
- Amparyup, P., W. Charoensapsri, and A. Tassanakajon. 2009. Two prophenoloxidases are important for the survival of *Vibrio harveyi* challenged shrimp *Penaeus monodon*. *Developmental and comparative immunology*. 33:247-256.
- Amparyup, P., J. Sutthangkul, W. Charoensapsri, and A. Tassanakajon. 2012. Pattern recognition protein binds to lipopolysaccharide and β -1, 3-glucan and activates shrimp prophenoloxidase system. *Journal of Biological Chemistry*. 287:10060-10069.
- Amparyup, P., K. Wiriyaukaradecha, W. Charoensapsri, and A. Tassanakajon. 2010. A clip domain serine proteinase plays a role in antibacterial defense but is not

- required for prophenoloxidase activation in shrimp. *Developmental and comparative immunology*. 34:168-176.
- Aravin, A.A., M. Lagos-Quintana, A. Yalcin, M. Zavolan, D. Marks, B. Snyder, T. Gaasterland, J. Meyer, and T. Tuschl. 2003. The small RNA profile during *Drosophila melanogaster* development. *Developmental cell*. 5:337-350.
- Bachère, E., Y. Gueguen, M. Gonzalez, J. De Lorgeril, J. Garnier, and B. Romestand. 2004. Insights into the anti-microbial defense of marine invertebrates: the penaeid shrimps and the oyster *Crassostrea gigas*. *Immunological reviews*. 198:149-168.
- Bangrak, P., P. Graidist, W. Chotigeat, and A. Phongdara. 2004. Molecular cloning and expression of a mammalian homologue of a translationally controlled tumor protein (TCTP) gene from *Penaeus monodon* shrimp. *Journal of biotechnology*. 108:219-226.
- Bartel, D.P. 2009. MicroRNAs: target recognition and regulatory functions. *Cell*. 136:215-233.
- Bentley, D.R., S. Balasubramanian, H.P. Swerdlow, G.P. Smith, J. Milton, C.G. Brown, K.P. Hall, D.J. Evers, C.L. Barnes, H.R. Bignell, J.M. Boutell, J. Bryant, R.J. Carter, R. Keira Cheetham, A.J. Cox, D.J. Ellis, M.R. Flatbush, N.A. Gormley, S.J. Humphray, L.J. Irving, M.S. Karbelashvili, S.M. Kirk, H. Li, X. Liu, K.S. Maisinger, L.J. Murray, B. Obradovic, T. Ost, M.L. Parkinson, M.R. Pratt, I.M. Rasolonjatovo, M.T. Reed, R. Rigatti, C. Rodighiero, M.T. Ross, A. Sabot, S.V. Sankar, A. Scally, G.P. Schroth, M.E. Smith, V.P. Smith, A. Spiridou, P.E. Torrance, S.S. Tzonev, E.H. Vermaas, K. Walter, X. Wu, L. Zhang, M.D. Alam, C. Anastasi, I.C. Aniebo, D.M. Bailey, I.R. Bancarz, S. Banerjee, S.G. Barbour, P.A. Baybayan, V.A. Benoit, K.F. Benson, C. Bevis, P.J. Black, A. Boodhun, J.S. Brennan, J.A. Bridgham, R.C. Brown, A.A. Brown, D.H. Buermann, A.A. Bundu, J.C. Burrows, N.P. Carter, N. Castillo, E.C.M. Chiara, S. Chang, R. Neil Cooley, N.R. Crake, O.O. Dada, K.D. Diakoumakos, B. Dominguez-Fernandez, D.J. Earnshaw, U.C. Egbujor, D.W. Elmore, S.S. Etchin, M.R. Ewan, M. Fedurco, L.J. Fraser, K.V. Fuentes Fajardo, W. Scott Furey, D. George, K.J. Gietzen, C.P. Goddard, G.S. Golda, P.A. Granieri, D.E. Green, D.L. Gustafson, N.F. Hansen, K. Harnish, C.D. Haudenschild, N.I.

- Heyer, M.M. Hims, J.T. Ho, A.M. Horgan, et al. 2008. Accurate whole human genome sequencing using reversible terminator chemistry. *Nature*. 456:53-59.
- Bohnsack, M.T., K. Czaplinski, and D. Gorlich. 2004. Exportin 5 is a RanGTP-dependent dsRNA-binding protein that mediates nuclear export of pre-miRNAs. *Rna*. 10:185-191.
- Boulias, K., and H.R. Horvitz. 2012. The *C. elegans* microRNA mir-71 acts in neurons to promote germline-mediated longevity through regulation of DAF-16/FOXO. *Cell metabolism*. 15:439-450.
- Braasch, D.A., and D.R. Corey. 2001. Locked nucleic acid (LNA): fine-tuning the recognition of DNA and RNA. *Chemistry & biology*. 8:1-7.
- Brennecke, J., D.R. Hipfner, A. Stark, R.B. Russell, and S.M. Cohen. 2003. bantam encodes a developmentally regulated microRNA that controls cell proliferation and regulates the proapoptotic gene hid in *Drosophila*. *Cell*. 113:25-36.
- Bushati, N., and S.M. Cohen. 2007. microRNA functions. *Annual review of cell and developmental biology*. 23:175-205.
- Cassar, N.J., and G.J. Hunter. 2013. SERPINS: FORM, FUNCTION, AND DYSFUNCTION. *Xjenza-Online*. 501:51.
- Charoensapsri, W., P. Amparyup, I. Hirono, T. Aoki, and A. Tassanakajon. 2009. Gene silencing of a prophenoloxidase activating enzyme in the shrimp, *Penaeus monodon*, increases susceptibility to *Vibrio harveyi* infection. *Developmental and comparative immunology*. 33:811-820.
- Chen, C., D.A. Ridzon, A.J. Broomer, Z. Zhou, D.H. Lee, J.T. Nguyen, M. Barbisin, N.L. Xu, V.R. Mahuvakar, M.R. Andersen, K.Q. Lao, K.J. Livak, and K.J. Guegler. 2005a. Real-time quantification of microRNAs by stem-loop RT-PCR. *Nucleic acids research*. 33:e179.
- Chen, C.Z., L. Li, H.F. Lodish, and D.P. Bartel. 2004. MicroRNAs modulate hematopoietic lineage differentiation. *Science*. 303:83-86.
- Chen, L.L., H.C. Wang, C.J. Huang, S.E. Peng, Y.G. Chen, S.J. Lin, W.Y. Chen, C.F. Dai, H.T. Yu, C.H. Wang, C.F. Lo, and G.H. Kou. 2002. Transcriptional analysis of the

- DNA polymerase gene of shrimp white spot syndrome virus. *Virology*. 301:136-147.
- Chen, M.-Y., K.-Y. Hu, C.-C. Huang, and Y.-L. Song. 2005b. More than one type of transglutaminase in invertebrates? A second type of transglutaminase is involved in shrimp coagulation. *Developmental & Comparative Immunology*. 29:1003-1016.
- Chen, X., X. Yu, Y. Cai, H. Zheng, D. Yu, G. Liu, Q. Zhou, S. Hu, and F. Hu. 2010. Next-generation small RNA sequencing for microRNAs profiling in the honey bee *Apis mellifera*. *Insect molecular biology*. 19:799-805.
- Cheng, W., I.H. Tsai, C.J. Huang, P.C. Chiang, C.H. Cheng, and M.S. Yeh. 2008. Cloning and characterization of hemolymph clottable proteins of kuruma prawn (*Marsupenaeus japonicus*) and white shrimp (*Litopenaeus vannamei*). *Developmental and comparative immunology*. 32:265-274.
- Chi, S.W., G.J. Hannon, and R.B. Darnell. 2012. An alternative mode of microRNA target recognition. *Nature structural & molecular biology*. 19:321-327.
- Chiang, H.R., L.W. Schoenfeld, J.G. Ruby, V.C. Auyeung, N. Spies, D. Baek, W.K. Johnston, C. Russ, S. Luo, J.E. Babiarz, R. Belloch, G.P. Schroth, C. Nusbaum, and D.P. Bartel. 2010. Mammalian microRNAs: experimental evaluation of novel and previously annotated genes. *Genes & development*. 24:992-1009.
- Chou, H.-Y., M.-C. Tung, C.-F. Chang, M.-S. Su, and G.-H. Kou. 1995a. Purification and genomic analysis of baculovirus associated with white spot syndrome (WSBV) of *Penaeus monodon*. *Dis Aquat Org*. 23:239-242.
- Chou, H., C. Huang, C. Wang, H. Chiang, and C. Lo. 1995b. Pathogenicity of a baculovirus infection causing white spot syndrome in cultured penaeid shrimp in Taiwan.
- Cullen, B.R. 2011. Viruses and microRNAs: RISCy interactions with serious consequences. *Genes & development*. 25:1881-1894.
- Deveraux, Q.L., and J.C. Reed. 1999. IAP family proteins--suppressors of apoptosis. *Genes & development*. 13:239-252.
- Dostie, J., Z. Mourelatos, M. Yang, A. Sharma, and G. Dreyfuss. 2003. Numerous microRNPs in neuronal cells containing novel microRNAs. *Rna*. 9:180-186.

- Durand, S., D. Lightner, R. Redman, and J.-R. Bonami. 1997. Ultrastructure and morphogenesis of white spot syndrome baculovirus (WSSV). *Diseases of aquatic organisms*. 29:205-211.
- Enright, A.J., B. John, U. Gaul, T. Tuschl, C. Sander, and D.S. Marks. 2003. MicroRNA targets in *Drosophila*. *Genome biology*. 5:R1.
- Escobedo-Bonilla, C.M., V. Alday-Sanz, M. Wille, P. Sorgeloos, M.B. Pensaert, and H.J. Nauwynck. 2008. A review on the morphology, molecular characterization, morphogenesis and pathogenesis of white spot syndrome virus. *Journal of fish diseases*. 31:1-18.
- Everett, H., and G. McFadden. 1999. Apoptosis: an innate immune response to virus infection. *Trends Microbiol.* 7:160-165.
- Flegel, T. 1997. Major viral diseases of the black tiger prawn (*Penaeus monodon*) in Thailand. *World Journal of Microbiology and Biotechnology*. 13:433-442.
- Flegel, T., and V. Alday-Sanz. 1998. The crisis in Asian shrimp aquaculture: current status and future needs. *Journal of Applied ichthyology*. 14:269-273.
- Flegel, T.W. 2007. Update on viral accommodation, a model for host-viral interaction in shrimp and other arthropods. *Developmental and comparative immunology*. 31:217-231.
- Forman, J.J., and H.A. Collier. 2010. The code within the code: microRNAs target coding regions. *Cell cycle*. 9:1533-1541.
- Friedlander, M.R., W. Chen, C. Adamidi, J. Maaskola, R. Einspanier, S. Knespel, and N. Rajewsky. 2008. Discovering microRNAs from deep sequencing data using miRDeep. *Nature biotechnology*. 26:407-415.
- Gillespie, J.P., M.R. Kanost, and T. Trenczek. 1997. Biological mediators of insect immunity. *Annual review of entomology*. 42:611-643.
- Git, A., H. Dvinge, M. Salmon-Divon, M. Osborne, C. Kutter, J. Hadfield, P. Bertone, and C. Caldas. 2010. Systematic comparison of microarray profiling, real-time PCR, and next-generation sequencing technologies for measuring differential microRNA expression. *Rna*. 16:991-1006.

- Glotzer, J.B., M. Saltik, S. Chiocca, A.I. Michou, P. Moseley, and M. Cotten. 2000. Activation of heat-shock response by an adenovirus is essential for virus replication. *Nature*. 407:207-211.
- Gorman, M.J., N.T. Dittmer, J.L. Marshall, and M.R. Kanost. 2008. Characterization of the multicopper oxidase gene family in *Anopheles gambiae*. *Insect biochemistry and molecular biology*. 38:817-824.
- Grad, Y., J. Aach, G.D. Hayes, B.J. Reinhart, G.M. Church, G. Ruvkun, and J. Kim. 2003. Computational and experimental identification of *C. elegans* microRNAs. *Molecular cell*. 11:1253-1263.
- Gregory, R.I., K.P. Yan, G. Amuthan, T. Chendrimada, B. Doratotaj, N. Cooch, and R. Shiekhattar. 2004. The Microprocessor complex mediates the genesis of microRNAs. *Nature*. 432:235-240.
- Hammond, S.M., E. Bernstein, D. Beach, and G.J. Hannon. 2000. An RNA-directed nuclease mediates post-transcriptional gene silencing in *Drosophila* cells. *Nature*. 404:293-296.
- Hancock, R.E., and G. Diamond. 2000. The role of cationic antimicrobial peptides in innate host defences. *Trends in microbiology*. 8:402-410.
- He, L., and G.J. Hannon. 2004. MicroRNAs: small RNAs with a big role in gene regulation. *Nature reviews. Genetics*. 5:522-531.
- He, P.A., Z. Nie, J. Chen, J. Chen, Z. Lv, Q. Sheng, S. Zhou, X. Gao, L. Kong, X. Wu, Y. Jin, and Y. Zhang. 2008. Identification and characteristics of microRNAs from *Bombyx mori*. *BMC genomics*. 9:248.
- Holtke, H.J., and C. Kessler. 1990. Non-radioactive labeling of RNA transcripts in vitro with the hapten digoxigenin (DIG); hybridization and ELISA-based detection. *Nucleic acids research*. 18:5843-5851.
- Homvises, T., A. Tassanakajon, and K. Somboonwiwat. 2010. *Penaeus monodon* SERPIN, *PmSERPIN6*, is implicated in the shrimp innate immunity. *Fish Shellfish Immunol*. 29:890-898.
- Huang, T., Y. Cui, and X. Zhang. 2014. Involvement of viral microRNA in the regulation of antiviral apoptosis in shrimp. *Journal of virology*. 88:2544-2554.

- Huang, T., D. Xu, and X. Zhang. 2012. Characterization of host microRNAs that respond to DNA virus infection in a crustacean. *BMC genomics*. 13:159.
- Huang, Y., Q. Zou, S.P. Wang, S.M. Tang, G.Z. Zhang, and X.J. Shen. 2011. The discovery approaches and detection methods of microRNAs. *Molecular biology reports*. 38:4125-4135.
- Hussain, M., and S. Asgari. 2010. Functional analysis of a cellular microRNA in insect host-ascovirus interaction. *Journal of virology*. 84:612-620.
- Hussain, M., R.J. Taft, and S. Asgari. 2008. An insect virus-encoded microRNA regulates viral replication. *Journal of virology*. 82:9164-9170.
- Hussain, M., S. Torres, E. Schnettler, A. Funk, A. Grundhoff, G.P. Pijlman, A.A. Khromykh, and S. Asgari. 2012. West Nile virus encodes a microRNA-like small RNA in the 3' untranslated region which up-regulates GATA4 mRNA and facilitates virus replication in mosquito cells. *Nucleic acids research*. 40:2210-2223.
- Hutvagner, G., and P.D. Zamore. 2002. A microRNA in a multiple-turnover RNAi enzyme complex. *Science*. 297:2056-2060.
- Jang, I.K., Z. Pang, J. Yu, S.K. Kim, H.C. Seo, and Y.R. Cho. 2011. Selectively enhanced expression of prophenoloxidase activating enzyme 1 (PPAE1) at a bacteria clearance site in the white shrimp, *Litopenaeus vannamei*. *BMC immunology*. 12:70.
- Jayachandran, B., M. Hussain, and S. Asgari. 2013. Regulation of *Helicoverpa armigera* ecdysone receptor by miR-14 and its potential link to baculovirus infection. *Journal of invertebrate pathology*. 114:151-157.
- Jiang, H., and M.R. Kanost. 2000. The clip-domain family of serine proteinases in arthropods. *Insect biochemistry and molecular biology*. 30:95-105.
- Johansson, M., and K. Soderhall. 1989. Cellular immunity in crustaceans and the proPO system. *Parasitology Today*. 5:171-176.
- Jopling, C.L., K.L. Norman, and P. Sarnow. 2006. Positive and negative modulation of viral and cellular mRNAs by liver-specific microRNA miR-122. *Cold Spring Harbor symposia on quantitative biology*. 71:369-376.

- Jopling, C.L., M. Yi, A.M. Lancaster, S.M. Lemon, and P. Sarnow. 2005. Modulation of hepatitis C virus RNA abundance by a liver-specific MicroRNA. *Science*. 309:1577-1581.
- Kang, R., H.J. Zeh, M.T. Lotze, and D. Tang. 2011. The Beclin 1 network regulates autophagy and apoptosis. *Cell death and differentiation*. 18:571-580.
- Kato, M., A. de Lencastre, Z. Pincus, and F.J. Slack. 2009. Dynamic expression of small non-coding RNAs, including novel microRNAs and piRNAs/21U-RNAs, during *Caenorhabditis elegans* development. *Genome biology*. 10:R54.
- Kevil, C.G., L. Walsh, F.S. Laroux, T. Kalogeris, M.B. Grisham, and J.S. Alexander. 1997. An improved, rapid Northern protocol. *Biochemical and biophysical research communications*. 238:277-279.
- Kiatpathomchai, W., S. Jitrapakdee, S. Panyim, and V. Boonsaeng. 2004. RT-PCR detection of yellow head virus (YHV) infection in *Penaeus monodon* using dried haemolymph spots. *Journal of virological methods*. 119:1-5.
- Kim, S.W., Z. Li, P.S. Moore, A.P. Monaghan, Y. Chang, M. Nichols, and B. John. 2010. A sensitive non-radioactive northern blot method to detect small RNAs. *Nucleic acids research*. 38:e98.
- Koh, W., C.T. Sheng, B. Tan, Q.Y. Lee, V. Kuznetsov, L.S. Kiang, and V. Tanavde. 2010. Analysis of deep sequencing microRNA expression profile from human embryonic stem cells derived mesenchymal stem cells reveals possible role of let-7 microRNA family in downstream targeting of hepatic nuclear factor 4 alpha. *BMC genomics*. 11 Suppl 1:S6.
- Kramer, M.F. 2011. Stem-loop RT-qPCR for miRNAs. *Current protocols in molecular biology*. Chapter 15:Unit 15 10.
- Krepstakies, M., J. Lucifora, C.H. Nagel, M.B. Zeisel, B. Holstermann, H. Hohenberg, I. Kowalski, T. Gutschmann, T.F. Baumert, K. Brandenburg, J. Hauber, and U. Protzer. 2012. A new class of synthetic peptide inhibitors blocks attachment and entry of human pathogenic viruses. *The Journal of infectious diseases*. 205:1654-1664.

- Kumar, M., and D. Mitra. 2005. Heat shock protein 40 is necessary for human immunodeficiency virus-1 Nef-mediated enhancement of viral gene expression and replication. *Journal of Biological Chemistry*. 280:40041-40050.
- Lagos-Quintana, M., R. Rauhut, W. Lendeckel, and T. Tuschl. 2001. Identification of novel genes coding for small expressed RNAs. *Science*. 294:853-858.
- Lagos-Quintana, M., R. Rauhut, A. Yalcin, J. Meyer, W. Lendeckel, and T. Tuschl. 2002. Identification of tissue-specific microRNAs from mouse. *Current biology : CB*. 12:735-739.
- Lahaye, X., A. Vidy, B. Fouquet, and D. Blondel. 2012. Hsp70 protein positively regulates rabies virus infection. *Journal of virology*. 86:4743-4751.
- Lai, E.C., P. Tomancak, R.W. Williams, and G.M. Rubin. 2003. Computational identification of Drosophila microRNA genes. *Genome biology*. 4:R42.
- Landgraf, P., M. Rusu, R. Sheridan, A. Sewer, N. Iovino, A. Aravin, S. Pfeffer, A. Rice, A.O. Kamphorst, M. Landthaler, C. Lin, N.D. Socci, L. Hermida, V. Fulci, S. Chiaretti, R. Foa, J. Schliwka, U. Fuchs, A. Novosel, R.U. Muller, B. Schermer, U. Bissels, J. Inman, Q. Phan, M. Chien, D.B. Weir, R. Choksi, G. De Vita, D. Frezzetti, H.I. Trompeter, V. Hornung, G. Teng, G. Hartmann, M. Palkovits, R. Di Lauro, P. Wernet, G. Macino, C.E. Rogler, J.W. Nagle, J. Ju, F.N. Papavasiliou, T. Benzing, P. Lichter, W. Tam, M.J. Brownstein, A. Bosio, A. Borkhardt, J.J. Russo, C. Sander, M. Zavolan, and T. Tuschl. 2007. A mammalian microRNA expression atlas based on small RNA library sequencing. *Cell*. 129:1401-1414.
- Lau, N.C., L.P. Lim, E.G. Weinstein, and D.P. Bartel. 2001. An abundant class of tiny RNAs with probable regulatory roles in *Caenorhabditis elegans*. *Science*. 294:858-862.
- Leclercq, M., A.B. Diallo, and M. Blanchette. 2013. Computational prediction of the localization of microRNAs within their pre-miRNA. *Nucleic acids research*. 41:7200-7211.
- Lee, R.C., and V. Ambros. 2001. An extensive class of small RNAs in *Caenorhabditis elegans*. *Science*. 294:862-864.

- Lee, R.C., R.L. Feinbaum, and V. Ambros. 1993. The *C. elegans* heterochronic gene *lin-4* encodes small RNAs with antisense complementarity to *lin-14*. *Cell*. 75:843-854.
- Lee, Y., C. Ahn, J. Han, H. Choi, J. Kim, J. Yim, J. Lee, P. Provost, O. Radmark, S. Kim, and V.N. Kim. 2003. The nuclear RNase III Drosha initiates microRNA processing. *Nature*. 425:415-419.
- Lee, Y., M. Kim, J. Han, K.H. Yeom, S. Lee, S.H. Baek, and V.N. Kim. 2004. MicroRNA genes are transcribed by RNA polymerase II. *The EMBO journal*. 23:4051-4060.
- Lewis, B.P., I.H. Shih, M.W. Jones-Rhoades, D.P. Bartel, and C.B. Burge. 2003. Prediction of mammalian microRNA targets. *Cell*. 115:787-798.
- Li, F., and J. Xiang. 2013. Recent advances in researches on the innate immunity of shrimp in China. *Developmental and comparative immunology*. 39:11-26.
- Li, J., X. Qian, and B. Sha. 2009. Heat shock protein 40: structural studies and their functional implications. *Protein and peptide letters*. 16:606-612.
- Li, L., S. Lin, and F. Yanga. 2005. Functional identification of the non-specific nuclease from white spot syndrome virus. *Virology*. 337:399-406.
- Li, P., J. Peng, J. Hu, Z. Xu, W. Xie, and L. Yuan. 2011. Localized expression pattern of miR-184 in *Drosophila*. *Molecular biology reports*. 38:355-358.
- Li, Q., Y. Chen, and F. Yang. 2004. Identification of a collagen-like protein gene from white spot syndrome virus. *Archives of virology*. 149:215-223.
- Li, W., X. Tang, J. Xing, X. Sheng, and W. Zhan. 2014. Proteomic analysis of differentially expressed proteins in *Fenneropenaeus chinensis* hemocytes upon white spot syndrome virus infection. *PloS one*. 9:e89962.
- Lightner, D.V. 1996. A handbook of shrimp pathology and diagnostic procedures for diseases of cultured penaeid shrimp.
- Lim, L.P., M.E. Glasner, S. Yekta, C.B. Burge, and D.P. Bartel. 2003a. Vertebrate microRNA genes. *Science*. 299:1540.
- Lim, L.P., N.C. Lau, E.G. Weinstein, A. Abdelhakim, S. Yekta, M.W. Rhoades, C.B. Burge, and D.P. Bartel. 2003b. The microRNAs of *Caenorhabditis elegans*. *Genes & development*. 17:991-1008.

- Lin, Y.C., B. Vaseeharan, C.F. Ko, T.T. Chiou, and J.C. Chen. 2007. Molecular cloning and characterisation of a proteinase inhibitor, alpha 2-macroglobulin (alpha2-M) from the haemocytes of tiger shrimp *Penaeus monodon*. *Molecular immunology*. 44:1065-1074.
- Liu, C.G., G.A. Calin, B. Meloon, N. Gamliel, C. Sevignani, M. Ferracin, C.D. Dumitru, M. Shimizu, S. Zupo, M. Dono, H. Alder, F. Bullrich, M. Negrini, and C.M. Croce. 2004. An oligonucleotide microchip for genome-wide microRNA profiling in human and mouse tissues. *Proceedings of the National Academy of Sciences of the United States of America*. 101:9740-9744.
- Liu, H., K. Soderhall, and P. Jiravanichpaisal. 2009a. Antiviral immunity in crustaceans. *Fish Shellfish Immunol*. 27:79-88.
- Liu, J., M.A. Valencia-Sanchez, G.J. Hannon, and R. Parker. 2005. MicroRNA-dependent localization of targeted mRNAs to mammalian P-bodies. *Nature cell biology*. 7:719-723.
- Liu, S., D. Li, Q. Li, P. Zhao, Z. Xiang, and Q. Xia. 2010. MicroRNAs of *Bombyx mori* identified by Solexa sequencing. *BMC genomics*. 11:148.
- Liu, S.G., S.H. Yuan, H.Y. Wu, C.S. Huang, and J. Liu. 2014. The programmed cell death 6 interacting protein insertion/deletion polymorphism is associated with non-small cell lung cancer risk in a Chinese Han population. *Tumour biology : the journal of the International Society for Oncodevelopmental Biology and Medicine*. 35:8679-8683.
- Liu, W., D. Qian, and X. Yan. 2011. Proteomic analysis of differentially expressed proteins in hemolymph of *Scylla serrata* response to white spot syndrome virus infection. *Aquaculture*. 314:53-57.
- Liu, X., and F. Yang. 2005. Identification and function of a shrimp white spot syndrome virus (WSSV) gene that encodes a dUTPase. *Virus research*. 110:21-30.
- Liu, Y., F. Li, B. Wang, B. Dong, X. Zhang, and J. Xiang. 2009b. A serpin from Chinese shrimp *Fenneropenaeus chinensis* is responsive to bacteria and WSSV challenge. *Fish Shellfish Immunol*. 26:345-351.

- Liu, Y.C., F.H. Li, B. Wang, B. Dong, Q.L. Zhang, W. Luan, X.J. Zhang, and J.H. Xiang. 2007. A transglutaminase from Chinese shrimp (*Fenneropenaeus chinensis*), full-length cDNA cloning, tissue localization and expression profile after challenge. *Fish Shellfish Immunol.* 22:576-588.
- Lo, C.-F., J.-H. Leu, C. Ho, C. Chen, S. Peng, Y. Chen, C. Chou, P. Yeh, C. Huang, and H. Chou. 1996. Detection of baculovirus associated with white spot syndrome (WSBV) in penaeid shrimps using polymerase chain reaction. *Diseases of aquatic organisms.* 25:133-141.
- Lu, D.P., R.L. Read, D.T. Humphreys, F.M. Battah, D.I. Martin, and J.E. Rasko. 2005. PCR-based expression analysis and identification of microRNAs. *Journal of RNAi and gene silencing : an international journal of RNA and gene targeting research.* 1:44-49.
- Lui, W.O., N. Pourmand, B.K. Patterson, and A. Fire. 2007. Patterns of known and novel small RNAs in human cervical cancer. *Cancer research.* 67:6031-6043.
- Marks, H. 2005. Genomics and transcriptomics of white spot syndrome virus. Wageningen Universiteit.
- Martinez, J., and T. Tuschl. 2004. RISC is a 5' phosphomonoester-producing RNA endonuclease. *Genes & development.* 18:975-980.
- Medzhitov, R., and C. Janeway, Jr. 2000. Innate immune recognition: mechanisms and pathways. *Immunol Rev.* 173:89-97.
- Mehrabadi, M., M. Hussain, and S. Asgari. 2013. MicroRNAome of *Spodoptera frugiperda* cells (Sf9) and its alteration following baculovirus infection. *The Journal of general virology.* 94:1385-1397.
- Metzker, M.L. 2010. Sequencing technologies - the next generation. *Nature reviews. Genetics.* 11:31-46.
- Mohan, C.V., K.M. Shankar, S. Kulkarni, and P.M. Sudha. 1998. Histopathology of cultured shrimp showing gross signs of yellow head syndrome and white spot syndrome during 1994 Indian epizootics. *Diseases of aquatic organisms.* 34:9-12.
- Molthathong, S., S. Senapin, S. Klinbunga, N. Puanglarp, J. Rojtinnakorn, and T.W. Flegel. 2008. Down-regulation of defender against apoptotic death (DAD1)

- after yellow head virus (YHV) challenge in black tiger shrimp *Penaeus monodon*. *Fish Shellfish Immunol.* 24:173-179.
- Moretti, F., R. Thermann, and M.W. Hentze. 2010. Mechanism of translational regulation by miR-2 from sites in the 5' untranslated region or the open reading frame. *Rna.* 16:2493-2502.
- Olsen, P.H., and V. Ambros. 1999. The lin-4 regulatory RNA controls developmental timing in *Caenorhabditis elegans* by blocking LIN-14 protein synthesis after the initiation of translation. *Developmental biology.* 216:671-680.
- Olson, A.J., J. Brennecke, A.A. Aravin, G.J. Hannon, and R. Sachidanandam. 2008. Analysis of large-scale sequencing of small RNAs. *Pacific Symposium on Biocomputing. Pacific Symposium on Biocomputing:*126-136.
- Ou, J., Y. Li, Z. Ding, Y. Xiu, T. Wu, J. Du, W. Li, H. Zhu, Q. Ren, W. Gu, and W. Wang. 2013. Transcriptome-wide identification and characterization of the *Procambarus clarkii* microRNAs potentially related to immunity against *Spiroplasma eriocheiris* infection. *Fish Shellfish Immunol.* 35:607-617.
- Overstreet, R.M., D.V. Lightner, K.W. Hasson, S. McIlwain, and J.M. Lotz. 1997. Susceptibility to Taura Syndrome Virus of Some Penaeid Shrimp Species Native to the Gulf of Mexico and the Southeastern United States. *Journal of invertebrate pathology.* 69:165-176.
- Park, J., Y. Lee, S. Lee, and Y. Lee. 1998. An infectious viral disease of penaeid shrimp newly found in Korea. *Diseases of aquatic organisms.* 34:71-75.
- Petrosino, J.F., S. Highlander, R.A. Luna, R.A. Gibbs, and J. Versalovic. 2009. Metagenomic pyrosequencing and microbial identification. *Clinical chemistry.* 55:856-866.
- Pfeffer, S., M. Zavolan, F.A. Grasser, M. Chien, J.J. Russo, J. Ju, B. John, A.J. Enright, D. Marks, C. Sander, and T. Tuschl. 2004. Identification of virus-encoded microRNAs. *Science.* 304:734-736.
- Ponprateep, S., S. Tharntada, K. Somboonwiwat, and A. Tassanakajon. 2012. Gene silencing reveals a crucial role for anti-lipoplysaccharide factors from *Penaeus monodon* in the protection against microbial infections. *Fish Shellfish Immunol.* 32:26-34.

- Portt, L., G. Norman, C. Clapp, M. Greenwood, and M.T. Greenwood. 2011. Anti-apoptosis and cell survival: a review. *Biochimica et biophysica acta*. 1813:238-259.
- Qasba, P.K., and S. Kumar. 1997. Molecular divergence of lysozymes and alpha-lactalbumin. *Critical reviews in biochemistry and molecular biology*. 32:255-306.
- Rajendran, K., K. Vijayan, T. Santiago, and R. Krol. 1999. Experimental host range and histopathology of white spot syndrome virus (WSSV) infection in shrimp, prawns, crabs and lobsters from India. *Journal of fish diseases*. 22:183-191.
- Ramkisson, S.H., L.A. Mainwaring, E.M. Sloand, N.S. Young, and S. Kajigaya. 2006. Nonisotopic detection of microRNA using digoxigenin labeled RNA probes. *Molecular and cellular probes*. 20:1-4.
- Raymond, C.K., B.S. Roberts, P. Garrett-Engle, L.P. Lim, and J.M. Johnson. 2005. Simple, quantitative primer-extension PCR assay for direct monitoring of microRNAs and short-interfering RNAs. *Rna*. 11:1737-1744.
- Rehmsmeier, M., P. Steffen, M. Hochsmann, and R. Giegerich. 2004. Fast and effective prediction of microRNA/target duplexes. *Rna*. 10:1507-1517.
- Reinhart, B.J., F.J. Slack, M. Basson, A.E. Pasquinelli, J.C. Bettinger, A.E. Rougvie, H.R. Horvitz, and G. Ruvkun. 2000. The 21-nucleotide let-7 RNA regulates developmental timing in *Caenorhabditis elegans*. *Nature*. 403:901-906.
- Ren, Q., Z.L. Xu, X.W. Wang, X.F. Zhao, and J.X. Wang. 2009. Clip domain serine protease and its homolog respond to *Vibrio* challenge in Chinese white shrimp, *Fenneropenaeus chinensis*. *Fish Shellfish Immunol*. 26:787-798.
- Rimphanitchayakit, V., and A. Tassanakajon. 2010. Structure and function of invertebrate Kazal-type serine proteinase inhibitors. *Developmental and comparative immunology*. 34:377-386.
- Rodriguez, J., B. Bayot, Y. Amano, F. Panchana, I. de Blas, V. Alday, and J. Calderon. 2003. White spot syndrome virus infection in cultured *Penaeus vannamei* (Boone) in Ecuador with emphasis on histopathology and ultrastructure. *Journal of fish diseases*. 26:439-450.

- Rolland, J.L., M. Abdelouahab, J. Dupont, F. Lefevre, E. Bachere, and B. Romestand. 2010. Stylicins, a new family of antimicrobial peptides from the Pacific blue shrimp *Litopenaeus stylirostris*. *Molecular immunology*. 47:1269-1277.
- Ruan, L., X. Bian, Y. Ji, M. Li, F. Li, and X. Yan. 2011. Isolation and identification of novel microRNAs from *Marsupenaeus japonicus*. *Fish Shellfish Immunol*. 31:334-340.
- Ruby, J.G., C. Jan, C. Player, M.J. Axtell, W. Lee, C. Nusbaum, H. Ge, and D.P. Bartel. 2006. Large-scale sequencing reveals 21U-RNAs and additional microRNAs and endogenous siRNAs in *C. elegans*. *Cell*. 127:1193-1207.
- Ruby, J.G., A. Stark, W.K. Johnston, M. Kellis, D.P. Bartel, and E.C. Lai. 2007. Evolution, biogenesis, expression, and target predictions of a substantially expanded set of *Drosophila* microRNAs. *Genome research*. 17:1850-1864.
- Ryan, B.M., A.I. Robles, and C.C. Harris. 2010. Genetic variation in microRNA networks: the implications for cancer research. *Nature reviews. Cancer*. 10:389-402.
- Schmittgen, T.D., E.J. Lee, J. Jiang, A. Sarkar, L. Yang, T.S. Elton, and C. Chen. 2008. Real-time PCR quantification of precursor and mature microRNA. *Methods*. 44:31-38.
- Sempere, L.F., N.S. Sokol, E.B. Dubrovsky, E.M. Berger, and V. Ambros. 2003. Temporal regulation of microRNA expression in *Drosophila melanogaster* mediated by hormonal signals and broad-Complex gene activity. *Developmental biology*. 259:9-18.
- Shi, R., and V.L. Chiang. 2005. Facile means for quantifying microRNA expression by real-time PCR. *BioTechniques*. 39:519-525.
- Shin, C., J.W. Nam, K.K. Farh, H.R. Chiang, A. Shkumatava, and D.P. Bartel. 2010. Expanding the microRNA targeting code: functional sites with centered pairing. *Molecular cell*. 38:789-802.
- Silver, S.J., J.W. Hagen, K. Okamura, N. Perrimon, and E.C. Lai. 2007. Functional screening identifies miR-315 as a potent activator of Wingless signaling. *Proceedings of the National Academy of Sciences of the United States of America*. 104:18151-18156.

- Singh, C.P., J. Singh, and J. Nagaraju. 2012. A baculovirus-encoded MicroRNA (miRNA) suppresses its host miRNA biogenesis by regulating the exportin-5 cofactor Ran. *Journal of virology*. 86:7867-7879.
- Singh, C.P., J. Singh, and J. Nagaraju. 2014. bmnvp-miR-3 facilitates BmNPV infection by modulating the expression of viral P6.9 and other late genes in *Bombyx mori*. *Insect biochemistry and molecular biology*. 49:59-69.
- Sir, D., and J.H. Ou. 2010. Autophagy in viral replication and pathogenesis. *Molecules and cells*. 29:1-7.
- Sithigorngul, P., P. Chauyuchwong, W. Sithigorngul, S. Longyant, P. Chaivisuthangkura, and P. Menasveta. 2000. Development of a monoclonal antibody specific to yellow head virus (YHV) from *Penaeus monodon*. *Diseases of aquatic organisms*. 42:27-34.
- Song, F., Y.C. Huang, X. Wang, S. Tang, and X. Shen. 2013. Bmo-miR-9A down regulates the expression of *Bm-ase* gene in vitro. *Bioorganicheskaia khimiia*. 39:194-199.
- Soowannayan, C., T.W. Flegel, P. Sithigorngul, J. Slater, A. Hyatt, S. Cramerri, T. Wise, M.S. Crane, J.A. Cowley, R.J. McCulloch, and P.J. Walker. 2003. Detection and differentiation of yellow head complex viruses using monoclonal antibodies. *Diseases of aquatic organisms*. 57:193-200.
- Stark, A., P. Kheradpour, L. Parts, J. Brennecke, E. Hodges, G.J. Hannon, and M. Kellis. 2007. Systematic discovery and characterization of fly microRNAs using 12 *Drosophila* genomes. *Genome research*. 17:1865-1879.
- Suzuki, H.I., and K. Miyazono. 2011. Emerging complexity of microRNA generation cascades. *Journal of biochemistry*. 149:15-25.
- Tan, T.T., M. Chen, J.A. Harikrishna, N. Khairuddin, M.I. Mohd Shamsudin, G. Zhang, and S. Bhassu. 2013. Deep parallel sequencing reveals conserved and novel miRNAs in gill and hepatopancreas of giant freshwater prawn. *Fish Shellfish Immunol*. 35:1061-1069.
- Tassanakajon, A., P. Amparyup, K. Somboonwiwat, and P. Supungul. 2011. Cationic antimicrobial peptides in penaeid shrimp. *Marine biotechnology*. 13:639-657.

- Tassanakajon, A., K. Somboonwiwat, P. Supungul, and S. Tang. 2013. Discovery of immune molecules and their crucial functions in shrimp immunity. *Fish & shellfish immunology*. 34:954-967.
- Tay, Y., J. Zhang, A.M. Thomson, B. Lim, and I. Rigoutsos. 2008. MicroRNAs to Nanog, Oct4 and Sox2 coding regions modulate embryonic stem cell differentiation. *Nature*. 455:1124-1128.
- Tong, C.Z., Y.F. Jin, and Y.Z. Zhang. 2006. Computational prediction of microRNA genes in silkworm genome. *Journal of Zhejiang University. Science. B*. 7:806-816.
- Tsai, M.F., H.T. Yu, H.F. Tzeng, J.H. Leu, C.M. Chou, C.J. Huang, C.H. Wang, J.Y. Lin, G.H. Kou, and C.F. Lo. 2000. Identification and characterization of a shrimp white spot syndrome virus (WSSV) gene that encodes a novel chimeric polypeptide of cellular-type thymidine kinase and thymidylate kinase. *Virology*. 277:100-110.
- Valoczi, A., C. Hornyik, N. Varga, J. Burgyan, S. Kauppinen, and Z. Havelda. 2004. Sensitive and specific detection of microRNAs by northern blot analysis using LNA-modified oligonucleotide probes. *Nucleic acids research*. 32:e175.
- Valouev, A., J. Ichikawa, T. Tonthat, J. Stuart, S. Ranade, H. Peckham, K. Zeng, J.A. Malek, G. Costa, K. McKernan, A. Sidow, A. Fire, and S.M. Johnson. 2008. A high-resolution, nucleosome position map of *C. elegans* reveals a lack of universal sequence-dictated positioning. *Genome research*. 18:1051-1063.
- van Hulten, M.C., J. Witteveldt, S. Peters, N. Kloosterboer, R. Tarchini, M. Fiers, H. Sandbrink, R.K. Lankhorst, and J.M. Vlak. 2001a. The white spot syndrome virus DNA genome sequence. *Virology*. 286:7-22.
- van Hulten, M.C., J. Witteveldt, M. Snippe, and J.M. Vlak. 2001b. White spot syndrome virus envelope protein VP28 is involved in the systemic infection of shrimp. *Virology*. 285:228-233.
- Varallyay, E., J. Burgyan, and Z. Havelda. 2008. MicroRNA detection by northern blotting using locked nucleic acid probes. *Nature protocols*. 3:190-196.
- Vaseeharan, B., S. Shanthi, and N.M. Prabhu. 2011. A novel clip domain serine proteinase (SPs) gene from the haemocytes of Indian white shrimp

- Fenneropenaeus indicus*: molecular cloning, characterization and expression analysis. *Fish Shellfish Immunol.* 30:980-985.
- Wang, L., B. Zhi, W. Wu, and X. Zhang. 2008. Requirement for shrimp caspase in apoptosis against virus infection. *Developmental and comparative immunology.* 32:706-715.
- Wang, X., and X. Wang. 2006. Systematic identification of microRNA functions by combining target prediction and expression profiling. *Nucleic acids research.* 34:1646-1652.
- Wang, Y., D.N. Keys, J.K. Au-Young, and C. Chen. 2009. MicroRNAs in embryonic stem cells. *Journal of cellular physiology.* 218:251-255.
- Warf, M.B., W.E. Johnson, and B.L. Bass. 2011. Improved annotation of *C. elegans* microRNAs by deep sequencing reveals structures associated with processing by Drosha and Dicer. *Rna.* 17:563-577.
- Watanabe, Y., N. Yachie, M. Tomita, and A. Kanai. 2006. Computational Prediction of Drosophila MicroRNA Targets and Analysis of Their Negative Feedback Control.
- Weaver, D.B., J.M. Anzola, J.D. Evans, J.G. Reid, J.T. Reese, K.L. Childs, E.M. Zdobnov, M.P. Samanta, J. Miller, and C.G. Elisk. 2007. Computational and transcriptional evidence for microRNAs in the honey bee genome. *Genome biology.* 8:R97. จุฬาลงกรณ์มหาวิทยาลัย
- Wei, J., W. Gao, C.J. Zhu, Y.Q. Liu, Z. Mei, T. Cheng, and Y.Q. Shu. 2011. Identification of plasma microRNA-21 as a biomarker for early detection and chemosensitivity of non-small cell lung cancer. *Chinese journal of cancer.* 30:407-414.
- Wheeler, B.M., A.M. Heimberg, V.N. Moy, E.A. Sperling, T.W. Holstein, S. Heber, and K.J. Peterson. 2009. The deep evolution of metazoan microRNAs. *Evolution & development.* 11:50-68.
- Witkos, T.M., E. Koscianska, and W.J. Krzyzosiak. 2011. Practical Aspects of microRNA Target Prediction. *Current molecular medicine.* 11:93-109.
- Witteveldt, J., M.C. Van Hulst, and J.M. Vlcek. 2001. Identification and phylogeny of a non-specific endonuclease gene of white spot syndrome virus of shrimp. *Virus genes.* 23:331-337.

- Wongteerasupaya, C., P. Pungchai, B. Withyachumnarnkul, V. Boonsaeng, S. Panyim, T.W. Flegel, and P.J. Walker. 2003. High variation in repetitive DNA fragment length for white spot syndrome virus (WSSV) isolates in Thailand. *Diseases of aquatic organisms*. 54:253-257.
- Wu, X., H. Xiong, Y. Wang, and H. Du. 2014. Immunomodulatory effects of hyperthermia on resisting WSSV infection in *Procambarus clarkii*. *Journal of fish diseases*.
- Wyban, J. 2007. Thailand's white shrimp revolution. *Global Aquaculture Advocate*. 10:56-58.
- Xu, P., S.Y. Vernooy, M. Guo, and B.A. Hay. 2003. The Drosophila microRNA Mir-14 suppresses cell death and is required for normal fat metabolism. *Current biology : CB*. 13:790-795.
- Yang, F., J. He, X. Lin, Q. Li, D. Pan, X. Zhang, and X. Xu. 2001. Complete genome sequence of the shrimp white spot bacilliform virus. *Journal of virology*. 75:11811-11820.
- Yang, G., L. Yang, Z. Zhao, J. Wang, and X. Zhang. 2012. Signature miRNAs involved in the innate immunity of invertebrates. *PloS one*. 7:e39015.
- Yeh, M.S., C.J. Huang, J.H. Leu, Y.C. Lee, and I.H. Tsai. 1999. Molecular cloning and characterization of a hemolymph clottable protein from tiger shrimp (*Penaeus monodon*). *European journal of biochemistry / FEBS*. 266:624-633.
- Yeh, M.S., L.R. Kao, C.J. Huang, and I.H. Tsai. 2006. Biochemical characterization and cloning of transglutaminases responsible for hemolymph clotting in *Penaeus monodon* and *Marsupenaeus japonicus*. *Biochimica et biophysica acta*. 1764:1167-1178.
- Yeh, M.S., C.H. Liu, C.W. Hung, and W. Cheng. 2009. cDNA cloning, identification, tissue localisation, and transcription profile of a transglutaminase from white shrimp, *Litopenaeus vannamei*, after infection by *Vibrio alginolyticus*. *Fish Shellfish Immunol*. 27:748-756.
- Yu, X., Q. Zhou, S.C. Li, Q. Luo, Y. Cai, W.C. Lin, H. Chen, Y. Yang, S. Hu, and J. Yu. 2008. The silkworm (*Bombyx mori*) microRNAs and their expressions in multiple developmental stages. *PloS one*. 3:e2997.

- Yu, X.Q., and M.R. Kanost. 2002. Binding of hemolin to bacterial lipopolysaccharide and lipoteichoic acid. An immunoglobulin superfamily member from insects as a pattern-recognition receptor. *European journal of biochemistry / FEBS*. 269:1827-1834.
- Zhang, J., Q. He, C.D. Zhang, X.Y. Chen, X.M. Chen, Z.Q. Dong, N. Li, X.X. Kuang, M.Y. Cao, C. Lu, and M.H. Pan. 2014a. Inhibition of BmNPV replication in silkworm cells using inducible and regulated artificial microRNA precursors targeting the essential viral gene *lef-11*. *Antiviral research*. 104:143-152.
- Zhang, X., Y. Zheng, G. Jagadeeswaran, R. Ren, R. Sunkar, and H. Jiang. 2014b. Identification of conserved and novel microRNAs in *Manduca sexta* and their possible roles in the expression regulation of immunity-related genes. *Insect biochemistry and molecular biology*. 47:12-22.
- Zhu, J.Y., M. Strehle, A. Frohn, E. Kremmer, K.P. Hofig, G. Meister, and H. Adler. 2010. Identification and analysis of expression of novel microRNAs of murine gammaherpesvirus 68. *Journal of virology*. 84:10266-10275.
- Zisoulis, D.G., M.T. Lovci, M.L. Wilbert, K.R. Hutt, T.Y. Liang, A.E. Pasquinelli, and G.W. Yeo. 2010. Comprehensive discovery of endogenous Argonaute binding sites in *Caenorhabditis elegans*. *Nature structural & molecular biology*. 17:173-179.



1. The 18th Biological Science Graduate Congress. January 6-8, 2014. Faculty of Science, University of Malaya, Kuala Lumpur, Malaysia. “Identification of miRNAs involved in WSSV infection *Penaeus monodon*” (Poster presentation)
Award: The Silver Medal Winner for poster presentation award in Cell and Molecular Biology theme
2. The 22nd Science Forum 2014. March 20-21, 2014. Faculty of Science, Chulalongkorn University, Bangkok, Thailand. “Identification and characterization of miRNAs involved in WSSV infection in *Penaeus monodon*” (Oral presentation)
3. The 4th International Biochemistry and Molecular Biology Conference. April 2-3, 2014. Rama Gardens Hotel & Resort, Bangkok, Thailand. “Identification of miRNAs involved in WSSV infection *Penaeus monodon*” (Oral presentation)
4. The Next Generation Sequencing for Genetic and Genomic Studies 2014, July 29-30, 2014. Winsor Hotel, Bangkok, Thailand. “Identification of microRNAs involved in WSSV infection from the black tiger shrimp, *Penaeus monodon*, by next generation sequencing” (Proceeding)

VITA

Mr. Napol Kaewkascholkul was born in March 14, 1990 in Bangkok. He graduated with the degree of Bachelor of Science (First class Honor) from the Department of Biochemistry, Faculty of Science, Chulalongkorn University in 2011. He has studied for the degree of Master of Science, Program in Biochemistry and Molecular biology, Department of Biochemistry, Faculty of Science, Chulalongkorn University since 2012. Then he got the scholarship from The Chulalongkorn University graduate scholarship to commemorate the 72nd Anniversary of His Majesty King Bhumibol Adulyadej and The 90th Anniversary of Chulalongkorn University Fund grant.

